



UNIVERSITY of  
RWANDA

COLLEGE OF SCIENCE  
AND TECHNOLOGY



AFRICAN CENTER OF  
EXCELLENCE IN ENERGY FOR  
SUSTAINABLE DEVELOPMENT

**TITLE: THERMAL EFFICIENCY ENHANCEMENT OF A COMMUNITY  
COOK-STOVE THROUGH DESIGN IMPROVEMENTS AND COMSOL-  
BASED SIMULATION.**

**Student Name:** Raban HABINEZA

**Registration Number:** 218005860

**A Thesis Submitted to the African Center of Excellence in Energy for  
Sustainable Development (ACE-ESD) College of Science and Technology  
University of Rwanda in Fulfilment of the Requirements for the Degree  
Of Masters of Science in Renewable Energy Engineering**

**Supervisor's Name:** Dr. Maxime BINAMA

**Co-Supervisor's Name:** Dr. Antoine MUSENGIMANA

**Month and Year of Submission:** October 2025

## Declaration


Declaration I, Raban HABINEZA, Student Number 218005860 declare that this thesis project is my original work, and has not presented for a degree at the University of Rwanda or any other university. All sources of materials used in the work have fully acknowledged in the correct academic format.

Printed by: Mr. Raban HABINEZA

Signature: ..... Date: 09/10/2025

This thesis has submitted for examination with my approval as a university advisor.

Approved by the Co-Supervisor: Dr. Antoine MUSENGIMANA

Signature:  ..... Date: 09/10/2025

Approved by the Supervisor: Dr. Maxime BINAMA

Signature: ..... Date: .....

## **Abstract**

In the wake of climate change, the widespread use of traditional biomass cook-stoves, particularly in rural and low-income communities especially in Africa, presents a critical challenge due to their low thermal efficiency those results in high fuel consumption. This High fuel Consumption can exacerbate deforestation, greenhouse gas emissions, and severe indoor air pollution, which negatively affect health of women and children mostly in developing countries. The poor performance of cooking stoves is due to week inefficient design of stove's combustion chambers and suboptimal selection of the insulation materials within the stove.

This research seeks to design and develop an improved community cook-stove that addresses these mentioned challenges. To achieve this, the study employs a simulation-based approach using COMSOL Multiphysics. Three geometries; cylindrical, conical, and rectangular of combustion chamber were modeled for better understanding their impact on stove performance. In addition, the process of selecting insulation material, which includes glass wool batt, swamp air gap insulator, Glass Fiber Blanket insulator and alumino-silicate fire clay bricks, was optimized through simulations. By both stationary and transient heat, temperature profiles, thermal performance, combustion efficiency, and Sensitivity analysis further explored the impact of insulation properties on overall stove performance.

The findings reveal that geometry and insulation material play a pivotal role in determining stove efficiency. The cylindrical combustion chamber, combined with high-performance insulation, achieved the best thermal retention and uniform heat distribution, significantly lowering fuel consumption. This optimized design offers a practical and sustainable improved clean cooking stove that reduce environmental impact, and improve public health in underserved communities. The work demonstrates a replicable model for advancing energy-efficient stove technologies through simulation-driven design.

## Table of Content

Declaration.....	i
Abstract.....	ii
Table of Content .....	iii
List of Figures.....	vi
List of Tables .....	viii
Acknowledgements.....	ix
Dedication.....	x
Chapter 1. Introduction.....	1
1.1 Background of the Study.....	1
1.2 Problems statement.....	3
1.3 Main Objective.....	3
1.4 Specific Objectives.....	3
1.5 Research Questions.....	3
1.5 Research Justification.....	4
1.6 Scope and Limitations of the Study.....	5
1.6.1 Scope.....	5
1.6.2. Limitations.....	5
1.7 Thesis Organization.....	6
Chapter 2. Literature Review.....	7
2.1 Overview on Cook-stove Designs.....	7
2.2 Basic Biomass Cook-Stove Concept.....	10
2.3 Similar Works.....	10
2.4 Summary of Previous Works and Gap Identification.....	12
Chapter 3. Methodology.....	13
3.1 Previous Methods.....	13
3.2 Data Collection Sources and Research Instrument.....	15
3.3 Design Conceptualization and Research Design models.....	17
3.3.1 Material Type and Properties Used for Community Cook stove.....	17

3.3.2 Combustion Chamber Geometry Models of Community Cook stove.....	19
3.3.2.1 Cylindrical Geometry Model of Community Cook stove Combustion Chamber.	21
3.3.2.2 Conical Geometry Model of Community Cook stove Combustion Chamber.....	32
3.3.2.3 Rectangular Geometry Model of Community Cook stove Combustion Chamber. .....	37
3.3.3 Comsol Multi-physics Heat Transfer Parametric Model.....	43
3.3.4 Optimal Design Selection of Community Cookstove Design Model.....	49
3.4 Parametric Mesh Type Selection.....	50
3.5.1 Implication of Mesh Selection.....	50
3.4.2 Mesh Statistics OF 3D Model Layers.....	51
3.5 Previous Experiment on Community Biomass Cook-Stove.....	52
3.5.1 Theory and Calculation of Experimental Material Set-Up.....	52
3.5.2 Thermal Efficiency Calculation.....	53
Chapter 4. Results and Discussions.....	55
4.1 Computational Simulation Analysis using COMSOL Multi-physics software.....	55
4.1.1 Stationary Study of COMSOL Multi-physics software-based simulation.....	56
4.1.1.1 Stationary Simulation Study of Cylindrical Combustion Chamber Geometry.....	56
4.1.1.2 Stationary Simulation Study of Conical Combustion Chamber Geometry.....	59
4.1.1.3 Stationary Simulation Study of Rectangular Combustion Chamber Geometry..	62
4.1.2 Time Dependent Study of COMSOL Multi-physics Software based Simulation.....	65
4.1.2.1 Time Dependent Simulation Study of Cylindrical Combustion Chamber Geometry.....	65
4.1.2.2 Time Dependent Simulation Study of Conical Combustion Chamber Geometry.	68
4.1.2.3 Time Dependent Simulation Study of Rectangular Combustion Chamber Geometry.....	70
4.2 Discussion on Performance Comparison for All Geometry Models.....	73
4.2.1 Data Analysis for All Combustion Chamber Geometries Comparison.....	73
4.2.2 Sensitivity Data Analysis for Different Insulation materials.....	74
Chapter 5. Conclusion and Recommendation.....	78
5.1 Conclusions.....	78
5.2 Recommendations.....	78

6. References.....	79
7. Appendix 1. Data Recording Process on Field. ....	81

## List of Figures

Figure 1.1 Biomass cook stove.....	2
Fig 2.1 Improved-cook-stove-with-forced-air-biomass-gasification.....	7
Fig 2.2 <b>A:</b> IIC Stove-World Food Program; <b>B:</b> Ecocina Stove.....	8
Fig 2.3 (1): Improved Double Mouth Cooking Stove Coupled with Single Mouth Cooking Stove having one common Chimney (Courtesy: IDCOL) and, (2): The National Biomass Cook-stoves Initiative (NCI).....	9
Figure 3.1 <b>A:</b> Hioki Temperature Hi-Tester 3443; <b>B:</b> EUTECH Eco-Scan Temp 6. ....	15
Figure 3.2: <b>(A):</b> Meter Rule; <b>(B):</b> Marker Pen Instrumentations.....	16
Fig 3.3 cylindrical combustion chamber deign model.....	20
Fig 3.4 Conical Combustion Chamber Deign Model .....	20
Fig 3.5 Rectangular combustion chamber design model. ....	21
Fig 3.6 Inner Sheet Metal with its dimensions of Cylindrical Cook-Stove Model.....	22
Fig 3.7 Alumino-silicate fire clay brick Insulator with its dimensions of Cylindrical Cook-Stove Model. ....	23
Fig 3.8 Middle Sheet Metal with its dimensions of Cylindrical Cook-Stove Model. ....	24
Fig 3.9 Glass Wool batt Insulator with its dimensions of Cylindrical Cook-Stove Model. ....	25
Fig 3.10 Outer Sheet Metal with its dimensions of Cylindrical Cook-Stove Model.....	26
Fig 3.11 Entranceway Sheet Metal with its dimensions of Cylindrical Cook-Stove Model. ....	27
Fig 3.12 Stove Top Ring Cover Sheet Metal with its dimensions of Cylindrical Cook-Stove Model. ....	27
Fig 3.13 Entry Wood Carrier Sheet and Tube Metals of Cylindrical cook-stove Model. ....	28
Fig 3.14 Entry Wood Carrier Side Tube Metals with their dimensions of Cylindrical Cook-Stove Model. ....	28
Fig 3.15 Entry Wood Carrier Frame with their dimensions of Cylindrical Cook-Stove Model. .	29
Fig 3.16 Base Stand with its dimensions of Cylindrical Cook-Stove Model. ....	29
Fig 3.17 Cooking Pot of Cylindrical Cook-Stove Model. ....	30
Fig 3.18 Cooking Pot Sheet Metal with its dimensions of Cylindrical Cook-Stove Model.....	31
Fig 3.19 Cooking Pot Ring Cover with its dimensions of Cylindrical Cook-Stove Model. ....	31
Fig 3.20 Stove Frame Tube Metal with its dimensions of Cylindrical Cook-Stove Model. ....	32
Fig 3.21 Inner Sheet Metal with its dimensions of Conical Cook-Stove Model. ....	33
Fig 3.22 Alumino-silicate fire clay brick Insulator with its dimensions of Conical Cook-Stove Model. ....	34
Fig 3.23 Inner Sheet Metal with its dimensions of Square Cook-Stove Model. ....	38
Fig 3.24 Alumino-silicate fire clay brick Insulator with its dimensions of Square Cook-Stove Model. ....	39
Fig 3.25: Comsol Design Model of Community Cook Stove.....	43
Figure 4.1: The Stationary Temperature Heat Distribution for Cylindrical Combustion Chamber. ....	56

Figure 4.2: The Stationary Isothermal Contour Distribution for Cylindrical Combustion Chamber Model. ....	57
Figure 4.3 The Stationary Temperature Distribution Within Water at each Point from Bottom to Top Layer of Cylindrical Model. ....	57
Figure 4.4 The Stationary Temperature Distribution Within Cooking at each Point from Both Sides to External wall body Layer of Cylindrical Model. ....	58
Figure 4.5 The Stationary Temperature Distribution Within Wall Thickness from Cylindrical Combustion Chamber to Outside Wall Body Surface. ....	58
Figure 4.6: The Stationary Temperature Heat Distribution for Conical Combustion Chamber... ..	59
Figure 4.7: Stationary Isothermal Contour Distribution for Conical Combustion Chamber Model. ....	60
Figure 4.8 Stationary Temperature Distribution Within Water at each Point from Bottom to Top Layer of Conical Model. ....	60
Figure 4.9 Stationary Temperature Distribution Within Cooking at each Point from Both Sides to External wall body Layer of Conical Combustion Chamber Model. ....	61
Figure 4.10 Stationary Temperature Distribution Within Wall Thickness from Conical Combustion Chamber Outside Wall. ....	61
Figure 4.11: The Stationary Temperature Heat Distribution for Rectangular Combustion Chamber Model. ....	62
Figure 4.12: Stationary Isothermal Contour Distribution for Rectangular Combustion Chamber Model. ....	63
Figure 4.7 Stationary Temperature Distribution Within Water at each Point from Bottom to Top Layer of Rectangular Combustion Chamber Model. ....	63
Figure 4.14 Stationary Temperature Distribution Within Cooking at each Point from Both Sides to External wall body Layer of Conical Combustion Chamber Model. ....	64
Figure 4.15 Stationary Temperature Distribution Within Wall Thickness from Rectangular Combustion Chamber to Outside Wall Surface. ....	64
Fig 4.16 Temperature Heat Distribution for Cylindrical Combustion Chamber/ Time Dependent. ....	66
Fig 4.15 Isothermal Contour Distribution for Cylindrical Combustion Chamber/ Time Dependent. ....	66
Fig 4.16 Time Dependent Graph of Temperature Heat Distribution within water Verse Time.. ..	67
Fig 4.17 Time Dependent Graph of Temperature Heat Distribution within Cook-pot Verse Time. ....	67
Fig 4.18 Temperature Heat Distribution for Conical Combustion Chamber/ Time Dependent.. ..	68
Fig 4.19 Isothermal Contour Distribution for Conical Combustion Chamber/ Time Dependent. ..	69
Fig 4.20 Time Dependent Graph of Temperature Heat Distribution within water Verse Time.. ..	69
Fig 4.21 Time Dependent Graph of Temperature Heat Distribution within Cooking Pot Verse Time. ....	70

Fig 4.24 Temperature Heat Distribution for Rectangular Combustion Chamber/ Time Dependent.	71
Fig 4.25 Isothermal Contour Distribution for Rectangular Combustion Chamber/ Time Dependent.	71
Fig 4.24 Time Dependent Graph of Temperature Heat Distribution within water Verse Time.	72
Fig 4.25 Time Dependent Graph of Temperature Heat Distribution within Cooking Pot Verse Time.	72
Fig 4.26 Temperature Heat Distribution within Water of the Three Different Combustion Chamber Geometries.	73
Figure 4.27 Temperature Heat Distribution within Cooking Pot of the Three Different Combustion geometry Models.	74
Fig 4.28 Temperature Heat Distribution within Water of the Three Different Insulators.	75
Fig 4.29 Temperature Heat Distribution within Cook Pot of the Three Different Insulators.	76
Fig 4.30 Temperature Heat Distribution within Cook Stove Wall Thickness for the Three Different Insulators.	77
Fig A1.6.1 Data recording on field (a), final manufactured stove model (b), and construction chamber model (c) of Community Stove at RP IPRC Tumba Colledge.	81

## List of Tables

Table 3.1 Data collected from the Community Cook-Stove on the field at RP Tumba College..	16
Table 3.2 Material Properties of Stainless-Steel Chromium Steel.	17
Table 3.3 Material Properties of Glass Wool Batt Insulator.	17
Table 3.4 Material Properties of Air.	17
Table 3.5 Material Properties of Alumino Silicate Fire Clay Brick Insulator.	18
Table 3.6 Material Properties of Water.	18
Table 3.7 Material Properties of Swamp Clay Insulator.	18
Table 3.8 Material Properties of Glass Fiber Blanket.	18
Table 3.9 Community Cook-Stove with Mesh type of Cylindrical, Conical and Rectangular Combustion Chamber Models.	50
Table 3.10 Mesh Statistics for biomass cookstove model.	51
Table 3.11 Experimental Temperature results of the previous Cook-Stove at RP Tumba College	52
Table 4.1 Different temperature of insulators used for sensitivity analysis on cylindrical geometry.	75

## **Acknowledgements.**

I would like to express my deepest gratitude and appreciation to all those who have supported me throughout the journey of completing this thesis. Without their guidance, encouragement, and assistance, this work would not have been possible.

In collaboration with Dr. BINAMA Maxime and Dr. Antoine MUSENGIMANA, thesis have conducted. In addition, I would like to express my sincere thanks to my supervisor and my co-supervisors for their exceptional motivation and unwavering support throughout this endeavor. From both industry expertise and academic expansive knowledge of my supervisors, have providing a multidimensional perspective to enrich this study research.

I would also like to acknowledge my family for continuous motivation, my brother Eng. Enock MBONIMPA, my former company manager Msc. Celestin NGENDABANGA, Mr. Gabriel IRAGUHA, as they have also helped me by providing their insights into different opinions critical feedback of my thesis and motivation. I acknowledge the administration of RP IPRC Tumba College for allowing me in data recoding for the research study.

My studies at University of Rwanda and life here in Rwanda has been possible with the partial scholarship I received from African Center of Excellence in Energy for Sustainable Development (ACE-ESD) College of Science and Technology University of Rwanda, I am indebted to institution for helping me to understand Engineering gaps and their respective solutions.

Moreover, I would like to express my heartfelt appreciation to my family, my friends, and my fellow classmates in Cohort 5 at the African Center of Excellence in Energy for Sustainable Development (ACE-ESD) College of Science and Technology University of Rwanda, whose constant support has consistently motivated and propelled me towards continuous improvement.

## **Dedication.**

To our parents, siblings, colleagues, supervisors, African Center of Excellence in Energy for Sustainable Development (ACE-ESD) College of Science and Technology University of Rwanda staff.

## **Chapter 1. Introduction.**

### **1.1 Background of the Study.**

The International Energy Agency (IEA) reports that 2.4 billion individuals globally utilize biomass for cooking, primarily employing traditional three-stone fires (TSF) in rural regions. TSF usage is linked to health concerns arising from open-fire burning and enhanced biomass cook-stoves (IBC) strive for effective combustion to minimize emissions through comprehension of these stoves entails research using experimental methods and mathematical models [1]. Approximately three billion people globally, representing 40% of the world's population, use open fire systems fuelled by biomass or coal for cooking and these traditional methods contribute to severe health issues due to indoor air pollution, causing about 4 million premature deaths annually, especially among women and children. Improved biomass cook-stoves aim to mitigate these risks through enhanced efficiency and reduced emissions, necessitating further research into their operational mechanisms and environmental impact [2].

Furthermore, the airflow within biomass cook-stoves significantly affects their performance in combustion chamber. While iterative prototyping and testing are making improvements, the effects of airflow conditions not fully understood, and adjusting the airflows rate holds substantial promise for enhancing biomass cook-stove efficiency [3].

Cook-stove design involves balancing priorities. Users might want fast ignition for efficiency, NGOs might target health benefits, governments might focus on reducing pollution, and manufacturers on affordability. A successful stove will consider these needs and combine various "design features" to meet the needs of multiple stakeholders [4].

Cook-stove designers mix and match materials to get the best properties, for instance, good insulation often crumbles easily. Therefore, designers might create a "sandwich" with a layer of insulation in the middle, protected by stronger materials on the outside, and insulation can be dangerous if it leaks, so care needed during assembly. Ideally, a cook-stove should trap heat for cooking, and Traditional fires waste most of their heat, while better designs like rocket stoves capture more, needing much less fuel. However, fig 1.1 shows how heat travels in three ways: directly touching (conduction), air currents (convection), and radiation where these play a big role

in how efficient a stove is leading how heat moves through a stove wall, highlighting how material choice and design impact how well a stove traps heat for cooking [4].

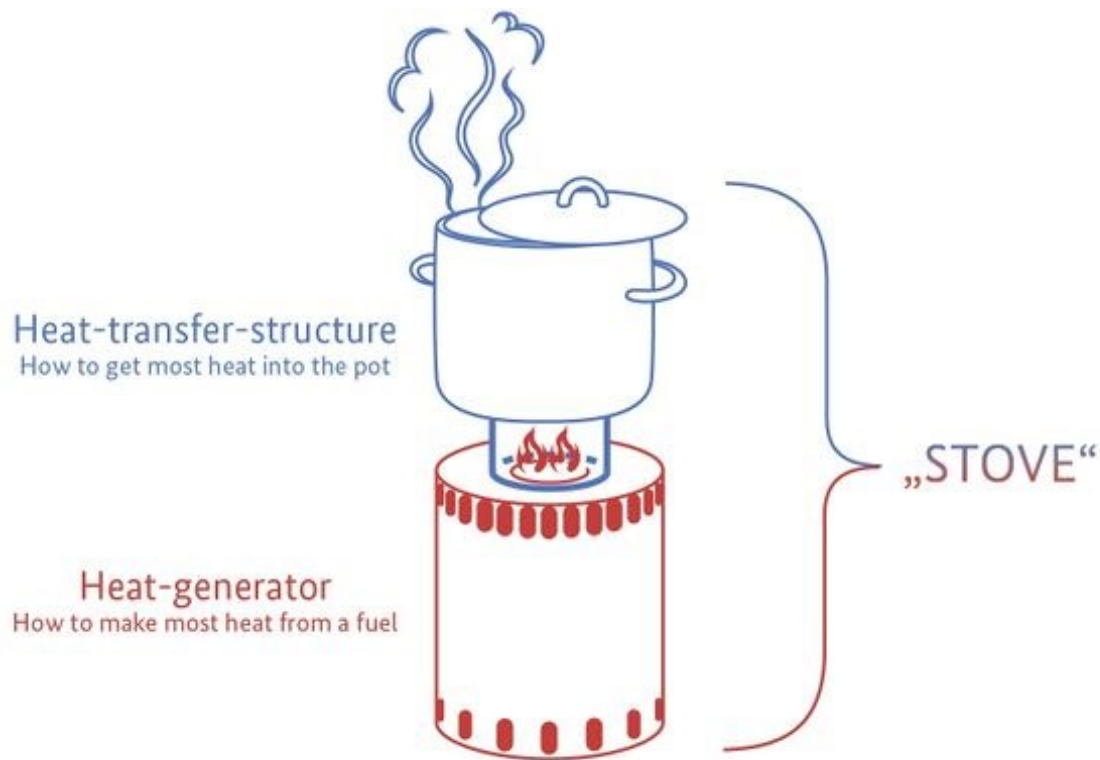


Figure 1.1 Biomass cook stove.

The efficient use of energy and heat transfer characteristics of cook-stove, particularly under different atmospheric pressures establish a three-dimensional numerical calculation and theoretical analysis model of impact flame heat transfer for integrated cook-stove widely used in China and investigates how decreased atmospheric pressure affects combustion intensity, flame combustion temperature, heat transfer rate, and total thermal efficiency of the stove.

## **1.2 Problems statement.**

A significant issue on much presence of heat losses often arises from utilization of cooking fuels as dry firewood that produces much heat comes from combustion chamber geometry design of manufactured community cook-stove at IPRC Tumba College. The improper balancing of heat transfer between the cooking fuels and the cook-stove leads to excessive fuel consumption, contributing to higher operational costs and environmental impacts.

## **1.3 Main Objective.**

The primary objective of this study is to develop an improved Community Cook-stove that minimizes heat loss and optimizes fuel efficiency. This will be achieved by enhancing heat transfer processes within the combustion chamber, ensuring that more energy from the fuel is effectively utilized for cooking. The goal is to create a stove design that not only conserves fuel but also reduces emissions, providing a sustainable and cost-effective solution for large-scale cooking needs in community and institutional settings.

## **1.4 Specific Objectives.**

- Analyse how different design elements (such as insulation and chamber geometry) influence heat transfer efficiency.
- Design and simulate various configurations of the combustion chamber to optimize heat transfer efficiency.
- Develop models with improved efficiency (e.g., improved insulation, chamber geometry) to mitigate these losses and enhance overall stove efficiency.
- Evaluate the practical implications of stove design modifications on cooking performance metrics (e.g., cooking uniformity temperature) and selection of best model.

## **1.5 Research Questions.**

Cooking stoves in low-income regions are essential but often inefficient, wasting fuel, causing environmental, and health issues due to incomplete combustion. This highlights the urgent need

for better stove designs that improve heat transfer efficiency and combustion stability, addressing both energy conservation and environmental concerns.

Here are corresponding research questions being reflected on the research objectives such as:

- How do different design elements within the combustion chamber (such as insulation materials and chamber geometry) affect heat transfer efficiency in cooking stoves?
- How can the design of combustion chamber optimized to maximize heat transfer efficiency while ensuring stable combustion of various cooking fuels?
- What design modifications would implemented to develop a stove model with improved efficiency that effectively mitigates heat losses and enhances thermal performance?
- How do design modifications aimed at improving heat transfer efficiency impact cooking performance metrics such as fuel consumption, and cooking temperature uniformity in real-world settings?

### **1.5 Research Justification.**

Recent Studies have done on the improved biomass cook stoves as long-duration energy dependence to the use of biomass cooking fuel. The energy resources, often priced beyond the reach of many challenges, designing and simulating an improved institutional cook-stove presents a critical opportunity to address not only energy efficiency but also public health concerns. Traditional cooking methods often rely on inefficient stoves that consume large amounts of biomass, leading to deforestation and increase greenhouse gas emissions due to heat losses, while also posing health risks.

This study justify the need for developing an improved community cook-stove by focusing on energy efficiency, and environmental sustainability. By incorporating advanced modeling and simulation techniques, the design will also consider affordability and accessibility, ensuring that the final product can be widely adopted in resource-limited settings. This improved cook-stove not only aligns with global efforts to reduce energy consumption and carbon emissions but also directly contributes to the well-being of communities by providing a safer, more efficient cooking solution.

## **1.6 Scope and Limitations of the Study.**

### **1.6.1 Scope.**

This study aims to improve the thermal performance of biomass cook-stoves by identifying and addressing major heat loss zones within the combustion chamber. It integrates computational modeling, particularly Computational Fluid Dynamics (CFD), to simulate and analyze different design configurations. The research explores how insulation, air intake, and combustion chamber geometry influence heat transfer. A key objective is to propose design modifications that reduce thermal losses and enhance energy efficiency. By examining heat transfer mechanisms in detail, the study provides a scientific basis for optimizing combustion chamber performance. Insulation materials also evaluated for their thermal performance and integration within the design. This research serves as a foundation for developing more effective and sustainable cookstove designs, offering practical insights that can to guide future prototypes and implementations in resource-limited settings, where fuel efficiency and thermal performance are critically important.

### **1.6.2. Limitations.**

Despite its focus on improving cookstove performance, the study faces several limitations. CFD simulations, while powerful, require high computational resources and expert knowledge, limiting accessibility for broader adoption or replication. The accuracy of the simulations is also dependent on assumed boundary conditions and material properties, which may not perfectly mirror real-world conditions. Additionally, insulation materials—though essential for heat retention—can pose health and safety risks if not properly handled, making practical implementation more complex. The scope of this research is confined to thermal efficiency and does not encompass other key performance aspects such as emissions, durability, or user experience. Moreover, the study is simulation-based and lacks immediate experimental validation. The effectiveness of proposed improvements will therefore require physical testing and long-term evaluation to confirm their performance under actual cooking conditions, including user variability and environmental factors not captured in the simulations.

## **1.7 Thesis Organization.**

This thesis proposal contains three main chapters; which are the following:

- Chapter 1 introduces the topic and provides a background of the work, Problem Statement and the main objective and specific objective of the study. Research questions, research Justification and scope of the study highlighted in this section.
- Chapter 2 provides an Overview on Cook-stove Designs, Theoretical Literature Review; Similar Works have been highlighted in this section. This section also contains the Summary of Previous Works and Gap Identification, and the chapter conclusion.
- Chapter 3, the methodology section provides the previous methods used by other researchers, and Proposed Method such as Design Conceptualization and simulation using COMSOL Multi-physics software.
- Chapter 4, the results sections highlight the computational simulation, graphs and Simulation Analysis for Design. Furthermore, the discussion section provides the interpretation and selection of the best combustion chamber model geometry for Community cook stove.
- Chapter 5, the conclusion section highlights the factors that lead best selection model of combustion chamber geometry of the good thermal efficiency and the recommendations for further research development.

## Chapter 2. Literature Review.

### 2.1 Overview on Cook-stove Designs.

New biomass cook-stoves, especially those that force air in (forced draft) figure 2.1, seem to burn cleaner and waste less fuel. However, real-world use is not always as good as lab tests and Computer simulations (CFD) can help design better stoves without needing as many tests [3].

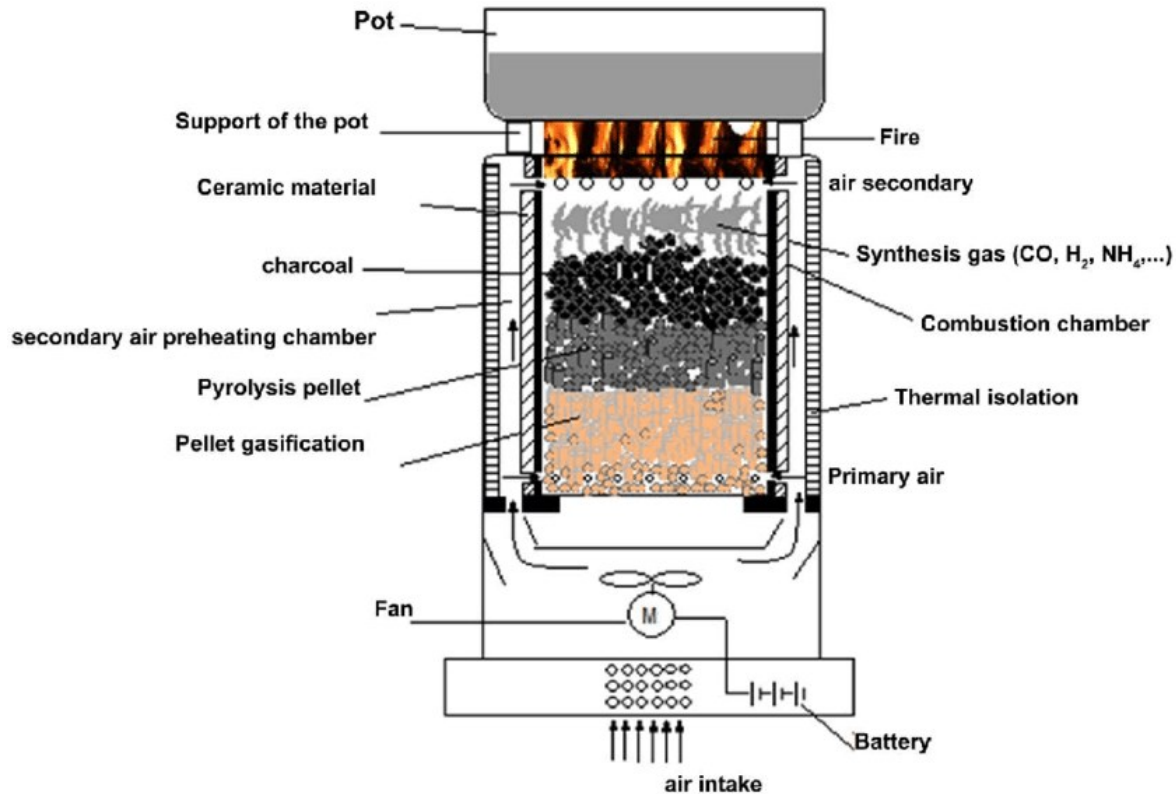
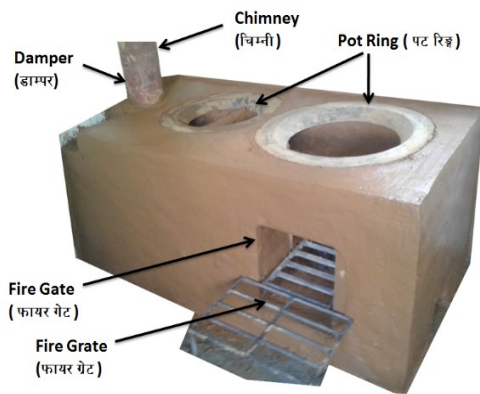


Fig 2.1 Improved-cook-stove-with-forced-air-biomass-gasification.

Traditional cook-stoves are inefficient and emit harmful pollutants, causing severe health issues and environmental damage due to lack of the advancements in cook-stove technology to enhance efficiency and reduce emissions without disrupting local cultures [5]. Previous improvements have been made through iterative prototyping and testing, but the full potential of airflow conditions has not explored.



(A)



(B)

Fig 2.2 (A): IIC Stove-World Food Program; (B): Ecocina Stove

High Moisture in the fuel reduces the efficiency and temperature of combustion, Cook-stove efficiency is like comparing what you get out to what you put in. We put in fuel, which burns to create heat. This heat cooks food shown by figure 2.2, but some escapes. Thermal efficiency is simply the percentage of heat used for cooking compared to the total heat produced by the fuel. Getting a fire going starts with heating the fuel with something external. With enough air, the fuel catches fire once it gets hot enough (around 300-500°C for wood, 350-400°C for charcoal). As long as there is air and the burning area stays hot, more fuel will light and keep burning steadily [4].

To enhance energy efficiency and lower emissions from biomass cooking stoves, the design of the combustion chamber is crucial. This chamber, where fuel burns to produce heat, significantly affects the stove's overall performance, including heat transfer, fuel use, and cooking efficiency. Given that biomass stoves remain a primary cooking method in many rural and developing areas, improving their efficiency is vital for addressing environmental and health issues.

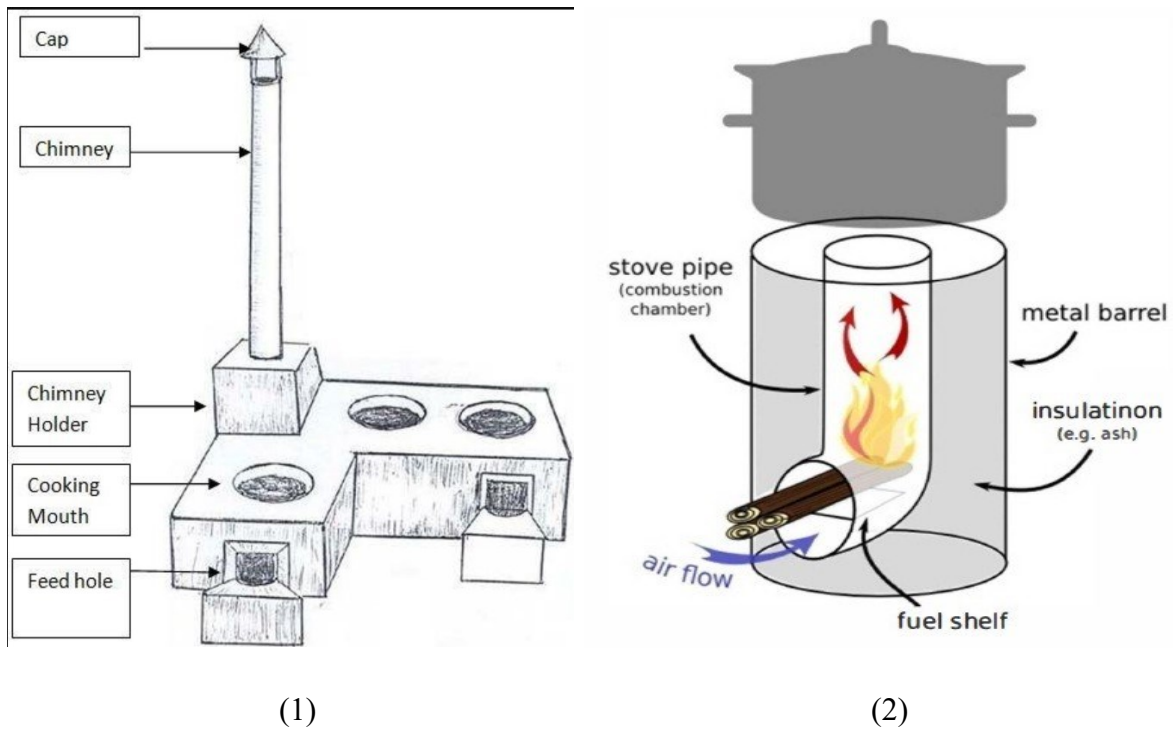


Fig 2.3 (1): Improved Double Mouth Cooking Stove Coupled with Single Mouth Cooking Stove having one common Chimney (Courtesy: IDCOL) and, (2): The National Biomass Cook-stoves Initiative (NCI)

Stove design often follows an iterative process involving building prototypes shown in figure 2.0.3, testing, and refining until achieving an acceptable design and this method is resource-intensive, time-consuming, and lacks insight into the physics of cook-stove performance where Computational modelling can complement this process, reducing time and resources and providing detailed physical insights for better stove designs. It allows the study of geometric parameters on combustion and mixing without costly and time-consuming testing where few studies have focused on cook-stove modelling as in fig 2.4, with fewer than thirty of the five hundred articles published in the last thirty years addressing it [6].

## **2.2 Basic Biomass Cook-Stove Concept.**

Early models, like Baldwin's heat transfer model, predicted the impact of channel dimensions on heat transfer but lacked experimental validation [7]. Agen-broad et al. developed a Bernoulli equation-based model to predict flow rates, validated with measurements for various fire-powers [8]. Shah and Date created a four-zone thermochemical model to predict thermal efficiency and combustion product composition, considering geometry and fuel characteristics [9]. CFD models are more computationally demanding but handle complex geometries with fewer assumptions, providing detailed heat transfer, mixing, and combustion information. For instance, Burnham-Slipper developed a CFD model including combustion in the gas phase, though it simplified geometry and neglected soot radiation [10].

## **2.3 Similar Works.**

Several critical factors essential using modelling and simulation for Developing an improved cook-stoves designs necessitates a comprehensive understanding of several empirical insights from existing research. These insights span across airflow optimization, heat transfer mechanisms, material properties, geometric design, and environmental conditions.

CFD simulations have demonstrated the critical role of airflow in enhancing biomass cook-stove performance where Proper airflow management can significantly improve combustion efficiency and reduce emissions. [3] Showed that varying airflow conditions can lead to different performance outcomes, highlighting the need for precise airflow control, the theoretical and numerical investigation of heat transfer characteristics under different atmospheric pressures emphasized how atmospheric pressure affects combustion intensity, flame temperature, and overall thermal efficiency, with efficiency dropping by 7.5% at lower pressures.

The selection of materials is crucial for achieving a balance between insulation and durability. Insulating materials such as low-density clay and porous stones, while effective in retaining heat, often lack the necessary strength and durability, requiring a sandwich structure with more durable materials like refractory ceramics for high temperatures and exterior cladding for strength [3].

The thermal performance and heat storage behaviour of the three-pot improved cook-stove illustrate how integrating materials with high heat storage capacity, such as bricks, sand, and

cement, can stabilize cooking temperatures and improve overall efficiency [2]. Studies have shown that smaller channel gaps and longer channel lengths can enhance heat transfer to the cooking pot. The three-pots improved cook-stove design utilize heat more effectively by allowing simultaneous cooking on multiple pots, reducing cooking time and fuel consumption by nearly 60% compared to traditional designs through Geometric modifications in the combustion chamber [2].

The CTARA stove model which includes a cylindrical clay outer body, a conical clay enclosure, a grate, and a metal enclosure, have developed by Rahul Shah [9] the combustion space is divided into four zones, each treated as a well-stirred reactor to simplify the modeling process. Rahul Shah [9], made the assumptions and simplifications in developing the CTARA stove describes how the air flow in the stove, driven by buoyancy forces, determines the wood burning rate and overall efficiencies and calculating the wood burning rate using a steady-state approach and introduces the Stefan-Flow model to estimate burning flux.

Validation through standardized testing methods such as the Water Boiling Test (WBT) and Energy Utilization Test (EUT) is essential for confirming the efficacy of design modifications, and these tests provide a comprehensive evaluation of cook-stove performance, including thermal efficiency, pollutant emissions, and practical usability [5].

Improvements by Phusrimuang and wongwuttanasatian [11] showed a new steaming stove design featuring double-wall construction filled with rice husk ash for insulation and enhance heat transfer by prolonging the path of exhaust gases. In addition, the new stove showed a thermal efficiency of 21.21%, compared to 15.17% for the conventional stove, demonstrating a significant improvement where it measured using a standard water-boiling test with Eucalyptus wood as fuel [11].

By integrating these empirical insights, researchers can develop institutional cook-stove designs that are efficient, durable, and adaptable to different environmental conditions. This comprehensive approach ensures that the cook-stoves not only meet thermal performance requirements but also address practical issues related to material durability and usability in diverse atmospheric pressures.

## **2.4 Summary of Previous Works and Gap Identification.**

Most of biomass cook-stove designs emphasizes in detailed analysis and developing both Water Boiling Tests (WBT) and Energy Utilization Tests (EUT) to evaluate biomass cook-stove performance, which is crucial for improving efficiency and reducing emissions. Furthermore, the use of Computational Fluid Dynamics (CFD) allows for a detailed understanding of the heat transfer, mixing, and combustion processes within the cook-stove. Moreover, Combining CFD analysis with experimental validation strengthens the reliability of the findings and provides a solid foundation for practical applications. Through optimization to enhance energy efficiency and reduce emissions, and for detailed description of the experimental setup and methodologies provides a clear understanding of how the tests conducted, enhancing reproducibility.

Accordingly, the CFD simulations are computationally intensive and may not be accessible to all researchers or practitioners, limiting the broader application of the findings, and the complexity of the experimental setup and procedures may pose challenges for replication and practical implementation in resource-limited settings.

The valuable insights into the optimization of biomass cook-stove performance through improved cook-stove design models, and effectively combining computational modelling with experimental validation, providing a robust foundation for further research and development. However, challenges related to the complexity and computational demands of their methodologies.

It reviews existing literature, noting a lack of detailed modelling for heat and mass transfer processes in stoves.

## **Chapter 3. Methodology.**

### **3.1 Previous Methods.**

In previous research studies provides a systematic approach to evaluating the improvements in stove design and their impact on efficiency, cost, and environmental sustainability [11]. The Research study [11] shows experimental setup (where the study involves setting up an experimental biomass stove with a specific design tailored for the steaming process). The thermal efficiency measurement (where the thermal efficiency of the stove is measured by comparing the amount of fuel consumed to the amount of energy transferred to the steaming process); and design modifications (where the stove design is modified and tested iteratively to achieve improvements in thermal efficiency). Furthermore, the study offers data collection (where data on fuel consumption, temperature, and steaming times collected to evaluate the stove's performance); and comparison (where the performance of the improved stove is compared with traditional stove designs to assess the improvements).

The study of [12] examines theoretical modeling (where it used theoretical models to investigate the heat transfer characteristics of a cook-stove under different atmospheric pressures) and Numerical Simulation (where numerical methods employed to solve the heat transfer equations and analyze the impact of varying atmospheric pressures on the stove's performance). Furthermore, the study offers comparative analysis (where the results from the theoretical models have compared against empirical data or previously established models to validate the accuracy and reliability of the predictions).

The study of [2] shows experimental testing (where the study involved experimental testing of the thermal performance and heat storage behavior of a three-pot improved cook-stove) and temperature measurement (where various temperature sensors have placed at strategic locations within the stove to monitor heat distribution and storage over time). Moreover, the study offers performance metrics (where the stove's performance was evaluated based on metrics such as heat transfer efficiency, fuel consumption, and cooking time) and comparative analysis (where the results have compared to those of traditional single-pot stoves to highlight the improvements made by the three-pot design).

The study of [9] emphasizes on thermochemical modeling (where this study developed a steady-state thermochemical model to simulate the combustion, heat transfer processes within a wood-burning cook-stove). And zonal analysis (where the combustion chamber was divided into multiple zones, each with specific thermochemical properties due to the model predicted the temperature distribution, composition of combustion products, and thermal efficiency for each zone). Furthermore, the study offers validation (where the model's predictions have validated through experimental data or comparison with existing models). Sensitivity analyses have conducted to assess the impact of different design parameters on the stove's performance and iterative refinement (where the model was refined iteratively based on discrepancies between the model's predictions and empirical observations).

The approach of the design and modeling process, an improved community cook-stove have developed that is efficient, durable, and suitable for diverse environmental conditions [3]. The study of [3], examines Computational Fluid Dynamics (CFD) Modeling where the study utilized CFD to simulate airflow, combustion, and heat transfer within a forced draft biomass cook-stove, and Mesh Generation where a detailed 3D model of the cook-stove was created, and a computational mesh was generated to facilitate the CFD simulations. Furthermore, the study offers Boundary Conditions where the simulation was run under various airflow conditions, with boundary conditions set to mimic real-world operating scenarios, and Validation where the CFD results were validated against experimental data to ensure accuracy and also the study explored the effects of different airflow configurations on stove performance, including temperature distribution, combustion efficiency, and emissions.

The Research study [13], emphasizes on the experimental design, where the study designed an Energy Utilization Test (EUT) to evaluate the performance of a biomass cook-stove under different airflow conditions, and controlled testing where a series of controlled experiments have conducted to measure fuel consumption, cooking time, and thermal efficiency under varying airflow settings. Furthermore, the study offers optimization (where the study aimed to develop an optimal airflow "recipe" that maximizes energy utilization and minimizes fuel wastage due to the airflow rates were systematically varied, and their impact on stove performance was recorded). Moreover, Data Analysis (where the experimental data analyzed to identify the airflow conditions that yielded the

best overall performance in such way that the findings used to guide design improvements for the cook-stove).

The literature review has described some of which numerous techniques that have used to simulate and study the behavior of cook stove models. In addition, most simulation software are the following the Computational Fluid Dynamics (CFD) Software (ANSYS Fluent; Open FOAM and COMSOL Multiphysics) and Thermodynamic Analysis Software (such as MATLAB/Simulink and EES (Engineering Equation Solver). Finite Element Analysis (FEA) Software (such as ABAQUS and SolidWorks Simulation), 3D Modeling and Design Software (such as SolidWorks and AutoCAD), Optimization Software (such as MODEFRONTIER and MATLAB), and Emission and Environmental Impact Modeling (such as GaBi and SimaPro) are adopted tools. Those software tolls applied to work together to create a comprehensive simulation environment for modeling, analyzing, and optimizing cook-stove designs, ensuring they are efficient, cost-effective, and environmentally friendly.

### 3.2 Data Collection Sources and Research Instrument.

Observation method through instrumentation have used to collect information from water boiling test standards. The different recording instruments used are digital Thermometers (such as ), meter rule, pens, papers as shown in fig 3.1, fig 3.2 and fig 3.3.

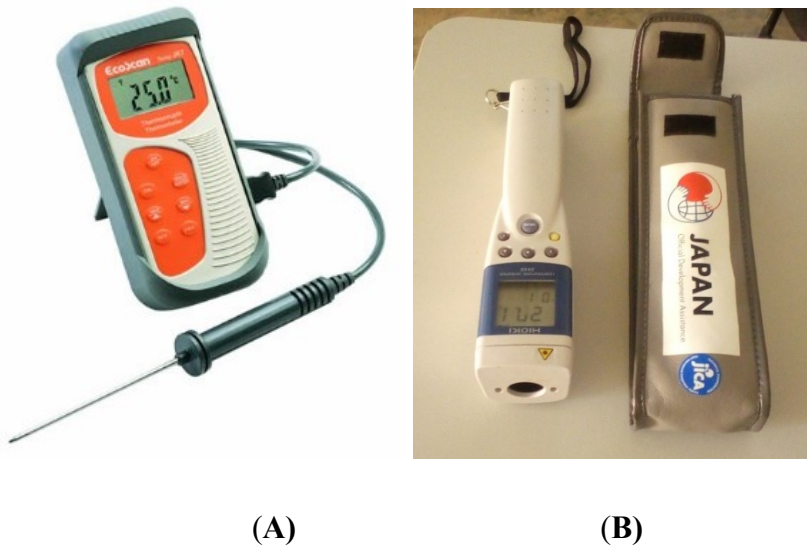
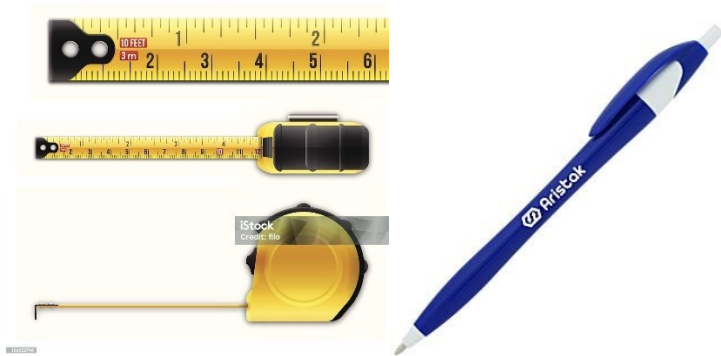


Figure 3.1 (A): Hioki Temperature Hi-Tester 3443; (B): EUTECH Eco-Scan Temp 6.



(A)

(B)

Figure 3.2: (A): Meter Rule; (B): Marker Pen Instrumentations.

Through the data collecting using the instruments on the working Cookstove model are described below: the weight of dry fire wood as , burning rate of firewood as , Burning Power Output of firewood as 1328.1 W, heat source of firewood as 2604.1 W/m<sup>2</sup>, cook-stove height of 960mm, cook-stove inner diameter of 806mm, cook-stove outer diameter of 1210mm and thickness of 120mm. The outer surface body temperature found to be 62.5 degC as shown in the table 3.0.1 below.

Table 3.1 Data collected from the Community Cook-Stove on the field at RP Tumba College.

NO	TIME (min)	Temperature in water (degC)	Temperature on outside Stove body (up) (degC)	Temperature on outside Stove body (Down) (degC)	Temperature on Bottom surface of Stove (degC)
1	0	50	30.9	40.1	57.2
2	10	53.7	33.1	42.7	68.4
3	20	69	35.3	45.9	72.5
4	30	79.3	39.8	49.3	83.5
5	40	88.8	43.2	52.4	91.6
6	50	93.6	45.4	58.8	99.3
7	56	95.8	52.8	65.7	144
8	60				

### 3.3 Design Conceptualization and Research Design models.

#### 3.3.1 Material Type and Properties Used for Community Cook stove.

Through CAD modeling design, several materials used in the Concepts for developing community cook-stove models are usually on the market. Here is material made of the community cook-stove model that are glass wool batt insulator, Stainless Steel Chromium Steel, Alumino-silicate fire clay brick insulator, air gap insulator, Glass fiber blanket insulator, and swamp clay insulator.

##### 1. Stainless Steel Chromium Steel.

Table 3.2 Material Properties of Stainless-Steel Chromium Steel.

Name	Value	Unit
Density	7850	kg/m <sup>3</sup>
Heat capacity at constant pressure	600	J/(kg·K)
Thermal conductivity	16	W/(m·K)

##### 2. Glass Wool Batt.

Table 3.3 Material Properties of Glass Wool Batt Insulator.

Description	Value	Unit
Density	22	kg/m <sup>3</sup>
Heat capacity at constant pressure	850	J/(kg·K)
Thermal conductivity	0.04	W/(m·K)

##### 3. Air.

Table 3.4 Material Properties of Air.

Description	Value	Unit
Thermal conductivity	0.026	W/(m·K)
Heat capacity at constant pressure	1005	J/(kg·K)
Density	1.225	kg/m <sup>3</sup>

#### 4. Alumino-silicate fire clay brick.

Table 3.5 Material Properties of Alumino Silicate Fire Clay Brick Insulator.

Description	Value	Unit
Density	1900	kg/m <sup>3</sup>
Thermal conductivity	1.5	W/(m·K)
Heat capacity at constant pressure	1000	J/(kg·K)

#### 5. Water.

Table 3.6 Material Properties of Water.

Description	Value	Unit
Heat capacity at constant pressure	4181	J/(kg·K)
Density	1000	kg/m <sup>3</sup>
Thermal conductivity	0.6	W/(m·K)

#### 6. Swamp Clay.

Table 3.7 Material Properties of Swamp Clay Insulator.

Description	Value	Unit
Thermal conductivity	0.8	W/(m·K)
Density	2000	kg/m <sup>3</sup>
Heat capacity at constant pressure	1000	J/(kg·K)

#### 7. Glass Fiber Blanket.

Table 3.8 Material Properties of Glass Fiber Blanket.

Description	Value	Unit
Thermal conductivity	0.03	W/(m·K)
Heat capacity at constant pressure	840	J/(kg·K)
Density	96	kg/m <sup>3</sup>

### 3.3.2 Combustion Chamber Geometry Models of Community Cook stove.

The Community cook-stove material and geometry have described by the following design variables that are:

- Combustion chamber diameter.
- Combustion chamber height.
- Gap between the shield and material sheet.
- Gap at the side edge of the cook pot,
- Gap between the shield (if included) and pot,
- Pot diameter,
- Height of the water in the pot based on its occupied volume,
- Stove combustion chamber body diameter,
- Stove body material conductivity,
- Height of the shield insulators.
- Diameter of the shield insulators.
- Thickness of the shield insulator materials.
- Shield Insulator materials conductivities.
- Specific gas constant of the shield insulators.
- Density of the shield insulators.

According to the many biomasses cook stoves, one of the main geometries being considered is the combustion chamber geometry. In combustion chamber, there will be a heat production from combustion process from burning wood as fuel type.

In this study, many different types of 3D Models designs have generated such as the cylindrical combustion chamber design model, rectangular combustion chamber design model, conical combustion chamber design model and rectangular combustion chamber design model as shown in the fig 3.4, fig 3.5 and fig 3.6.

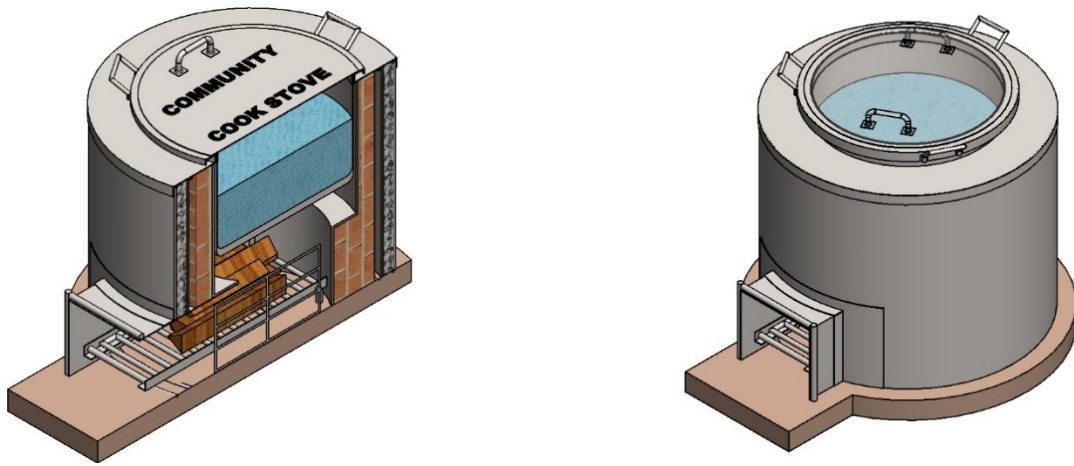


Fig 3.3 cylindrical combustion chamber deign model

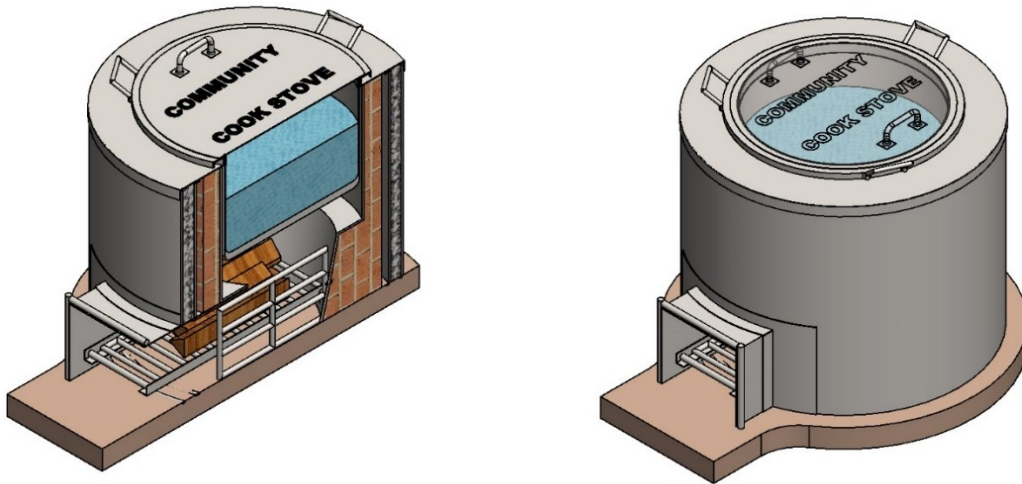


Fig 3.4 Conical Combustion Chamber Deign Model

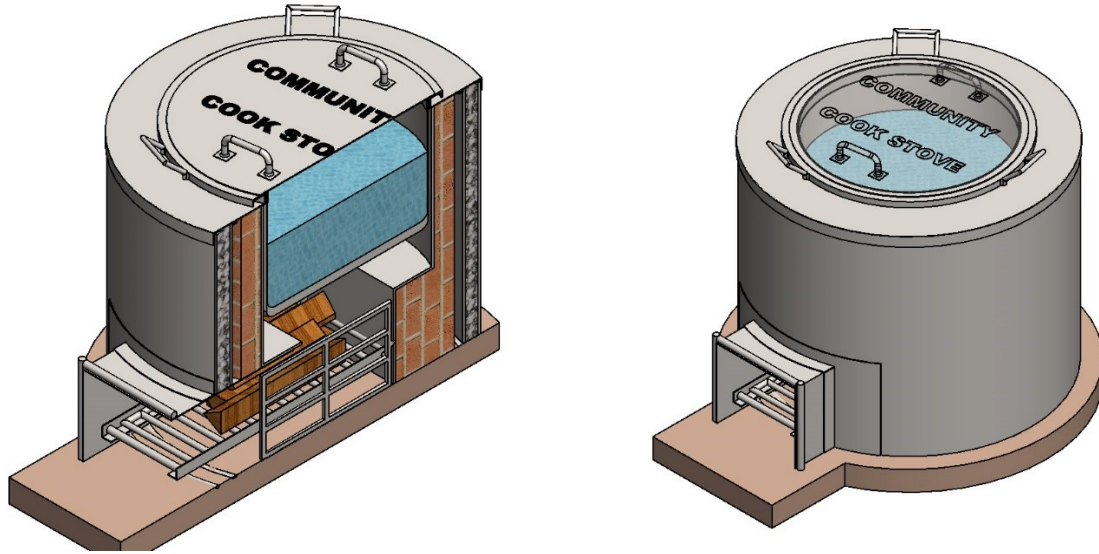


Fig 3.5 Rectangular combustion chamber design model.

### 3.3.2.1 Cylindrical Geometry Model of Community Cook stove Combustion Chamber.

Community cook stove have many material parts that composed it where some are insulators and other are metal sheets.

It has several parts that made it such as inner sheet metal, bricks, air gap, top ring cover, middle sheet metal, wool bat, outer sheet metal, stove base, entrance way, entry wood Career.

#### 1. Inner sheet metal made of Stainless-Steel Chromium Steel.

The material part that made this sheet has their material properties such as thermal conductivity (K) of 16 W/(m.K) , density ( $\rho$ ) of 7850 Kg/m<sup>3</sup>, Heat capacity at constant pressure (C<sub>p</sub>) of 600 J/(kg.K) , Electrical conductivity of 1.3[MS/m]. Moreover, the dimensions used for this Stainless-Steel Chromium Steel material have shown in the figure below and they are all in in the millimetre [mm]. The variables with dimensions are outer diameter (D<sub>Osh</sub>), inner diameter (D<sub>Ish</sub>), Height of Entrance way (H<sub>E</sub>), Width of Entrance way (W<sub>E</sub>), Height of insulator material (H<sub>Sh</sub>), and thickness of sheet metal material (t<sub>sh</sub>). Note that, the length of the sheet metal calculated as multiplying pi ( $\pi$ ) by the outer diameter as shown in the fig 3.7 below.

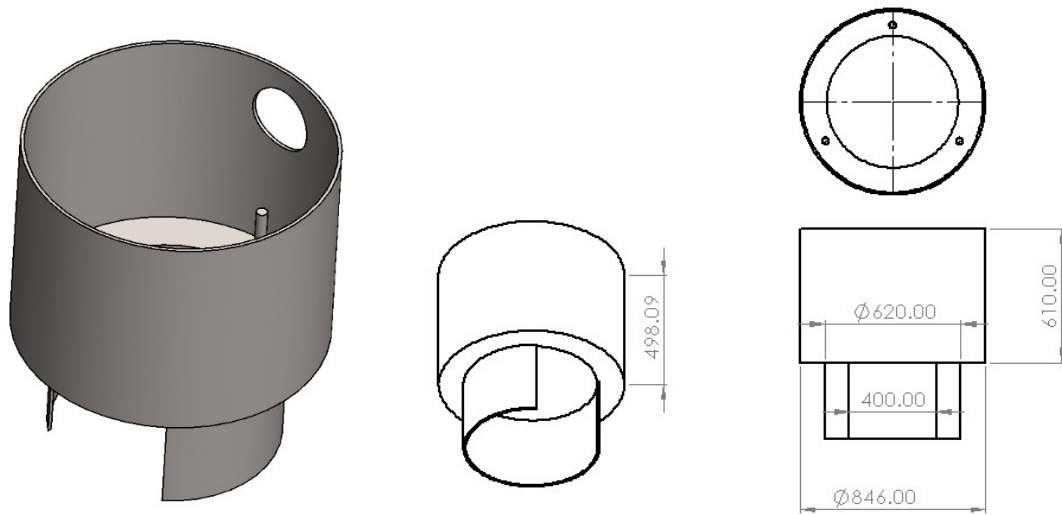


Fig 3.6 Inner Sheet Metal with its dimensions of Cylindrical Cook-Stove Model.

## 2. Insulator One made of Alumino-silicate fire clay brick [solid].

The material part that made this sheet has their material properties such as thermal conductivity (K) of 1.5 W/(m.K) , density ( $\rho$ ) of 1900 Kg/m<sup>3</sup> , Heat capacity at constant pressure (Cp) of 1200 J/(kg.K). Moreover, the dimensions used for this Alumino-silicate fire clay brick Insulator material have shown in the figure below and they are all in in the millimetre [mm]. The Alumino-silicate fire clay brick Insulator variables with dimensions are outer diameter ( $D_{OIns}$ ), inner diameter ( $D_{IIns}$ ), Height of Entrance way ( $H_E$ ), Width of Entrance way ( $W_E$ ), Height of insulator material ( $H_{Ins}$ ), and thickness of insulator material ( $t_{Ins}$ ) as shown in the fig 3.8 below.

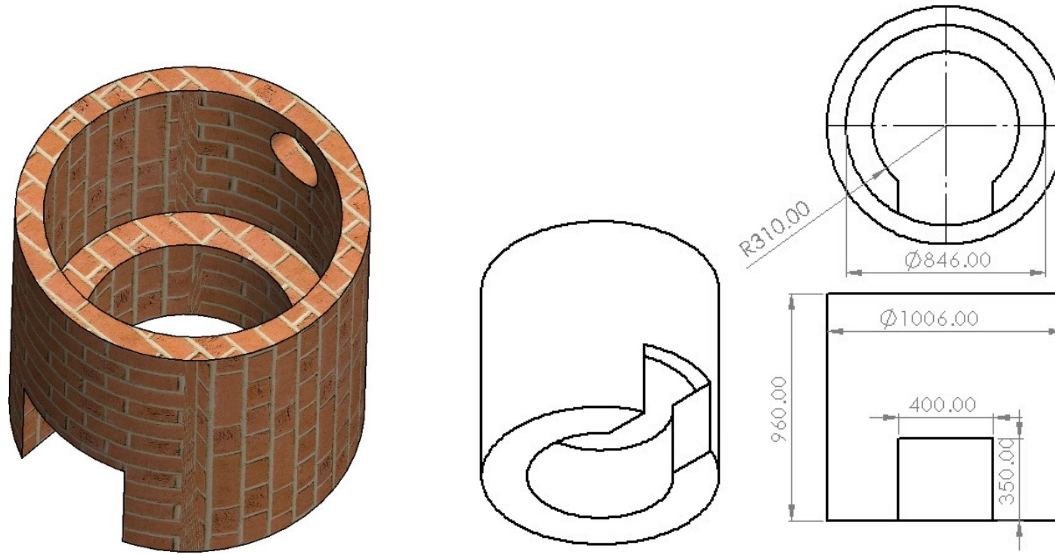


Fig 3.7 Alumino-silicate fire clay brick Insulator with its dimensions of Cylindrical Cook-Stove Model.

### 3. Insulator two made of Air Gap at 20 degrees Celsius.

The material part that are made of this insulator has the following different material properties. Those are thermal conductivity ( $K$ ) of  $0.026 \text{ W/(m.K)}$ , density ( $\rho$ ) of  $1.225 \text{ Kg/(m}^3\text{)}$ ; Heat capacity at constant pressure ( $C_p$ ) of  $1005 \text{ J/(kg.K)}$ , Electrical conductivity of  $0 \text{ [S/m]}$ , Mean molar mass of  $0.02897 \text{ kg/(mol)}$ , Ratio of specific heats of  $1.4$ , Specific gas constant of  $287 \text{ J/(kg.K)}$ . Moreover, the dimensions used for this air insulator material have described in the Cook stove model and they are all in the millimetre [mm]. The air-gap insulator variables with dimensions are outer diameter ( $D_o$ ), inner diameter ( $D_i$ ), Height of Entrance way ( $H_E$ ), Width of Entrance way ( $W_E$ ), Height of insulator material ( $H_{Ins}$ ), and thickness of insulator material ( $t_{Ins}$ ).

### 4. Middle sheet metal made of Stainless-Steel Chromium Steel

The material part that made this sheet has their material properties such as thermal conductivity ( $K$ ) of  $16 \text{ W/(m.K)}$ , density ( $\rho$ ) of  $7850 \text{ Kg/m}^3$ , Heat capacity at constant pressure ( $C_p$ ) of  $600 \text{ J/(kg.K)}$ , Electrical conductivity of  $1.3 \text{ [MS/m]}$ . Moreover, the dimensions used for this Stainless-Steel Chromium Steel material have shown in the figure below and they are all in in the millimetre [mm]. The variables with dimensions are outer diameter ( $D_{Osh}$ ), inner diameter ( $D_{Ish}$ ), Height of Entrance way ( $H_E$ ), Width of Entrance way ( $W_E$ ), Height of insulator material ( $H_{Sh}$ ), and thickness

of sheet metal material ( $t_{sh}$ ). Note that, the length of the sheet metal has calculated as multiplying pi ( $\pi$ ) by the outer diameter as shown in the fig 3.9 below.

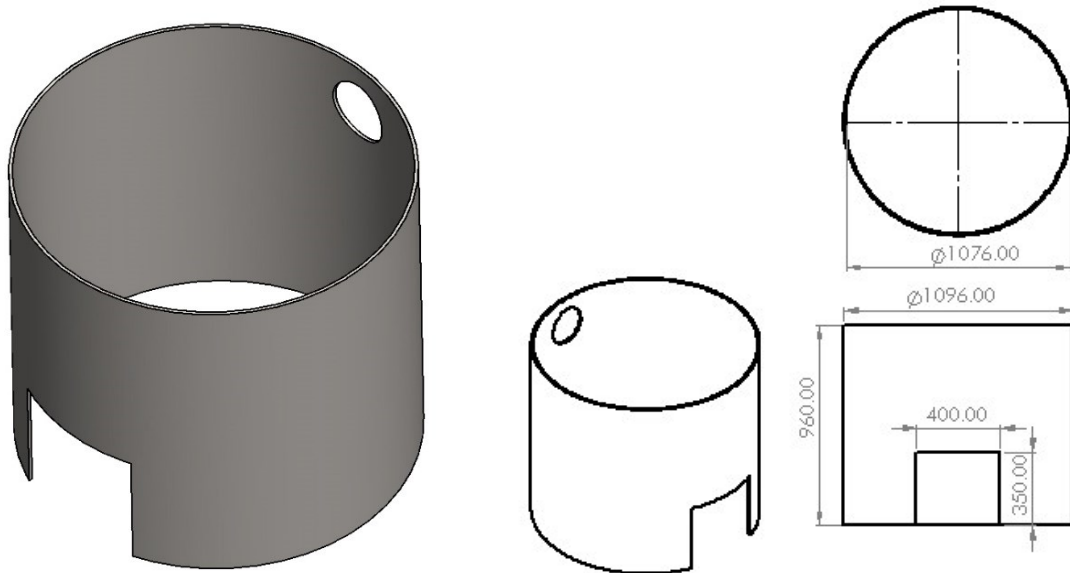


Fig 3.8 Middle Sheet Metal with its dimensions of Cylindrical Cook-Stove Model.

### 5. Insulator three made of Glass wool batt

The material part that made this sheet has their material properties such as thermal conductivity ( $K$ ) of  $0.035 \text{ W/(m.K)}$ , density ( $\rho$ ) of  $22 \text{ Kg/m}^3$ , Heat capacity at constant pressure ( $C_p$ ) of  $850 \text{ J/(kg.K)}$ , Vapor resistance factor of  $1.2$ , Diffusion coefficient of  $1e-14 \text{ m}^2/\text{s}$ . Moreover, the dimensions used for this glass wool batt insulator material have described and shown in the Cook stove model and they are all in the millimetre [mm]. The glass wool batt insulator variables with dimensions are outer diameter ( $D_{Oins}$ ), inner diameter ( $D_{Iins}$ ), Height of Entrance way ( $H_E$ ), Width of Entrance way ( $W_E$ ), Height of insulator material ( $H_{Ins}$ ), and thickness of insulator material ( $t_{Ins}$ ). Note that, the length of the glass wool batt calculated as multiplying pi ( $\pi$ ) by the outer diameter as shown in the fig 3.10 below.

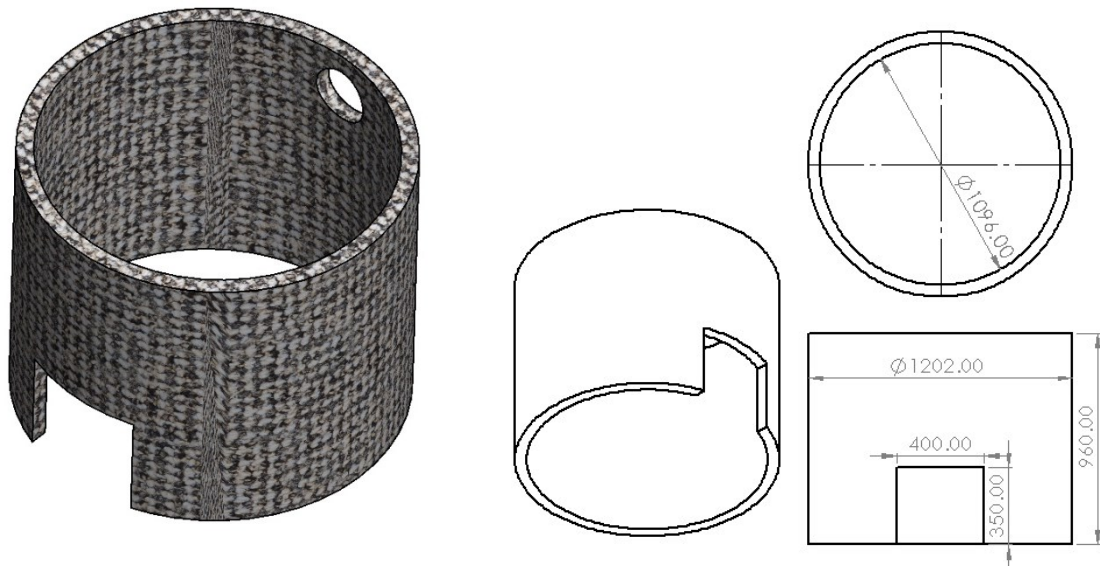


Fig 3.9 Glass Wool batt Insulator with its dimensions of Cylindrical Cook-Stove Model.

#### 6. Outer sheet metal made of Stainless-Steel Chromium Steel.

The material part that made this sheet has their material properties such as thermal conductivity (K) of 16 W/(m.K) , density ( $\rho$ ) of 7850 Kg/m<sup>3</sup>, Heat capacity at constant pressure (Cp) of 600 J/(kg.K) , Electrical conductivity of 1.3[MS/m]. Moreover, the dimensions used for this Stainless-Steel Chromium Steel material have shown in the figure below and they are all in in the millimetre [mm]. The outer sheet metal variables with dimensions are outer diameter ( $D_{Osh}$ ), inner diameter ( $D_{Ish}$ ), Height of Entrance way ( $H_E$ ), Width of Entrance way ( $W_E$ ), Height of insulator material ( $H_{Sh}$ ), and thickness of sheet metal material ( $t_{sh}$ ). Note that, the length of the sheet metal has calculated as multiplying pi ( $\pi$ ) by the outer diameter as shown in the fig 3.11 below.

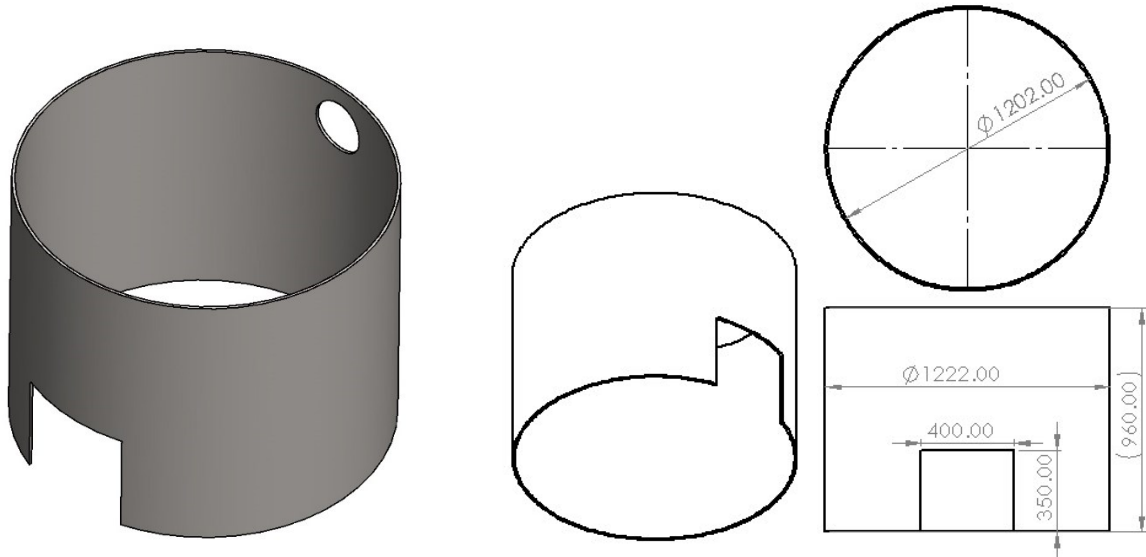


Fig 3.10 Outer Sheet Metal with its dimensions of Cylindrical Cook-Stove Model.

### 7. Entranceway sheet metal made of Stainless-Steel Chromium Steel.

The material part that made this sheet has their material properties such as thermal conductivity (K) of 16 W/(m.K) , density ( $\rho$ ) of 7850 Kg/m<sup>3</sup>, Heat capacity at constant pressure (Cp) of 600 J/(kg.K) , Electrical conductivity of 1.3[MS/m]. Moreover, the dimensions used for this Stainless-Steel Chromium Steel material have shown in the figure below and they are all in in the millimetre [mm]. The tube metal variables with dimensions are tube outer diameter ( $D_{OTb}$ ), tube inner diameter ( $D_{ITb}$ ), and the different lengths of the tube metal ( $L_{Tb}$ ). The entrance sheet variables are entrance sheet metal width ( $W_{ESh}$ ), entrance sheet metal length ( $L_{ESh}$ ), and thickness of entrance sheet metal material ( $t_{ESh}$ ). Note that, the length of the small sheet metal has calculated as multiplying pi ( $\pi$ ) by the outer diameter as shown in the fig 3.12 below.

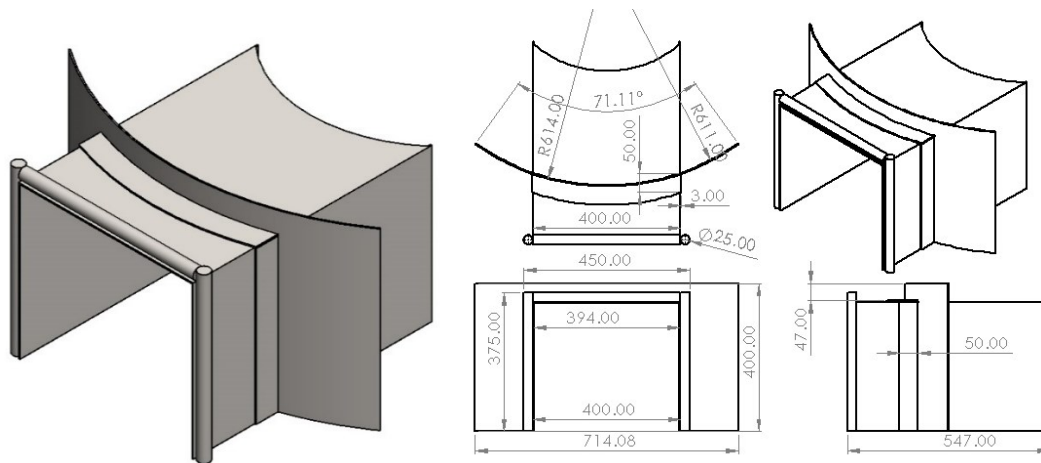


Fig 3.11 Entranceway Sheet Metal with its dimensions of Cylindrical Cook-Stove Model.

### 8. Stove Top Ring sheet metal Cover made of Stainless-Steel Chromium Steel.

The material part that made this sheet has their material properties such as thermal conductivity (K) of 16 W/(m.K) , density ( $\rho$ ) of 7850 Kg/m<sup>3</sup>, Heat capacity at constant pressure (Cp) of 600 J/(kg.K) , Electrical conductivity of 1.3[MS/m]. Moreover, the dimensions used for this Stainless-Steel Chromium Steel material have shown in the figure below and they are all in in the millimetre [mm]. The stove-ring cover variables with dimensions are stove-ring cover sheet outer diameter (D<sub>OSCSH</sub>); stove-ring cover sheet inner diameter (D<sub>ISCSH</sub>); different heights of stove-ring cover sheet metal (H<sub>SCSH</sub>), and thickness of stove-ring cover sheet metal material (t<sub>SCSH</sub>). Note that, the length of the sheet metal has calculated as multiplying pi ( $\pi$ ) by the outer diameter as shown in the fig 3.13 below.

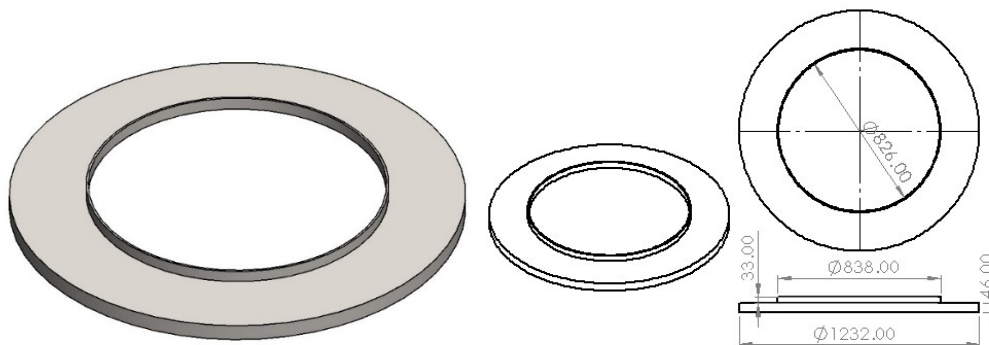


Fig 3.12 Stove Top Ring Cover Sheet Metal with its dimensions of Cylindrical Cook-Stove Model.

### 9. Entry wood Carrier metal tube made of Stainless-Steel Chromium Steel.

The material part that made this sheet has their material properties such as thermal conductivity (K) of 16 W/(m.K) , density ( $\rho$ ) of 7850 Kg/m<sup>3</sup>, Heat capacity at constant pressure (Cp) of 600 J/(kg.K) , Electrical conductivity of 1.3[MS/m]. Moreover, the dimensions used for this Stainless-Steel Chromium Steel material have shown in the figure below and they are all in in the millimetre [mm]. The tube metal variables with dimensions are tube outer diameter ( $D_{OTb}$ ), tube inner diameter ( $D_{ITb}$ ), and the different lengths of the tube metal ( $L_{Tb}$ ). The small sheet variables are small sheet metal width ( $W_{SSH}$ ), length of small sheet metal ( $L_{SSH}$ ), and thickness of small sheet metal material ( $t_{SSH}$ ). Note that, the length of the small sheet metal has calculated as multiplying pi ( $\pi$ ) by the outer diameter as shown in the fig 3.14, fig 3.15 and fig 3.16 below.

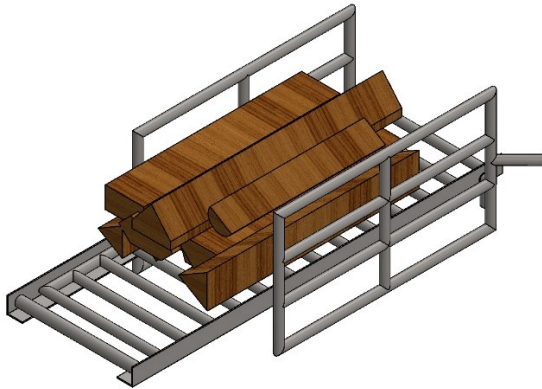


Fig 3.13 Entry Wood Carrier Sheet and Tube Metals of Cylindrical cook-stove Model.

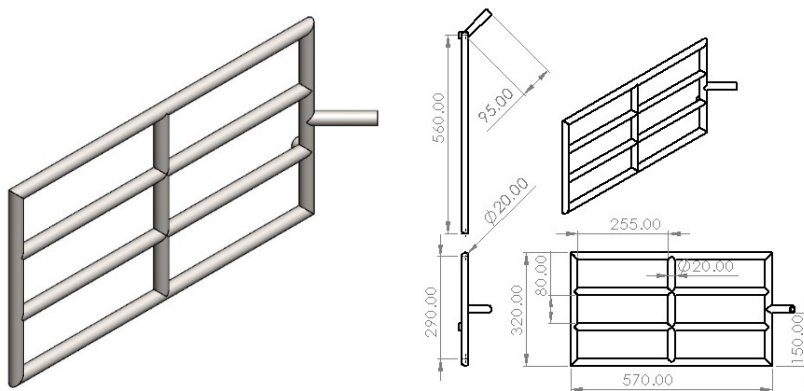


Fig 3.14 Entry Wood Carrier Side Tube Metals with their dimensions of Cylindrical Cook-Stove Model.

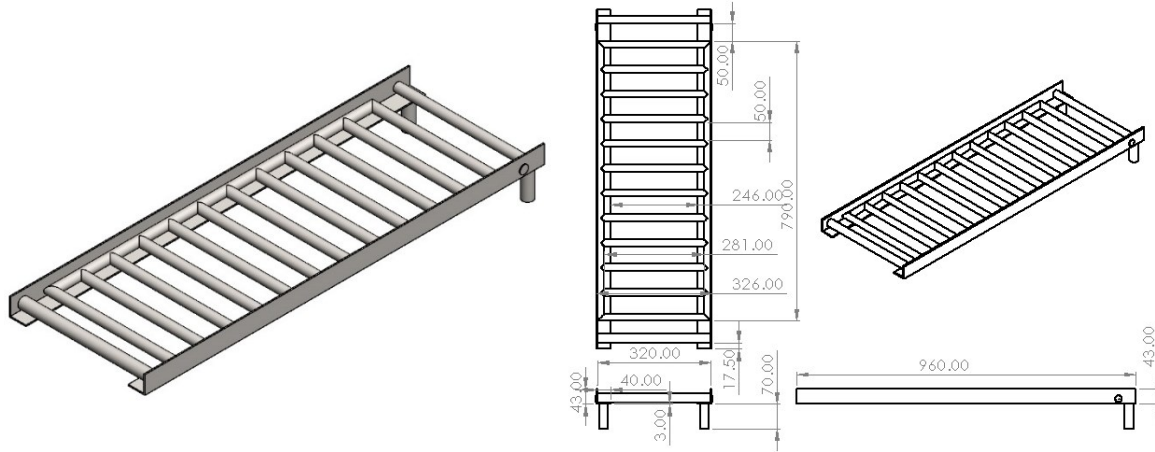


Fig 3.15 Entry Wood Carrier Frame with their dimensions of Cylindrical Cook-Stove Model.

**10. Cook-Stove Base Stand made of Alumino-silicate fire clay brick [solid].**

The material part that made this sheet has their material properties such as thermal conductivity (K) of 1.5 W/(m.K) , density ( $\rho$ ) of 1900 Kg/m<sup>3</sup> , Heat capacity at constant pressure (Cp) of 1200 J/(kg.K). Moreover, the dimensions used for this Alumino-silicate fire clay brick Insulator material have shown in the figure below and they are all in in the millimetre [mm]. The Alumino-silicate fire clay brick Insulator variables with dimensions are outer diameter ( $D_{OBase}$ ), inner diameter ( $D_{Ins}$ ), Width of stove base ( $W_{Base}$ ), Depth of stove base ( $d_{Base}$ ), and thickness of insulator material ( $t_{Ins}$ ) as shown in the fig 3.17 below.

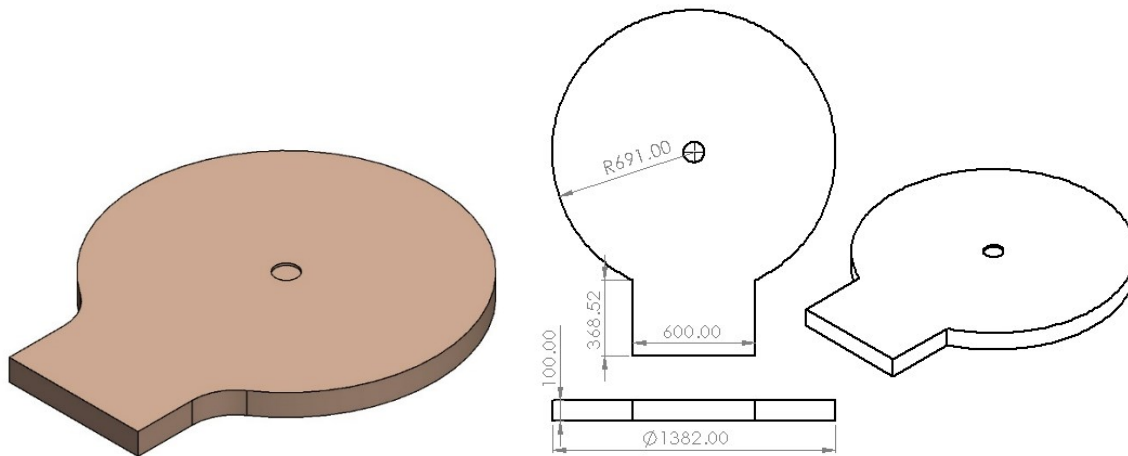


Fig 3.16 Base Stand with its dimensions of Cylindrical Cook-Stove Model.

## 11. Cooking Pot made of Stainless-Steel Chromium Steel.

The material part that made this sheet has their material properties such as thermal conductivity (K) of 16 W/(m.K) , density ( $\rho$ ) of 7850 Kg/m<sup>3</sup>, Heat capacity at constant pressure (Cp) of 600 J/(kg.K) , Electrical conductivity of 1.3[MS/m]. Moreover, the dimensions used for this Stainless Steel Chromium Steel tube metal and sheet metal have shown in the figure below and they are all in in the millimetre [mm]. The cook-pot ring cover variables are cover sheet outer diameter ( $D_{OCsh}$ ); cover sheet inner diameter ( $D_{ICsh}$ ); height of tube metal ( $H_{Tb}$ ); height of cover sheet metal ( $H_{Csh}$ ), and thickness of cover sheet metal material ( $t_{Csh}$ ). The tube metal variables are tube metal outer diameter ( $D_{OTb}$ ); tube metal inner diameter ( $D_{ITb}$ ); the length of the tube metal ( $L_{Tb}$ ). The cook-pot also have its variables such as cook-pot sheet outer diameter ( $D_{OCPSh}$ ), and cook-pot sheet inner diameter ( $D_{ICPSh}$ ), cook-pot sheet height ( $H_{CPSH}$ ). Note that, the length of the small sheet metal has calculated as multiplying pi ( $\pi$ ) by the outer diameter of sheet as shown in the fig 3.18, fig 3.19.and fig 3.20 below.



Fig 3.17 Cooking Pot of Cylindrical Cook-Stove Model.

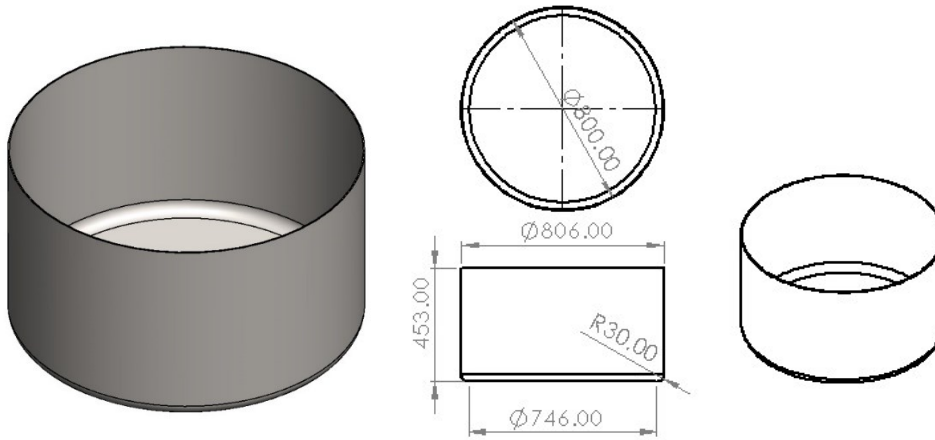


Fig 3.18 Cooking Pot Sheet Metal with its dimensions of Cylindrical Cook-Stove Model.

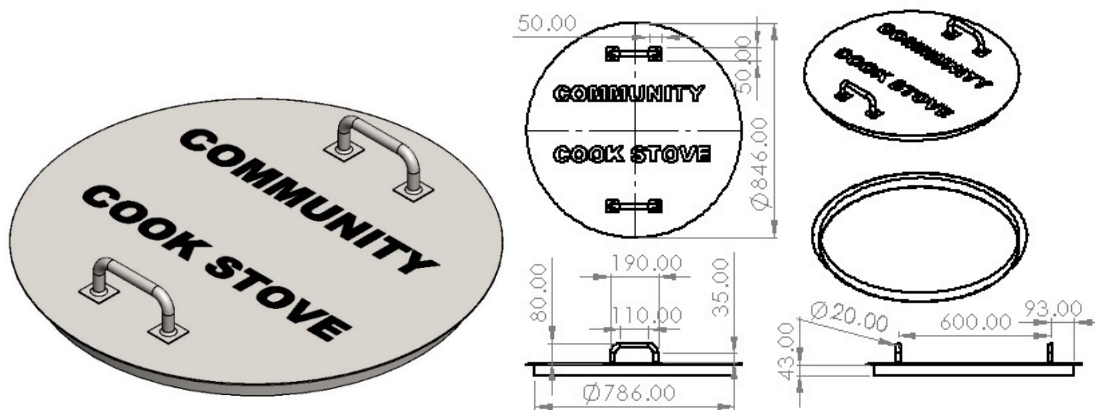


Fig 3.19 Cooking Pot Ring Cover with its dimensions of Cylindrical Cook-Stove Model.

## 12. Stove Frame Tube metal made of Stainless-Steel Chromium Steel.

The material part that made this sheet has their material properties such as thermal conductivity (K) of 16 W/(m.K) , density ( $\rho$ ) of 7850 Kg/m<sup>3</sup>, Heat capacity at constant pressure (Cp) of 600 J/(kg.K) , Electrical conductivity of 1.3[MS/m]. Moreover, the dimensions used for this Stainless-Steel Chromium Steel tube material have shown in the figure below and they are all in in the millimetre [mm]. The tube metal variables with dimensions are tube outer diameter ( $D_{OTb}$ ), tube inner diameter ( $D_{ITb}$ ), and the different lengths of the tube metal ( $L_{Tb}$ ). The small sheet variables are small sheet outer diameter ( $D_{OSSh}$ ), small sheet inner diameter ( $D_{ISSh}$ ), and thickness of small

sheet metal material ( $t_{SSH}$ ). Note that, the length of the small sheet metal has calculated as multiplying pi ( $\pi$ ) by the outer diameter as shown in the fig 3.21 below.

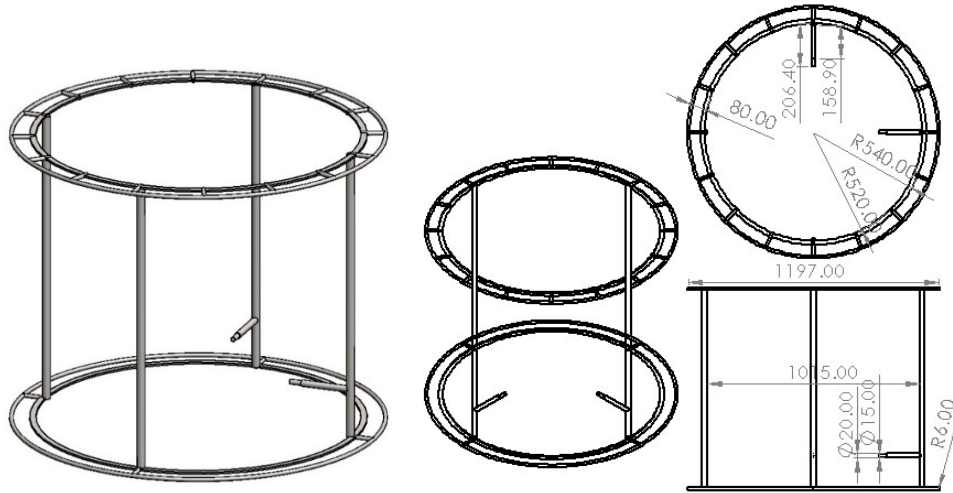


Fig 3.20 Stove Frame Tube Metal with its dimensions of Cylindrical Cook-Stove Model.

### 3.3.2.2 Conical Geometry Model of Community Cook stove Combustion Chamber.

Community cook-stove have many material parts that composed it where some are insulators, tube metal and other are metal sheets.

It has several parts that made it such as inner sheet metal, bricks, air gap, top ring cover, middle sheet metal, wool bat, outer sheet metal, stove base, entrance way, entry wood Carrier.

#### 1. Inner sheet metal made of Stainless-Steel Chromium Steel.

The material part that made this sheet has their material properties such as thermal conductivity (K) of 16 W/(m.K) , density ( $\rho$ ) of 7850 Kg/m<sup>3</sup>, Heat capacity at constant pressure (Cp) of 600 J/(kg.K) , Electrical conductivity of 1.3[MS/m]. Moreover, the dimensions used for this Stainless-Steel Chromium Steel material have shown in the figure below and they are all in in the millimetre [mm]. The variables with dimensions are outer diameter ( $D_{OSh}$ ), inner diameter ( $D_{Ish}$ ), Height of Entrance way ( $H_E$ ), Width of Entrance way ( $W_E$ ), Height of insulator material ( $H_{Sh}$ ), and thickness of sheet metal material ( $t_{Sh}$ ). Note that, the length of the sheet metal will be calculated as multiplying pi ( $\pi$ ) by the outer diameter as shown in the fig 3.22 below.

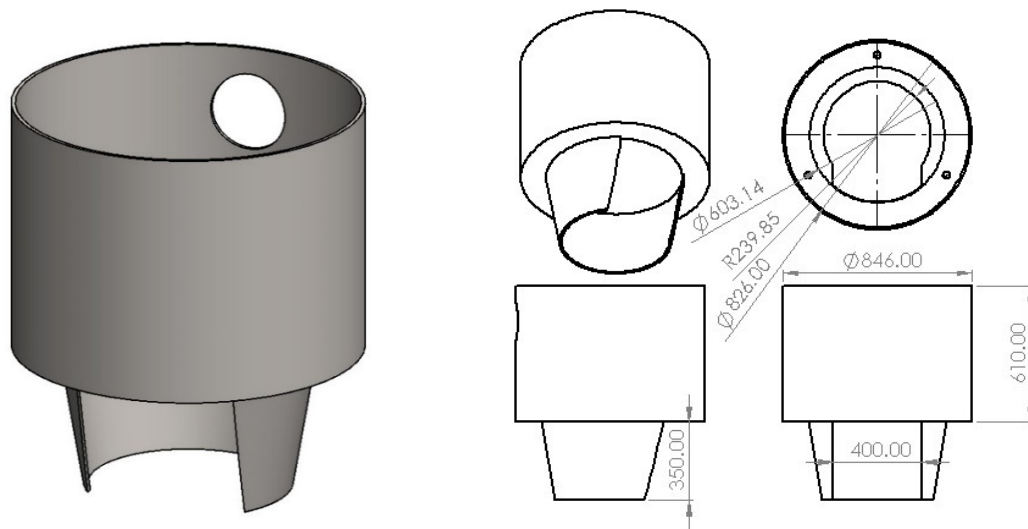


Fig 3.21 Inner Sheet Metal with its dimensions of Conical Cook-Stove Model.

## 2. Insulator one made of Alumino-silicate fire clay brick [solid]

The material part that made this sheet has their material properties such as thermal conductivity (K) of 1.5 W/(m.K) , density ( $\rho$ ) of 1900 Kg/m<sup>3</sup> , Heat capacity at constant pressure (Cp) of 1200 J/(kg.K). Moreover, the dimensions used for this Alumino-silicate fire clay brick Insulator material have shown in the figure below and they are all in in the millimetre [mm]. The Alumino-silicate fire clay brick Insulator variables with dimensions are outer diameter ( $D_{OIns}$ ), inner diameter ( $D_{IIns}$ ), Height of Entrance way ( $H_E$ ), Width of Entrance way ( $W_E$ ), Height of insulator material ( $H_{Ins}$ ), and thickness of insulator material ( $t_{Ins}$ ) as shown in the fig 3.23 below.

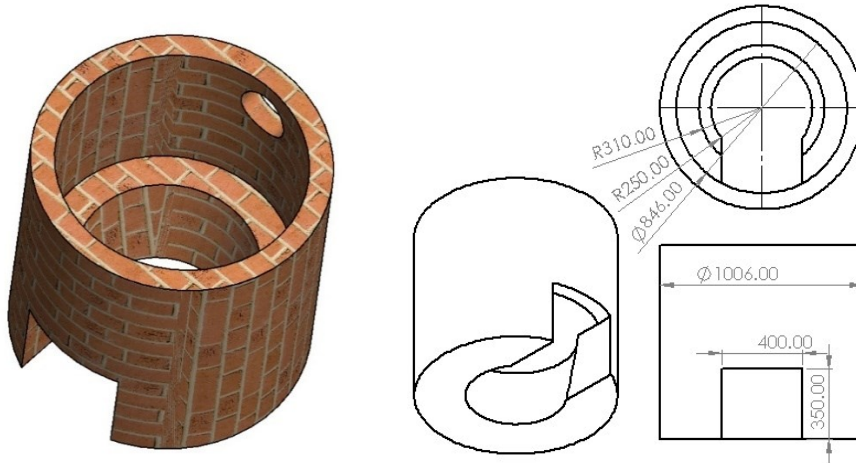


Fig 3.22 Alumino-silicate fire clay brick Insulator with its dimensions of Conical Cook-Stove Model.

### 3. Insulator two made of Air Gap at 20 degrees Celsius

The material part that are made of this insulator has the following different material properties. Those are thermal conductivity (K) of 0.026 W/(m.K), density ( $\rho$ ) of 1.225 Kg/(m<sup>3</sup>); Heat capacity at constant pressure (Cp) of 1005 J/(kg.K), Electrical conductivity of 0[S/m], Mean molar mass of 0.02897 kg/(mol), Ratio of specific heats of 1.4, Specific gas constant of 287 J/(kg.K). Moreover, the dimensions used for this air insulator material have described in the Cook stove model and they are all in the millimetre [mm]. The air-gap insulator variables with dimensions are outer diameter (D<sub>O</sub>), inner diameter (D<sub>i</sub>), Height of Entrance way (H<sub>E</sub>), Width of Entrance way (W<sub>E</sub>), Height of insulator material (H<sub>Ins</sub>), and thickness of insulator material (t<sub>Ins</sub>).

### 4. Middle sheet metal made of Stainless-Steel Chromium Steel

The material part that made this sheet has their material properties such as thermal conductivity (K) of 16 W/(m.K) , density ( $\rho$ ) of 7850 Kg/m<sup>3</sup>, Heat capacity at constant pressure (Cp) of 600 J/(kg.K) , Electrical conductivity of 1.3[MS/m]. Moreover, the dimensions used for this Stainless-Steel Chromium Steel material have shown in the figure below and they are all in in the millimetre [mm]. The variables with dimensions are outer diameter (D<sub>Osh</sub>), inner diameter (D<sub>Ish</sub>), Height of Entrance way (H<sub>E</sub>), Width of Entrance way (W<sub>E</sub>), Height of insulator material (H<sub>Sh</sub>), and thickness

of sheet metal material ( $t_{sh}$ ). Note that, the length of the sheet metal has calculated as multiplying pi ( $\pi$ ) by the outer diameter.

### **5. Insulator three made of Glass wool batt.**

The material part that made this sheet has their material properties such as thermal conductivity (K) of 0.035 W/(m.K) , density ( $\rho$ ) of 22 Kg/m<sup>3</sup> , Heat capacity at constant pressure (Cp) of 850 J/(kg.K) , Vapor resistance factor of 1.2 , Diffusion coefficient of 1e-14 m<sup>2</sup>/s. Moreover, the dimensions used for this glass wool batt insulator material have described and shown in the Cook stove model and they are all in the millimetre [mm]. The glass wool batt insulator variables with dimensions are outer diameter ( $D_{Oins}$ ), inner diameter ( $D_{Iins}$ ), Height of Entrance way ( $H_E$ ), Width of Entrance way ( $W_E$ ), Height of insulator material ( $H_{Ins}$ ), and thickness of insulator material ( $t_{ins}$ ). Note that, the length of the glass wool batt calculated as multiplying pi ( $\pi$ ) by the outer diameter.

### **6. Outer sheet metal made of Stainless-Steel Chromium Steel.**

The material part that made this sheet has their material properties such as thermal conductivity (K) of 16 W/(m.K) , density ( $\rho$ ) of 7850 Kg/m<sup>3</sup>, Heat capacity at constant pressure (Cp) of 600 J/(kg.K) , Electrical conductivity of 1.3[MS/m]. Moreover, the dimensions used for this Stainless-Steel Chromium Steel material have shown in the figure below and they are all in in the millimetre [mm]. The outer sheet metal variables with dimensions are outer diameter ( $D_{Osh}$ ), inner diameter ( $D_{Ish}$ ), Height of Entrance way ( $H_E$ ), Width of Entrance way ( $W_E$ ), Height of insulator material ( $H_{Sh}$ ), and thickness of sheet metal material ( $t_{sh}$ ). Note that, the length of the sheet metal has calculated as multiplying pi ( $\pi$ ) by the outer diameter.

### **7. Entranceway sheet metal made of Stainless-Steel Chromium Steel.**

The material part that made this sheet has their material properties such as thermal conductivity (K) of 16 W/(m.K) , density ( $\rho$ ) of 7850 Kg/m<sup>3</sup>, Heat capacity at constant pressure (Cp) of 600 J/(kg.K) , Electrical conductivity of 1.3[MS/m]. Moreover, the dimensions used for this Stainless-Steel Chromium Steel material have shown in the figure below and they are all in in the millimetre [mm]. The tube metal variables with dimensions are tube outer diameter ( $D_{OTb}$ ), tube inner diameter ( $D_{ITb}$ ), and the different lengths of the tube metal ( $L_{Tb}$ ). The entrance sheet variables are entrance sheet metal width ( $W_{ESh}$ ), entrance sheet metal length ( $L_{ESh}$ ), and thickness of entrance

sheet metal material ( $t_{ESH}$ ). Note that, the length of the small sheet metal has calculated as multiplying pi ( $\pi$ ) by the outer diameter.

#### **8. Stove Top Ring sheet metal Cover made of Stainless-Steel Chromium Steel.**

The material part that made this sheet has their material properties such as thermal conductivity (K) of 16 W/(m.K) , density ( $\rho$ ) of 7850 Kg/m<sup>3</sup>, Heat capacity at constant pressure (Cp) of 600 J/(kg.K) , Electrical conductivity of 1.3[MS/m]. Moreover, the dimensions used for this Stainless-Steel Chromium Steel material have shown in the figure below and they are all in in the millimetre [mm]. The stove-ring cover variables with dimensions are stove-ring cover sheet outer diameter ( $D_{OSCSH}$ ); stove-ring cover sheet inner diameter ( $D_{ISCSH}$ ); different heights of stove-ring cover sheet metal ( $H_{SCSH}$ ), and thickness of stove-ring cover sheet metal material ( $t_{SCSH}$ ). Note that, the length of the sheet metal has calculated as multiplying pi ( $\pi$ ) by the outer diameter.

#### **9. Entry wood Carrier metal tube made of Stainless-Steel Chromium Steel.**

The material part that made this sheet has their material properties such as thermal conductivity (K) of 16 W/(m.K) , density ( $\rho$ ) of 7850 Kg/m<sup>3</sup>, Heat capacity at constant pressure (Cp) of 600 J/(kg.K) , Electrical conductivity of 1.3[MS/m]. Moreover, the dimensions used for this Stainless-Steel Chromium Steel material have shown in the figure below and they are all in in the millimetre [mm]. The tube metal variables with dimensions are tube outer diameter ( $D_{OTb}$ ), tube inner diameter ( $D_{ITb}$ ), and the different lengths of the tube metal ( $L_{Tb}$ ). The small sheet variables are small sheet metal width ( $W_{SSH}$ ), length of small sheet metal ( $L_{SSH}$ ), and thickness of small sheet metal material ( $t_{SSH}$ ). Note that, the length of the small sheet metal has calculated as multiplying pi ( $\pi$ ) by the outer diameter.

#### **10. Cook stove Base stand made of Alumino-silicate fire clay brick [solid].**

The material part that made this sheet has their material properties such as thermal conductivity (K) of 1.5 W/(m.K) , density ( $\rho$ ) of 1900 Kg/m<sup>3</sup> , Heat capacity at constant pressure (Cp) of 1200 J/(kg.K). Moreover, the dimensions used for this Alumino-silicate fire clay brick Insulator material have shown in the figure below and they are all in in the millimetre [mm]. The Alumino-silicate fire clay brick Insulator variables with dimensions are outer diameter ( $D_{OBase}$ ), inner diameter

( $D_{Ins}$ ), Width of stove base ( $W_{Base}$ ), Depth of stove base ( $d_{Base}$ ), and thickness of insulator material ( $t_{Ins}$ ).

### **11. Cooking Pot made of Stainless-Steel Chromium Steel.**

The material part that made this sheet has their material properties such as thermal conductivity (K) of 16 W/(m.K) , density ( $\rho$ ) of 7850 Kg/m<sup>3</sup>, Heat capacity at constant pressure ( $C_p$ ) of 600 J/(kg.K) , Electrical conductivity of 1.3[MS/m]. Moreover, the dimensions used for this Stainless-Steel Chromium Steel tube metal and sheet metal have shown in the figure below and they are all in in the millimetre [mm]. The cook-pot ring cover variables are cover sheet outer diameter ( $D_{OCSh}$ ); cover sheet inner diameter ( $D_{ICSh}$ ); height of tube metal ( $H_{Tb}$ ); height of cover sheet metal ( $H_{CSh}$ ), and thickness of cover sheet metal material ( $t_{CSh}$ ). The tube metal variables are tube metal outer diameter ( $D_{OTb}$ ); tube metal inner diameter ( $D_{ITb}$ ); the length of the tube metal ( $L_{Tb}$ ). The cook-pot also have its variables such as cook-pot sheet outer diameter ( $D_{OCPSH}$ ), and cook-pot sheet inner diameter ( $D_{OCPSH}$ ), cook-pot sheet height ( $H_{CPSH}$ ). Note that, the length of the small sheet metal has calculated as multiplying pi ( $\pi$ ) by the outer diameter of sheet.

### **12. Stove Frame Tube metal made of Stainless-Steel Chromium Steel.**

The material part that made this sheet has their material properties such as thermal conductivity (K) of 16 W/(m.K) , density ( $\rho$ ) of 7850 Kg/m<sup>3</sup>, Heat capacity at constant pressure ( $C_p$ ) of 600 J/(kg.K) , Electrical conductivity of 1.3[MS/m]. Moreover, the dimensions used for this Stainless-Steel Chromium Steel tube material have shown in the figure below and they are all in in the millimetre [mm]. The tube metal variables with dimensions are tube outer diameter ( $D_{OTb}$ ), tube inner diameter ( $D_{ITb}$ ), and the different lengths of the tube metal ( $L_{Tb}$ ). The small sheet variables are small sheet outer diameter ( $D_{OSSh}$ ), small sheet inner diameter ( $D_{ISSh}$ ), and thickness of small sheet metal material ( $t_{SSh}$ ). Note that, the length of the small sheet metal has calculated as multiplying pi ( $\pi$ ) by the outer diameter.

### **3.3.2.3 Rectangular Geometry Model of Community Cook stove Combustion Chamber.**

Community cook stove have many material parts that composed it where some are insulators, round tube metals and other are metal sheets.

It has several parts that made it such as inner sheet metal, bricks, air gap, top ring cover, middle sheet metal, wool bat, outer sheet metal, stove base, entrance way, entry wood Career.

### 1. Inner sheet metal made of Stainless-Steel Chromium Steel.

The material part that made this sheet has their material properties such as thermal conductivity (K) of 16 W/(m.K) , density ( $\rho$ ) of 7850 Kg/m<sup>3</sup>, Heat capacity at constant pressure (Cp) of 600 J/(kg.K) , Electrical conductivity of 1.3[MS/m]. Moreover, the dimensions used for this Stainless-Steel Chromium Steel material have shown in the figure below and they are all in in the millimetre [mm]. The variables with dimensions are outer diameter ( $D_{Osh}$ ), inner diameter ( $D_{Ish}$ ), Height of Entrance way ( $H_E$ ), Width of Entrance way ( $W_E$ ), Height of insulator material ( $H_{Sh}$ ), and thickness of sheet metal material ( $t_{sh}$ ). Note that, the length of the sheet metal calculated as multiplying pi ( $\pi$ ) by the outer diameter as shown in the fig 3.37 below.

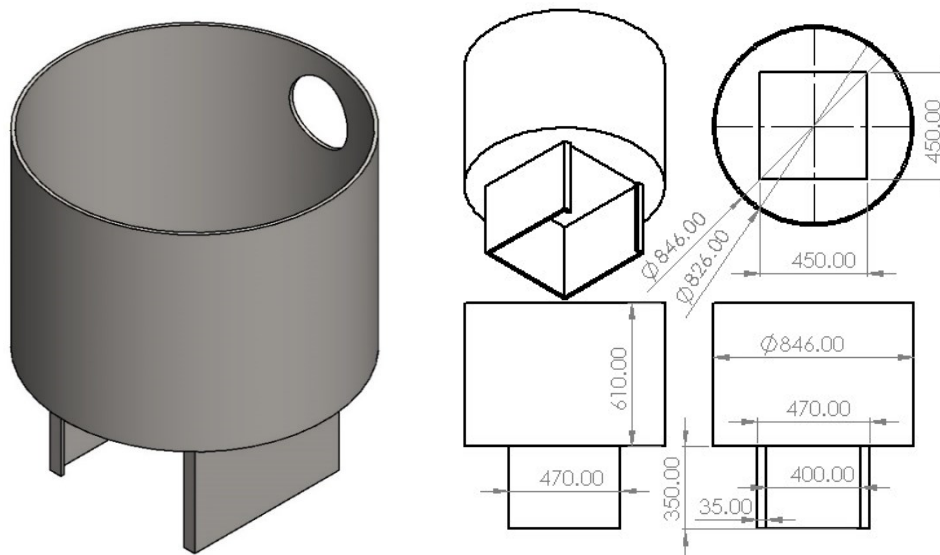


Fig 3.23 Inner Sheet Metal with its dimensions of Square Cook-Stove Model.

### 2. Insulator one made of Alumino-silicate fire clay brick [solid].

The material part that made this sheet has their material properties such as thermal conductivity (K) of 1.5 W/(m.K) , density ( $\rho$ ) of 1900 Kg/m<sup>3</sup> , Heat capacity at constant pressure (Cp) of 1200 J/(kg.K). Moreover, the dimensions used for this Alumino-silicate fire clay brick Insulator material have shown in the figure below and they are all in in the millimetre [mm].

The Alumino-silicate fire clay brick Insulator variables with dimensions are outer diameter ( $D_{OIns}$ ), inner diameter ( $D_{IIns}$ ), Height of Entrance way ( $H_E$ ), Width of Entrance way ( $W_E$ ), Height of insulator material ( $H_{Ins}$ ), and thickness of insulator material ( $t_{Ins}$ ) as shown in the fig 3.38 below.

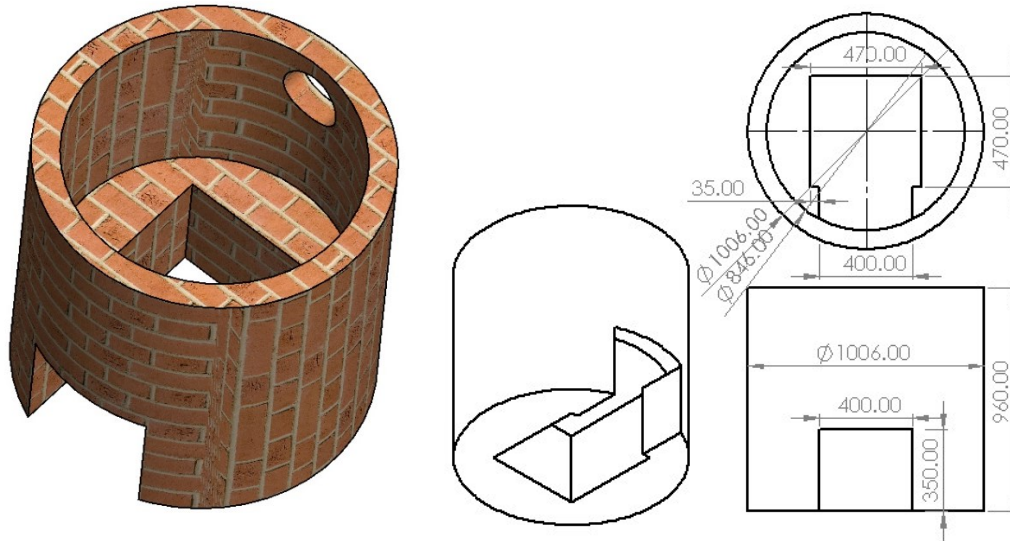


Fig 3.24 Alumino-silicate fire clay brick Insulator with its dimensions of Square Cook-Stove Model.

### 3. Insulator two made of Air Gap at 20 degrees Celsius.

The material part that are made of this insulator has the following different material properties. Those are thermal conductivity ( $K$ ) of 0.026 W/(m.K), density ( $\rho$ ) of 1.225 Kg/(m<sup>3</sup>); Heat capacity at constant pressure ( $C_p$ ) of 1005 J/(kg.K), Electrical conductivity of 0[S/m], Mean molar mass of 0.02897 kg/(mol), Ratio of specific heats of 1.4, Specific gas constant of 287 J/(kg.K). Moreover, the dimensions used for this air insulator material have described in the Cook stove model and they are all in the millimetre [mm].

The air-gap insulator variables with dimensions are outer diameter ( $D_o$ ), inner diameter ( $D_i$ ), Height of Entrance way ( $H_E$ ), Width of Entrance way ( $W_E$ ), Height of insulator material ( $H_{Ins}$ ), and thickness of insulator material ( $t_{Ins}$ ).

### 4. Middle sheet metal made of Stainless-Steel Chromium Steel.

The material part that made this sheet has their material properties such as thermal conductivity (K) of 16 W/(m.K) , density ( $\rho$ ) of 7850 Kg/m<sup>3</sup>, Heat capacity at constant pressure (Cp) of 600 J/(kg.K) , Electrical conductivity of 1.3[MS/m]. Moreover, the dimensions used for this Stainless-Steel Chromium Steel material have shown in the figure below and they are all in in the millimetre [mm]. The variables with dimensions are outer diameter ( $D_{Osh}$ ), inner diameter ( $D_{Ish}$ ), Height of Entrance way ( $H_E$ ), Width of Entrance way ( $W_E$ ), Height of insulator material ( $H_{Sh}$ ), and thickness of sheet metal material ( $t_{Sh}$ ). Note that, the length of the sheet metal has calculated as multiplying pi ( $\pi$ ) by the outer diameter.

### **5. Insulator Three made of Glass wool batt.**

The material part that made this sheet has their material properties such as thermal conductivity (K) of 0.035 W/(m.K) , density ( $\rho$ ) of 22 Kg/m<sup>3</sup> , Heat capacity at constant pressure (Cp) of 850 J/(kg.K) , Vapor resistance factor of 1.2 , Diffusion coefficient of 1e-14 m<sup>2</sup>/s. Moreover, the dimensions used for this glass wool batt insulator material have described and shown in the Cook stove model and they are all in the millimetre [mm]. The glass wool batt insulator variables with dimensions are outer diameter ( $D_{Oins}$ ), inner diameter ( $D_{Iins}$ ), Height of Entrance way ( $H_E$ ), Width of Entrance way ( $W_E$ ), Height of insulator material ( $H_{Ins}$ ), and thickness of insulator material ( $t_{Ins}$ ). Note that, the length of the glass wool batt calculated as multiplying pi ( $\pi$ ) by the outer diameter.

### **6. Outer sheet metal made of Stainless-Steel Chromium Steel.**

The material part that made this sheet has their material properties such as thermal conductivity (K) of 16 W/(m.K) , density ( $\rho$ ) of 7850 Kg/m<sup>3</sup>, Heat capacity at constant pressure (Cp) of 600 J/(kg.K) , Electrical conductivity of 1.3[MS/m]. Moreover, the dimensions used for this Stainless-Steel Chromium Steel material have shown in the figure below and they are all in in the millimetre [mm].

The outer sheet metal variables with dimensions are outer diameter ( $D_{Osh}$ ), inner diameter ( $D_{Ish}$ ), Height of Entrance way ( $H_E$ ), Width of Entrance way ( $W_E$ ), Height of insulator material ( $H_{Sh}$ ), and thickness of sheet metal material ( $t_{Sh}$ ). Note that, the length of the sheet metal has calculated as multiplying pi ( $\pi$ ) by the outer diameter.

### **7. Entranceway sheet metal made of Stainless-Steel Chromium Steel.**

The material part that made this sheet has their material properties such as thermal conductivity (K) of 16 W/(m.K) , density ( $\rho$ ) of 7850 Kg/m<sup>3</sup>, Heat capacity at constant pressure (Cp) of 600 J/(kg.K) , Electrical conductivity of 1.3[MS/m]. Moreover, the dimensions used for this Stainless-Steel Chromium Steel material have shown in the figure below and they are all in in the millimetre [mm]. The tube metal variables with dimensions are tube outer diameter ( $D_{OTb}$ ), tube inner diameter ( $D_{ITb}$ ), and the different lengths of the tube metal ( $L_{Tb}$ ). The entrance sheet variables are entrance sheet metal width ( $W_{ESh}$ ), entrance sheet metal length ( $L_{ESh}$ ), and thickness of entrance sheet metal material ( $t_{ESh}$ ). Note that, the length of the small sheet metal has calculated as multiplying pi ( $\pi$ ) by the outer diameter.

### **8. Stove Top Ring sheet metal Cover made of Stainless-Steel Chromium Steel.**

The material part that made this sheet has their material properties such as thermal conductivity (K) of 16 W/(m.K) , density ( $\rho$ ) of 7850 Kg/m<sup>3</sup>, Heat capacity at constant pressure (Cp) of 600 J/(kg.K) , Electrical conductivity of 1.3[MS/m]. Moreover, the dimensions used for this Stainless-Steel Chromium Steel material have shown in the figure below and they are all in in the millimetre [mm].

The stove-ring cover variables with dimensions are stove-ring cover sheet outer diameter ( $D_{OSCSH}$ ); stove-ring cover sheet inner diameter ( $D_{ISCSH}$ ); different heights of stove-ring cover sheet metal ( $H_{SCSH}$ ), and thickness of stove-ring cover sheet metal material ( $t_{SCSH}$ ). Note that, the length of the sheet metal has calculated as multiplying pi ( $\pi$ ) by the outer diameter.

### **9. Entry wood Carrier metal tube made of Stainless-Steel Chromium Steel.**

The material part that made this sheet has their material properties such as thermal conductivity (K) of 16 W/(m.K) , density ( $\rho$ ) of 7850 Kg/m<sup>3</sup>, Heat capacity at constant pressure (Cp) of 600 J/(kg.K) , Electrical conductivity of 1.3[MS/m]. Moreover, the dimensions used for this Stainless-Steel Chromium Steel material have shown in the figure below and they are all in in the millimetre [mm].

The tube metal variables with dimensions are tube outer diameter ( $D_{OTb}$ ), tube inner diameter ( $D_{ITb}$ ), and the different lengths of the tube metal ( $L_{Tb}$ ). The small sheet variables are small sheet metal width ( $W_{SSh}$ ), length of small sheet metal ( $L_{SSh}$ ), and thickness of small sheet metal material

( $t_{SSh}$ ). Note that, the length of the small sheet metal has calculated as multiplying pi ( $\pi$ ) by the outer diameter.

### **10. Cook stove Base stand made of Alumino-silicate fire clay brick [solid].**

The material part that made this sheet has their material properties such as thermal conductivity (K) of 1.5 W/(m.K) , density ( $\rho$ ) of 1900 Kg/m<sup>3</sup> , Heat capacity at constant pressure (Cp) of 1200 J/(kg.K). Moreover, the dimensions used for this Alumino-silicate fire clay brick Insulator material have shown in the figure below and they are all in in the millimetre [mm]. The Alumino-silicate fire clay brick Insulator variables with dimensions are outer diameter ( $D_{OBase}$ ), inner diameter ( $D_{IIns}$ ), Width of stove base ( $W_{Base}$ ), Depth of stove base ( $d_{Bbase}$ ), and thickness of insulator material ( $t_{Ins}$ ).

### **11. Cooking Pot made of Stainless-Steel Chromium Steel.**

The material part that made this sheet has their material properties such as thermal conductivity (K) of 16 W/(m.K) , density ( $\rho$ ) of 7850 Kg/m<sup>3</sup>, Heat capacity at constant pressure (Cp) of 600 J/(kg.K) , Electrical conductivity of 1.3[MS/m]. Moreover, the dimensions used for this Stainless-Steel Chromium Steel tube metal and sheet metal have shown in the figure below and they are all in in the millimetre [mm]. The cook-pot ring cover variables are cover sheet outer diameter ( $D_{OCSh}$ ); cover sheet inner diameter ( $D_{ICSh}$ ); height of tube metal ( $H_{Tb}$ ); height of cover sheet metal ( $H_{CSh}$ ), and thickness of cover sheet metal material ( $t_{CSh}$ ). The tube metal variables are tube metal outer diameter ( $D_{OTb}$ ); tube metal inner diameter ( $D_{ITb}$ ); the length of the tube metal ( $L_{Tb}$ ). The cook-pot also have its variables such as cook-pot sheet outer diameter ( $D_{OCPSH}$ ), and cook-pot sheet inner diameter ( $D_{OCPSH}$ ), cook-pot sheet height ( $H_{CPSH}$ ). Note that, the length of the small sheet metal has calculated as multiplying pi ( $\pi$ ) by the outer diameter of sheet.

### **12. Stove Frame Tube metal made of Stainless-Steel Chromium Steel.**

The material part that made this sheet has their material properties such as thermal conductivity (K) of 16 W/(m.K) , density ( $\rho$ ) of 7850 Kg/m<sup>3</sup>, Heat capacity at constant pressure (Cp) of 600 J/(kg.K) , Electrical conductivity of 1.3[MS/m]. Moreover, the dimensions used for this Stainless Steel Chromium Steel tube material have shown in the figure below and they are all in in the millimetre [mm]. The tube metal variables with dimensions are tube outer diameter ( $D_{OTb}$ ), tube

inner diameter ( $D_{ITb}$ ), and the different lengths of the tube metal ( $L_{Tb}$ ). The small sheet variables are small sheet outer diameter ( $D_{OSSh}$ ), small sheet inner diameter ( $D_{ISSh}$ ), and thickness of small sheet metal material ( $t_{SSh}$ ). Note that, the length of the small sheet metal has calculated as multiplying pi ( $\pi$ ) by the outer diameter.

### 3.3.3 Comsol Multi-physics Heat Transfer Parametric Model.

The simulating tool used for developing the temperature heat transfer of the Community cook-stove is Comsol multi-physics. The following parameters have considered building the Comsol model ready for simulation as shown in the fig 3.52 below.

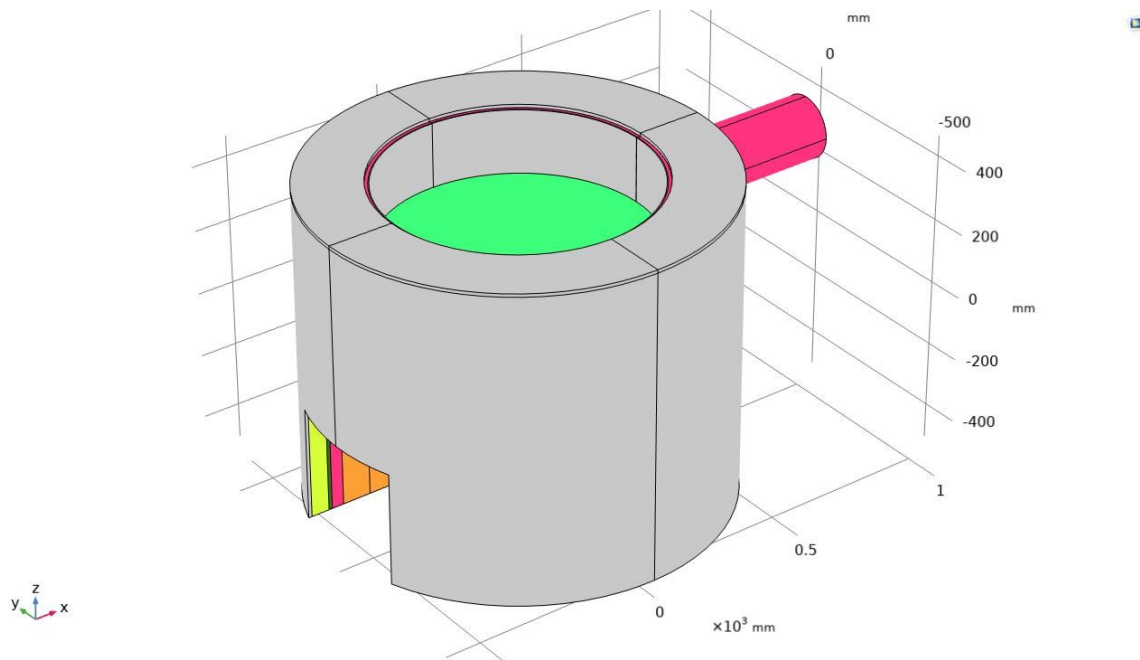


Fig 3.25: Comsol Design Model of Community Cook Stove.

There are further expressions formula used for simulating the different 3D Model designs of Comsol Multi-physics. Those mathematical model formulas are the following:

#### 1. The Energy Equation,

$$\rho C_p \left( \frac{DT}{Dt} \right) = \nabla \cdot (k \nabla T) + \dot{Q}_v + S_r$$

Where ,

- $\rho$  = Density of the gas mixture (kg/m<sup>3</sup>)
- $C_p$  = Specific heat capacity (J/kg·K)
- $T$  = Temperature (K)
- $k$  = Thermal conductivity (W/m·K)
- $\dot{Q}_v$  = Volumetric heat source term (W/m<sup>3</sup>)
- $S_r$  = Radiation heat source (W/m<sup>3</sup>)

## 2. Burning firewood mass rate and Heat released rate (or Heat input).

$$Q = \dot{m} \times CV \quad \text{And} \quad \dot{m} = \frac{\Delta m}{\Delta t}$$

Accounting to the airflow and efficiency,  $Q_{useful} = \dot{m} \times CV \times \eta$

Where,

- $\dot{m}$  is mass burn rate ( kg/s)
- $CV$  is calorific value of firewood ( J/Kg or MJ/Kg)
- $Q$  Is Heat energy released ( W or J/s)
- $\Delta m$  is mass of firewood burned ( Kg)
- $\Delta t$  is time taken for combustion ( s or h)
- $\eta$  is the combustion and heat transfer efficiency ( range in 0.7-0.9)

## 3. Convection Heat flux and Volumetric heat source for biomass combustion.

$$\dot{Q}_v = \frac{\dot{m}CV}{V} \quad \text{And} \quad \dot{q}_c = \frac{\dot{m}CV}{A} = h \times \Delta T$$

Where,

- $\dot{m}$  is mass burn rate ( kg/s)
- $CV$  is calorific value of firewood  $i$  ( J/Kg)
- $\dot{q}_c$  Is Heat Flux at the combustion surface ( W/ m<sup>2</sup>s)
- $\dot{Q}_v$  is Volumetric heat generation rate ( W/m<sup>3</sup>)
- $V$  is volume of combustion zone ( m<sup>3</sup>)
- $A$  is Surface area of Combustion ( m<sup>2</sup>)

- $h$  is the heat transfer coefficient ( $\text{W}/\text{m}^2\cdot\text{K}$ )
- $\Delta T$  is the temperature difference between Flame and surrounding Temperature (K)

#### 4. Combustion transport of Diluted species or reacting flow interface.

$$R_i = \left(\frac{\partial C_i}{\partial t}\right) + \nabla \cdot (-D_i \nabla C_i + u C_i)$$

Where,

- $R_i$  is Reaction rate source term for species  $i$  ( $\text{kg}/\text{m}^3\cdot\text{s}$ )
- $D_i$  is Diffusivity of species  $i$  ( $\text{m}^2/\text{s}$ )
- $u$  is velocity field ( $\text{m}/\text{s}$ )
- $C_i$  is Concentration of species  $i$  ( $\text{kg}/\text{m}^3$ )

#### 5. The Radiation Heat Flux refers: $\dot{q}_R = \sigma \epsilon (T_S^4 - T_\infty^4)$

Where ,

- $\sigma$  is Stefan-Boltzmann constant ( $5.67 \times 10^{-8} \text{ W}/\text{m}^2 \cdot \text{K}^4$ )
- $\epsilon$  is emissivity of firewood/ flame (range between  $\sim 0.8-0.95$ )
- $T_S^4$  is the Flame/Surface Temperature (K)
- $T_\infty^4$  is surrounding Temperature (K)
- $\dot{q}_R$  is Radiative Heat Flux at the surface ( $\text{W}/\text{m}^2$ )

#### 6. The flame/surface temperature and Film temperature.

$$T_S = T_{amb} + \frac{\dot{m}CV}{\dot{m}_{air}C_p} \quad \text{and} \quad T_f = \left(\frac{T_S + T_{amb}}{2}\right)$$

Where

- $C_p$  is Specific capacity of air ( $\text{J}/\text{Kg}\cdot\text{K}$ )
- $T_f$  is the film temperature (K)
- $T_S$  is the Flame/Surface Temperature (K)
- $T_{amb}$  is surrounding/ambient Temperature (K)
- $\dot{m}_{air}$  is mass flow rate of air ( $\text{Kg}/\text{s}$ )
- $\dot{m}$  is the burning rate of firewood ( $\text{Kg}/\text{s}$ )
- $CV$  is the calorific value of the firewood ( $\text{J}/\text{Kg}$  or  $\text{MJ}/\text{Kg}$ )

## 7. The Grashof number, Nursselt number, and Reynolds Number.

$$G_r = \frac{g\beta(T_s+T_\infty)L^3}{\nu^2} \quad \text{and} \quad N_u = C(G_r \cdot P_r)^n = \frac{h \times L}{k} \quad \text{and} \quad R_e = \sqrt{G_r} = \frac{V_{air} \times L}{\nu}$$

Where

- $G_r$  is the Grashof number.
- $N_u$  is the Nursselt number.
- $R_e$  is the Reynold number.
- $T_s$  is the Flame/Surface Temperature (K)
- $T_\infty$  is surrounding/ambient Temperature (K)
- $h$  is the convective heat transfer Coefficient ( W/m<sup>2</sup>.K)
- $V_{air}$  is the velocity of air (m/s)
- $L$  is the characteristic length (m)
- $\beta$  is the coefficient of thermal expansions (  $1/T_{film}$  in K<sup>-1</sup>)
- $\nu$  is the kinetic viscosity (m<sup>2</sup>/s)

## 8. Heat transfer into steam and Heat loss in flue gas.

$$Q_{st} = (m_w C_{pw} \Delta T) + m_e L_w \quad \text{And} \quad Q_g = \rho \times A_s \times V_f \times C_p \times (T_g - T_a) + m_e L_w$$

Where

- $C_p$  is Specific capacity of air ( J/Kg.K)
- $C_{pw}$  is the Water heat capacity constant , (4.18 kJ/kg.K)
- $V_f$  is the Flue gas velocity (m/s)
- $T_g$  is the Flue gas Temperature (K)
- $T_a$  is ambient Temperature (K)
- $m_e$  is the mass of evaporated steam (Kg)
- $m_w$  is the Initial mass of water (Kg)
- $L_w$  is the Latent heat of water (2,257.2 kJ/kg)
- $\Delta T$  is the Temperature difference from initial to boiling point (K)
- $Q_{st}$  is the heat transfer into steam
- $Q_g$  is the heat loss in flue gas.

### 9. Heat loss through convection and Heat loss through radiation.

$$Q_{IC} = h_{aw} \times A_w \times (T_w - T_a) \quad \text{And} \quad Q_{IR} = \rho \times \varepsilon \times A_w \times (T_w^4 - T_a^4)$$

Where

- $h_{aw}$  is Convective heat transfer coefficient of air on stove wall side (W/m<sup>2</sup>-oK)
- $A_w$  is the Wall surface areas (m<sup>2</sup>)
- $\varepsilon$  is the emissivity of brick wall (0.93)
- $T_w$  is the wall Temperature (K)
- $T_a$  is ambient Temperature (K)
- $\rho$  is the density of flue gas (kg/m<sup>3</sup>)
- $Q_{IR}$  is the heat loss through radiation.
- $Q_{IC}$  is the heat loss through convection.

### 10. Heat loss in unburned carbon and Heat loss in moisture.

$$Q_{lf} = C_r \times (33,826 \times m_r) \quad \text{and}$$

$$Q_{lmoist} = [m_f \times (\%moist_{fuel})] \times [2250 + (1.91 \times (T_g - T_a))]$$

Where

- $Q_{lf}$  is the heat lost in unburned carbon.
- $Q_{lmoist}$  is the heat lost in the moisture.
- $C_r$  is the Carbon composition in fuel.
- $m_r$  is the Mass of unburned fuel (Kg)
- $T_g$  is the Flue gas Temperature (K)
- $T_a$  is ambient Temperature (K)
- $\%moist_{fuel}$  is the percentage of moist content

### 11. The Combustion efficiency within combustion chamber.

$$\eta_c = \frac{m_w \times C_p \times \Delta T}{m_{fuel} \times C_v} \dots\dots$$

$$\rho_{fuel} = \frac{m_{fuel}}{V_{Required}} \quad \text{and} \quad V_{Required} = \frac{\pi \times d^2 \times L}{4}$$

Where

- $\eta_C$  is the Combustion efficiency (%).
- $m_{fuel}$  is the mass of fuel (Kg).
- $L$  is the Length of Combustion chamber (m).
- $d$  is the combustion chamber diameter (m).
- $m_w$  is the Mass of water (Kg).
- $\Delta T$  is the water temperature change (K)
- $V_{Required}$  is Volume of Combustion ( $m^3$ )
- $\rho_{fuel}$  is the density of fuel content ( $Kg/m^3$ )

## 12. The thermal efficiency of cookstove.

$$\eta = \left[ \frac{(m_w \times Cp_w \times \Delta T) + (\Delta m_w \times \lambda)}{\mu \times C_v} \right] \times 100\%$$

Where,

- $\eta$  is the Cookstove efficiency (%).
- $\Delta m_w$  is the mass of water evaporated (kg) (difference between initial and final mass of water).
- $\lambda$  is the Latent heat of vaporization of water (Kj/kg).
- $\mu$  is the equivalent mass of dry biomass consumed (kg)?
- $m_w$  is the Mass of water taken (kg)?
- $\Delta T$  is the water temperature change from initial to final temperature (K).
- $Cp_w$  is specific heat of water (kJ/kg,K)
- $C_v$  is the calorific value of fuel/biomass consumed (kJ/kg?K)

### **3.3.4 Optimal Design Selection of Community Cookstove Design Model.**

Through conducting the design modelling of community cookstove, the optimal design selection of a community cookstove model centers on achieving high thermal efficiency, minimal heat loss, and sustainable fuel use. Using COMSOL Multiphysics, three combustion chamber geometries such as cylindrical, conical, and rectangular, were modeled and analyzed for heat transfer and temperature distribution. Each design incorporated a multi-layer structure with stainless steel chromium steel, alumino-silicate fire clay brick, air gaps, and glass wool batt insulation to limit heat loss and improve energy efficiency.

Parametric studies examined insulation thickness, combustion chamber geometry, and material properties to identify a configuration that maximizes internal heat retention while reducing fuel consumption. These materials, combined with optimal chamber dimensions, reduce external surface temperatures and improve safety. The design strategy emphasized computational modeling to shorten development time and guide iterative improvements, ensuring a cost-effective and environmentally friendly solution.

COMSOL Multiphysics software was employed to simulate heat distribution and combustion behavior for each geometry under both steady-state and time-dependent conditions. Key parameters included chamber diameter and height, insulator thickness, and material thermal properties. The simulations examined temperature gradients within the stove walls, cooking pot, and water, enabling direct comparison of heat retention and transfer efficiency. These analyses demonstrated how chamber shape influences airflow, combustion stability, and the rate of heat delivery to the cooking vessel.

rapid and stable heating of the cooking pot while maintaining lower external surface temperatures, reducing fuel consumption and enhancing user safety. The conical design improved natural draft and combustion but exhibited slightly higher heat loss, while the rectangular model suffered from uneven heating and reduced efficiency.

Overall, the design model selection process demonstrated that systematic simulation and material testing can effectively identify a combustion chamber geometry that maximizes thermal efficiency and supports sustainable biomass utilization for institutional cookstove applications. In addition,

the final combustion chamber geometry model meets community-scale needs by balancing durability, affordability, and energy efficiency. It provides a replicable framework for large-scale cooking applications in resource-limited settings, contributing to reduced biomass dependency and improved air quality.

### 3.4 Parametric Mesh Type Selection.

#### 3.5.1 Implication of Mesh Selection.

In COMSOL Multi-physics, different types of mesh are used to discretize the computational domain for solving partial differential equations. The choice of mesh type depends on the geometry, physics, and accuracy requirements of the simulation. Tetrahedral mesh have selected for selection with the finer mesh level for irregular biomass stove designs while enabling mesh refinement in critical regions. Tetrahedral mesh uses four-faced elements (tetrahedral) ideal for meshing complex 3D geometries. It adapts easily to curved and irregular shapes, making it suitable for multi-physics simulations. Tetrahedral mesh supports automatic generation and adaptive refinement, offering flexibility and reasonable accuracy. It is widely used in heat transfer, structural, and fluid simulations where geometric complexity is high.

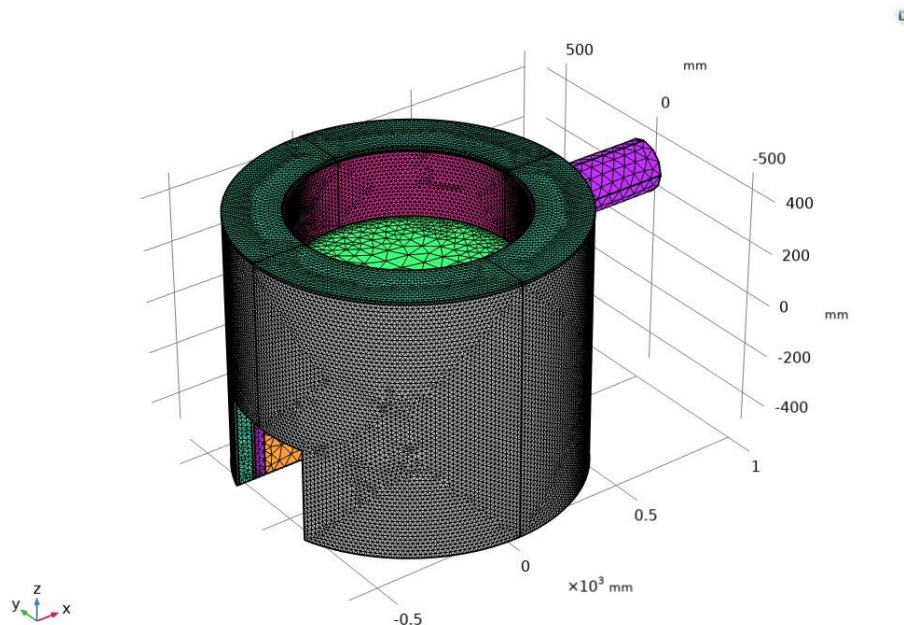


Table 3.9 Community Cook-Stove with Mesh type of Cylindrical, Conical and Rectangular Combustion Chamber Models.

### Why It is Ideal for Heat Transfer:

- Adapts to complex or irregular geometries (e.g., curved surfaces and intricate structures) with automatic mesh generation.
- Compatible with **Adaptive Mesh Refinement (AMR)** for refining areas with large temperature gradients.

The "**Finer**" mesh setting in COMSOL Multiphysics offers high-resolution discretization, ideal for simulations involving sharp gradients, such as heat transfer, fluid flow, or multiphysics. It generates smaller elements than the "Normal" mesh, improving accuracy near boundaries, curved surfaces, and narrow gaps. This setting is especially effective in modeling biomass cookstoves where thermal gradients occur near the combustion chamber and cooking pot. "Finer" mesh ensures better capture of localized effects like conduction across materials and convection in airflow zones. However, it increases computational load, requiring more memory and solve time. It strikes a balance between accuracy and performance for moderately complex geometries. It's best used with boundary layer meshes or in combination with adaptive refinement for optimal results. Start with "Finer" for critical regions, then perform a mesh convergence study to validate accuracy. It is a reliable choice when more detail is needed without the heavy cost of "Extra Fine" mesh.

### 3.4.2 Mesh Statistics OF 3D Model Layers.

Table 3.10 Mesh Statistics for biomass cookstove model.

Description	Value
Status	Complete mesh
Mesh vertices	442100
Tetrahedra	2497748
Triangles	464537
Edge elements	9931
Vertex elements	179
Number of elements	2497748
Minimum element quality	0.06495

Description	Value
Average element quality	0.6547
Element volume ratio	6.8516E-5
Mesh volume	8.954E8 mm <sup>3</sup>
Maximum element size	88.6
Minimum element size	6.44
Curvature factor	0.4
Resolution of narrow regions	0.7
Maximum element growth rate	1.4
Predefined size	Finer

### 3.5 Previous Experiment on Community Biomass Cook-Stove.

Referring on the previous work/ model that manufactured to be useful as first previous biomass cookstove model where it shows the performance and efficiency regarding on the combustion chamber efficiency.

#### 3.5.1 Theory and Calculation of Experimental Material Set-Up.

Through the experiment setup using different materials used such as high temperature thermometers, marker pen, papers .... etc. The previous research provides the temperature results for showing the temperature change of water and temperature of cookstove body temperature after a certain period. The initial temperature of water was 25 degC (298K) and initial temperature of cookstove body was 25 degC (298K) too.

The outcomes of research experiment have shown in the following table below:

Table 3.11 Experimental Temperature results of the previous Cook-Stove at RP Tumba College

NO	TIME (min)	Temperature in water (degC)	Temperature on outside Stove body (up) (degC)	Temperature on outside Stove body (Down) (degC)
1	0	50	30.9	40.1

2	10	53.7	33.1	42.7
3	20	69	35.3	45.9
4	30	79.3	39.8	49.3
5	40	88.8	43.2	52.4
6	50	93.6	45.4	58.8
7	56	95.8	52.8	65.7
8	60	98.9	52.9	65.9

---

### 3.5.2 Thermal Efficiency Calculation.

Biomass fuel contains moisture, and a portion of its energy consumed in evaporating this moisture during combustion. Therefore, to determine the actual amount of biomass contributing solely to cooking, the fraction used for moisture removal must be excluded. In this case, the biomass has a moisture content of 10%. Evaporating one kilogram of water requires about 2260 kJ of energy, which corresponds to approximately 12.55% of the biomass's calorific value. Consequently, if the biomass contains *mst* percent moisture (wet basis), the effective mass of biomass available for heating the cooking pot reduced by approximately a factor of  $(1 - 1.1255mst)$ , as the energy used to vaporize the moisture.

The thermal efficiency of cookstove is the ratio of work done by heating and evaporation of water to the energy produced by burning biomass. The numerator comprises of two parts: (i) the energy used in increasing the temperature of water and (ii) the energy needed for phase change of water to vapor. The denominator is the amount of energy produced by biomass combustion.

The thermal efficiency of cookstove calculated using the following formulas:

$$\eta = \left[ \frac{(m_w \times c_{p_w} \times \Delta T) + (\Delta m_w \times \lambda)}{\mu \times CV} \right] \times 100\%$$

$$\mu = [1 - (1.1255 \times mst)] \times (m_{fuel}) \text{ For showing the moisture content.}$$

Where:

- $\eta$  is the Cookstove efficiency (%).
- $\Delta m_w$  is the mass of water evaporated (kg) (difference between initial and final mass of water).
- $\lambda$  is the Latent heat of vaporization of water (Kj/kg).
- $\mu$  is the equivalent mass of dry biomass consumed (kg).
- $m_w$  is the Mass of water taken (kg).
- $\Delta T$  is the water temperature change from initial to final temperature (K).
- $Cp_w$  is specific heat of water (kJ/kg,K)
- $CV$  is the calorific value of fuel/biomass consumed (kJ/kg,K)
- $mst$  is the moisture content of biomass fuel (%)

$$\mu = [1 - (1.1255 \times 0.1)] \times (6.83) = [0.88745 \times 6.83] = \mathbf{6.0612 \text{ kg}}$$

$$\eta = \left[ \frac{(96.5 \times 4.18 \times 75) + (3.5 \times 2260)}{6.0612 \times 16,000} \right] \times 100\% = \left[ \frac{(30,252.75) + (7,910)}{96,979.2} \right] \times 100\% = \mathbf{39.35\%}$$

The mass of biomass consumed ( $m_{fuel}$ ) of 6.83kg, the equivalent mass of dry biomass consumed ( $\mu$ ) of 6.083kg, the Latent heat of vaporization of water ( $\lambda$ ) of 2260 kJ/kg, the mass of water evaporated ( $\Delta m_w$ ) of 3.5Kg, the Mass of water taken ( $m_w$ ) of 96.5Kg, the water temperature change from initial to final temperature ( $\Delta T$ ) of 75K have used. However, the specific heat of water ( $Cp_w$ ) of 4.18 kJ/kg-K, the calorific value of fuel/biomass consumed dry woof ( $CV$ ) of 16000 kJ/kg-K, the moisture content within biomass fuel ( $mst$ ) of 10%, provide the cook stove thermal efficiency of 39.35%.

## **Chapter 4. Results and Discussions.**

The research problem is on much presence of heat losses due to utilization of cooking fuels that produces much heat comes from combustion chamber geometry design of community cook-stove. An experimental simulation and CDF Analysis study of Heat transfer in solid and fluid occurs as the suitable alternative when conducting research on the community cook-stove design improvement. The 3D model combustion chamber geometries of a cook-stove are important because, in the COMSOL Multi-physics software, designing data are required to find the geometry patterns in simulation process.

### **4.1 Computational Simulation Analysis using COMSOL Multi-physics software.**

Utilizing Computational Fluid Dynamics (CFD) software COMSOL Multi-physics is one of the tool used in heat transfer simulation of many biomass cook-stoves models. The combustion process and heat transfer within the different cook-stove model design configurations are evaluate their thermal performance and identify optimal designs using the COMSOL Multi-physics software. The community cook-stove, benefit from using COMSOL Multi-physics software to simulate and analyze the heat transfer behavior of the temperature within the combustion chamber geometry design models such as cylindrical, conical and square.

Conduct thermal analysis or COMSOL Multi-physics software-based simulation to assess heat distribution of temperature through time dependent and stationary simulation analysis in various structural materials designs models made of combustion chamber geometry of community cook stoves.

This study Perform two different parametric studies to understand how temperature changes in design parameters such as insulation material thickness and combustion chamber geometries to analyze the effect performance. For the optimal performance, the two different parametric studies that shows heat transfer of temperature distribution are the following below:

- Stationary Study of COMSOL Multi-physics software-based simulation.
- Time Dependent Study of COMSOL Multi-physics software-based simulation.

### 4.1.1 Stationary Study of COMSOL Multi-physics software-based simulation.

Conducting the stationary study with COMSOL based simulation, allows showing the temperature distribution within the combustion chamber to each part of cooking pot for better performance of community cook-stove model. This study analyzes the different combustion chamber geometry models that showing the temperature or heat distribution within the community cook-stove. Those the different combustion chamber geometry models are cylindrical combustion chamber model, conical combustion chamber model and square combustion chamber model.

#### 4.1.1.1 Stationary Simulation Study of Cylindrical Combustion Chamber Geometry.

Through conducting the stationary study with COMSOL-based simulation, the boundary condition have initiated where the temperature used in combustion chamber have assumed that it will be 600 degree Celsius. The heat source of  $2604.1 \text{ W/m}^2$  used and surface ambient temperature of  $25 \text{ }^\circ\text{C}$  (298K) used and outer surface temperature of the community cook-stove model assumed as  $25 \text{ }^\circ\text{C}$  (298K) as shown in the fig 4.1, fig 4.2(a) and (b), and fig 4.3.

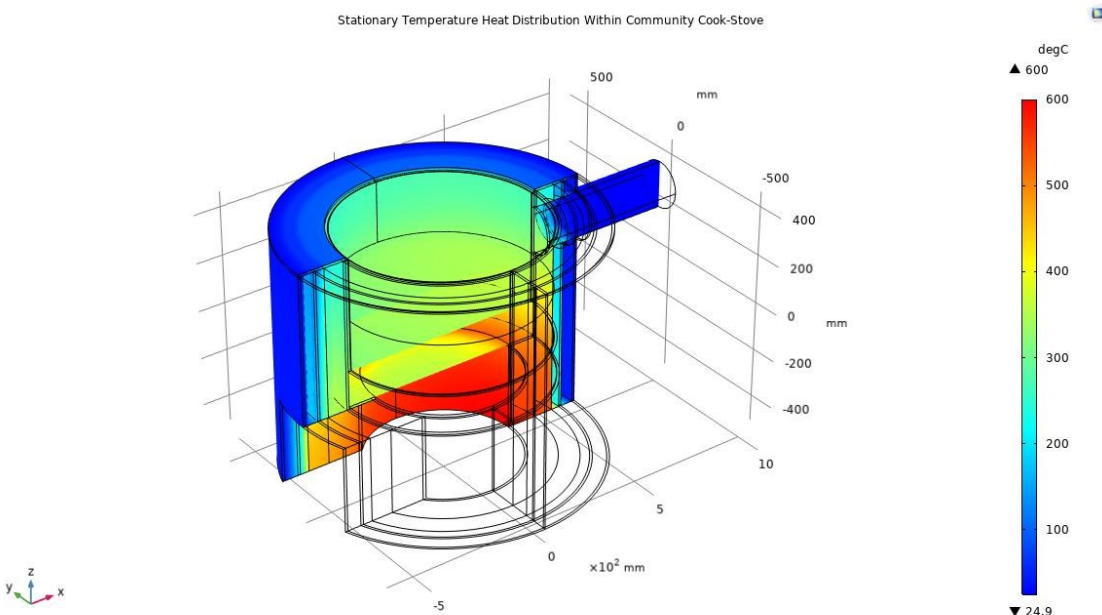


Figure 4.1: The Stationary Temperature Heat Distribution for Cylindrical Combustion Chamber.

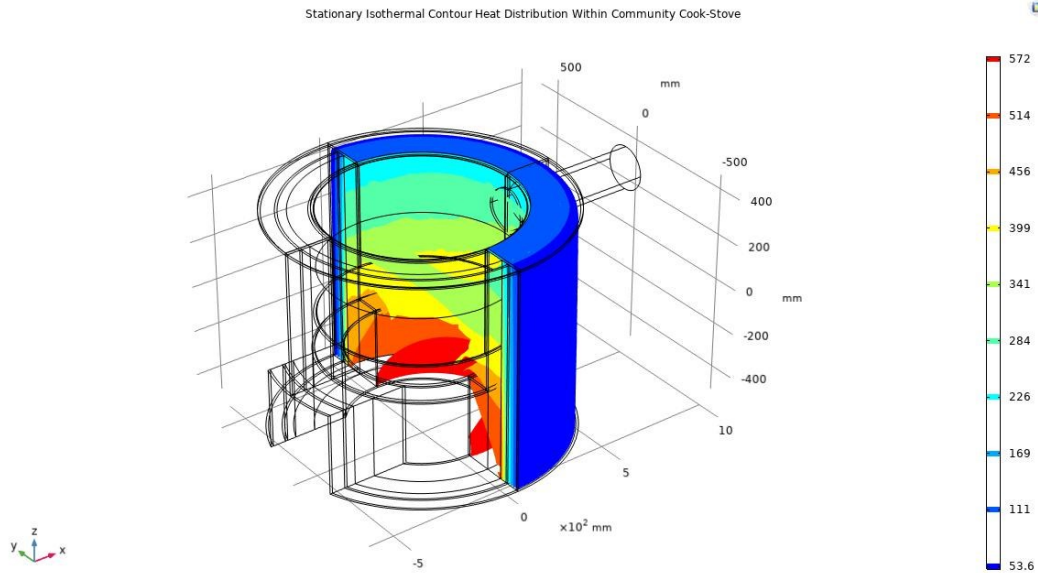


Figure 4.2: The Stationary Isothermal Contour Distribution for Cylindrical Combustion Chamber Model.

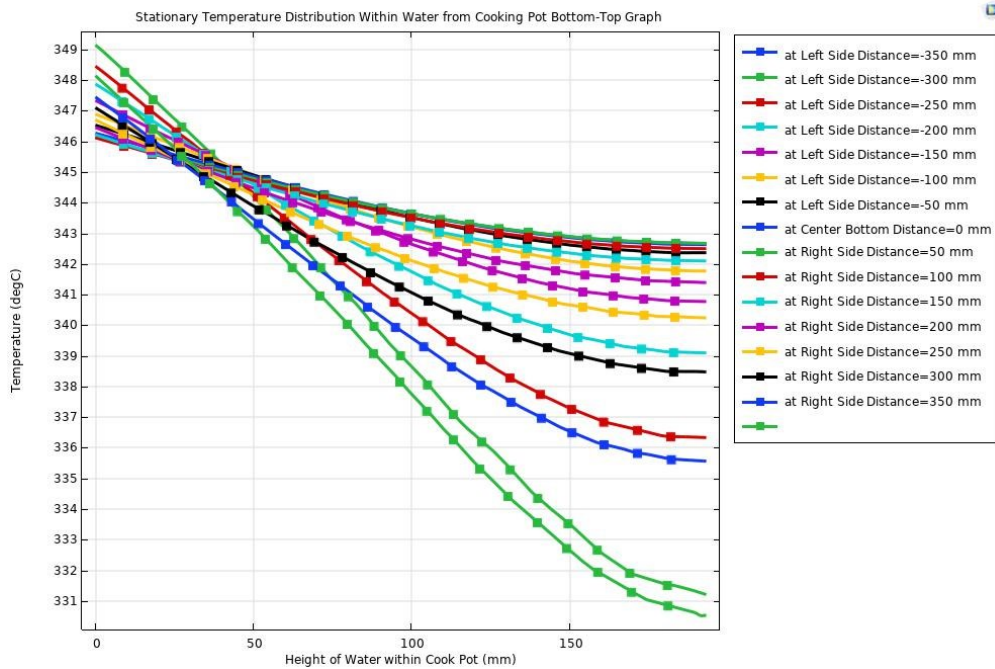


Figure 4.3 The Stationary Temperature Distribution Within Water at each Point from Bottom to Top Layer of Cylindrical Model.

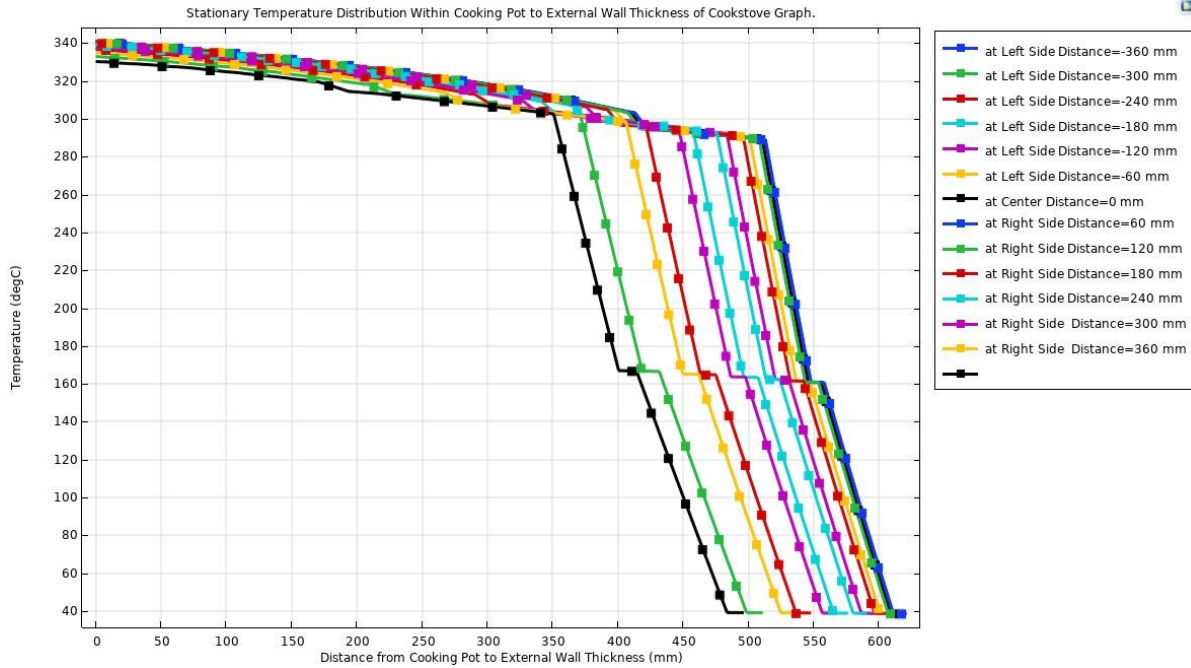


Figure 4.4 The Stationary Temperature Distribution Within Cooking at each Point from Both Sides to External wall body Layer of Cylindrical Model.

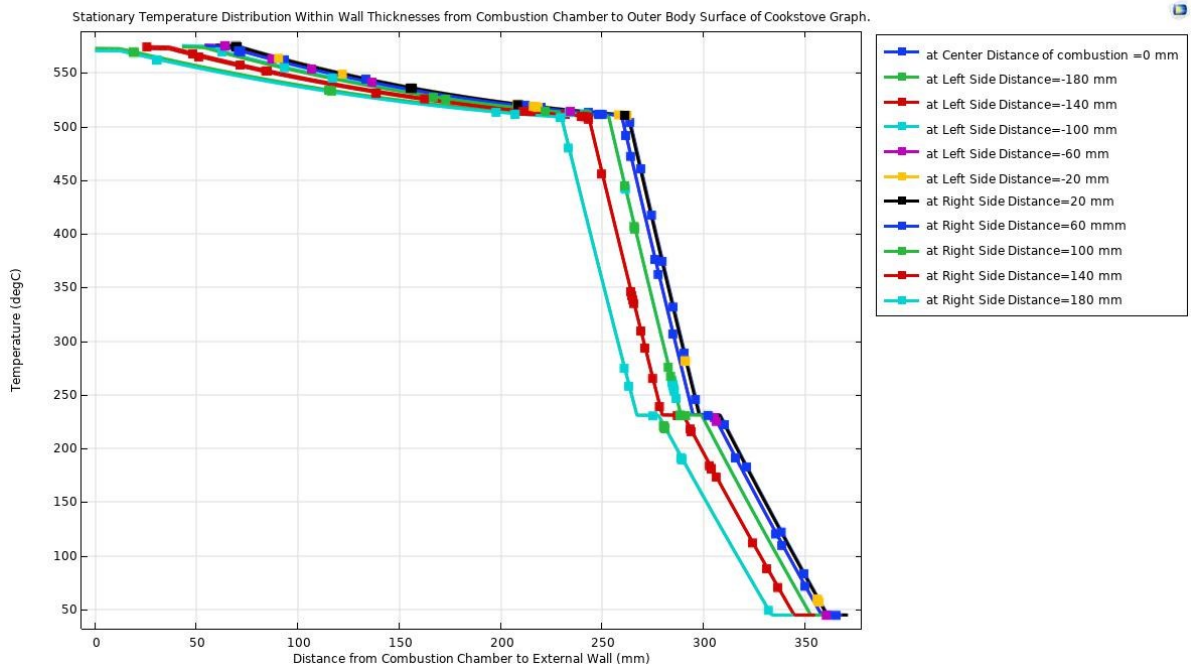


Figure 4.5 The Stationary Temperature Distribution Within Wall Thickness from Cylindrical Combustion Chamber to Outside Wall Body Surface.

#### 4.1.1.2 Stationary Simulation Study of Conical Combustion Chamber Geometry.

Through conducting the stationary study with COMSOL-based simulation, the boundary condition has initiated where the temperature used in combustion chamber have assumed that it will be 600 degrees Celsius. The heat source of  $2604.1 \text{ W}/(\text{m}^2)$  used, surface ambient temperature of  $25 \text{ }^\circ\text{C}$  (298K) used and outer surface temperature of the community cook-stove model assumed as  $25 \text{ }^\circ\text{C}$  (298K) as shown in the fig 4.4, figure 4.5(a) and (b), and figure 4.6

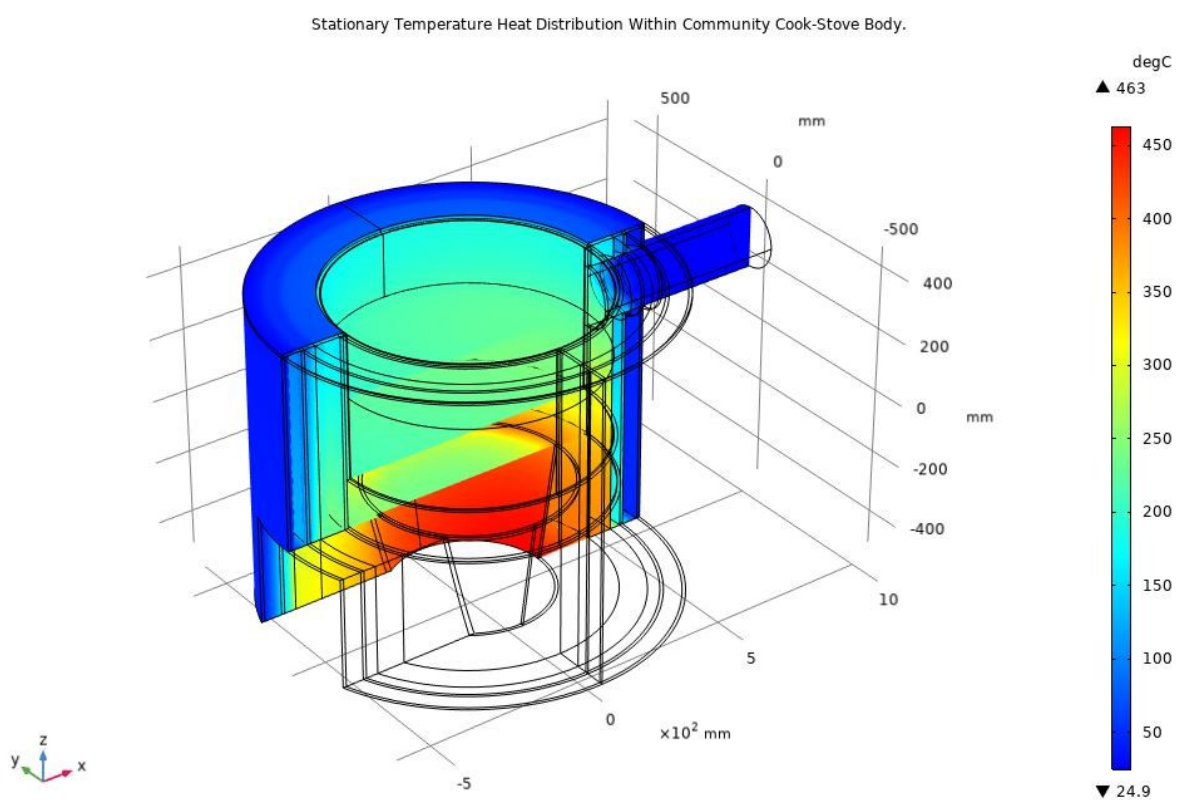


Figure 4.6: The Stationary Temperature Heat Distribution for Conical Combustion Chamber.

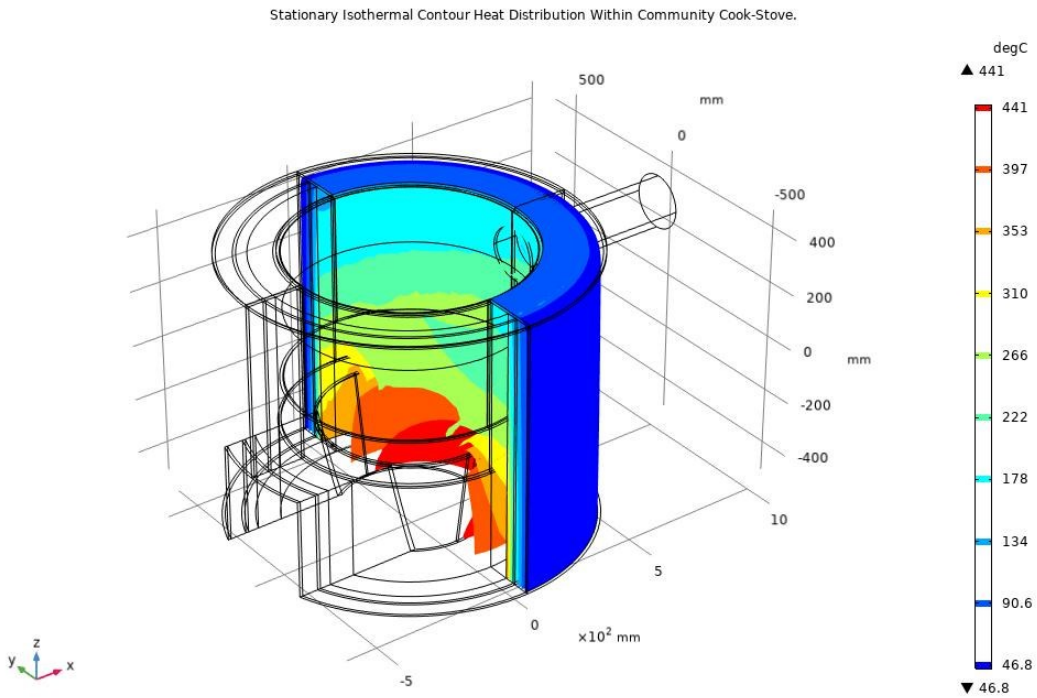


Figure 4.7: Stationary Isothermal Contour Distribution for Conical Combustion Chamber Model.

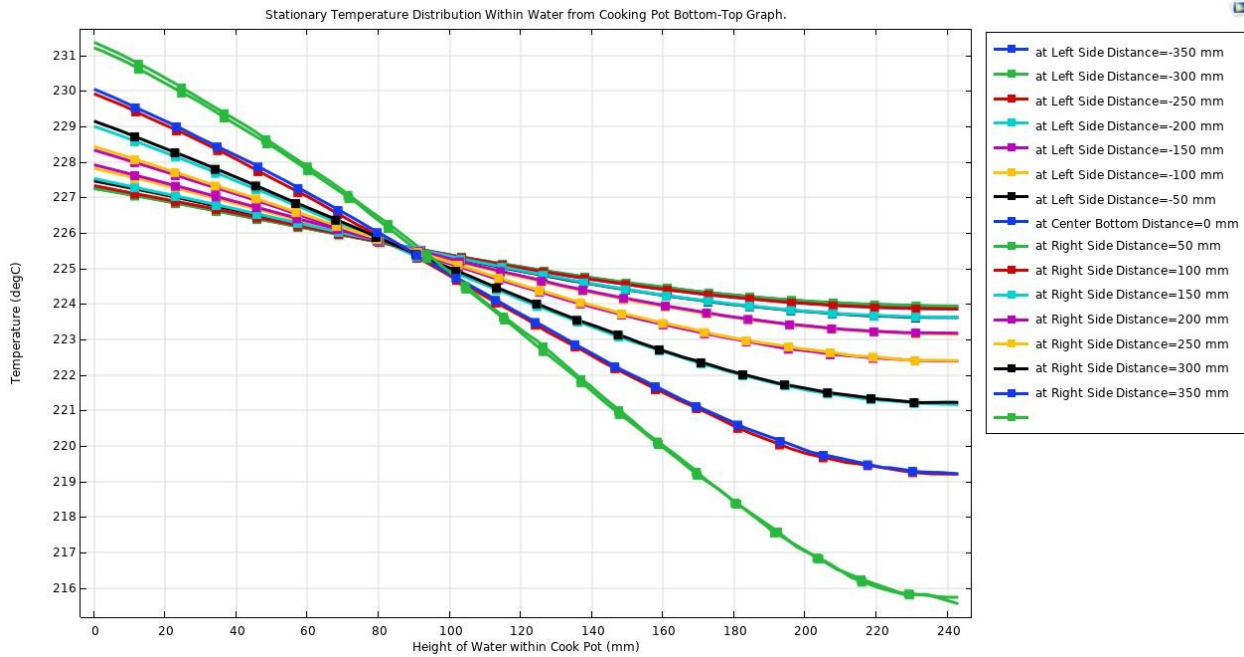


Figure 4.8 Stationary Temperature Distribution Within Water at each Point from Bottom to Top Layer of Conical Model.

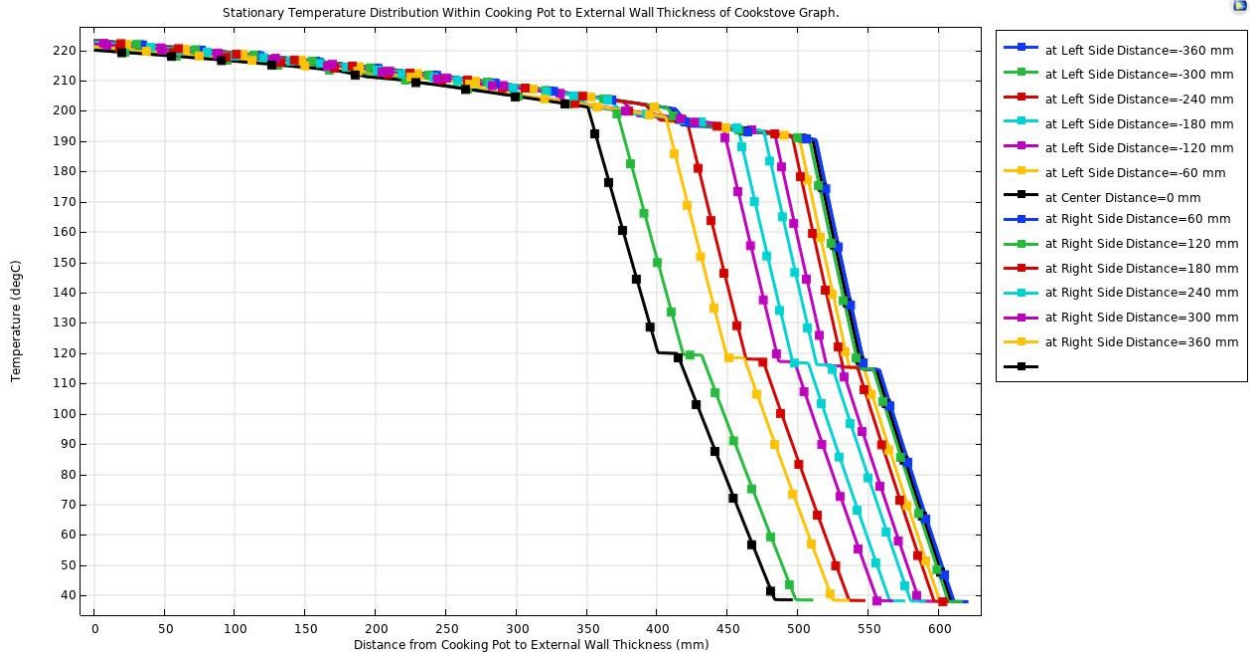


Figure 4.9 Stationary Temperature Distribution Within Cooking at each Point from Both Sides to External wall body Layer of Conical Combustion Chamber Model.

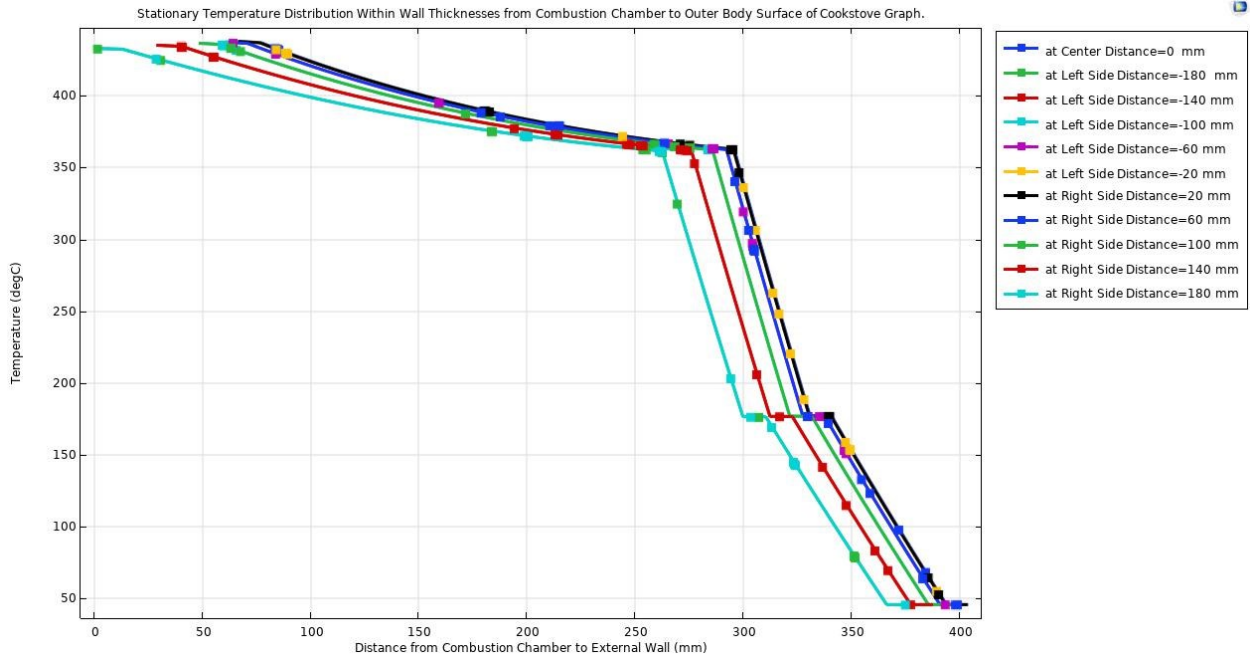


Figure 4.10 Stationary Temperature Distribution Within Wall Thickness from Conical Combustion Chamber Outside Wall.

### 4.1.1.3 Stationary Simulation Study of Rectangular Combustion Chamber Geometry.

Through conducting the stationary study with COMSOL-based simulation, the boundary condition has initiated where the temperature used in combustion chamber have assumed that it will be 600 degrees Celsius. The heat source of  $2604.1 \text{ W}/(\text{m}^2)$  used and surface ambient temperature of  $25^\circ\text{C}$  ( $298\text{K}$ ) used and outer surface temperature of the community cook-stove model assumed as  $25^\circ\text{C}$  ( $298\text{K}$ ) as shown in the fig 4.7, fig 4.8 (a) and (b), and fig 4.9.

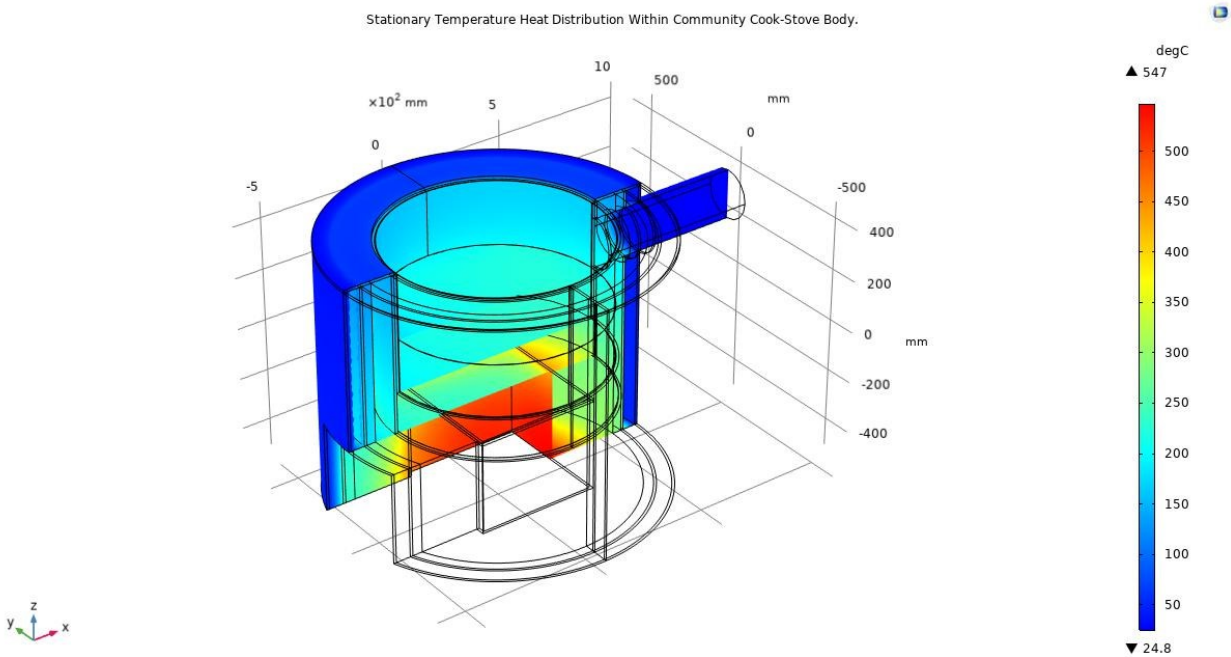


Figure 4.11: The Stationary Temperature Heat Distribution for Rectangular Combustion Chamber Model.

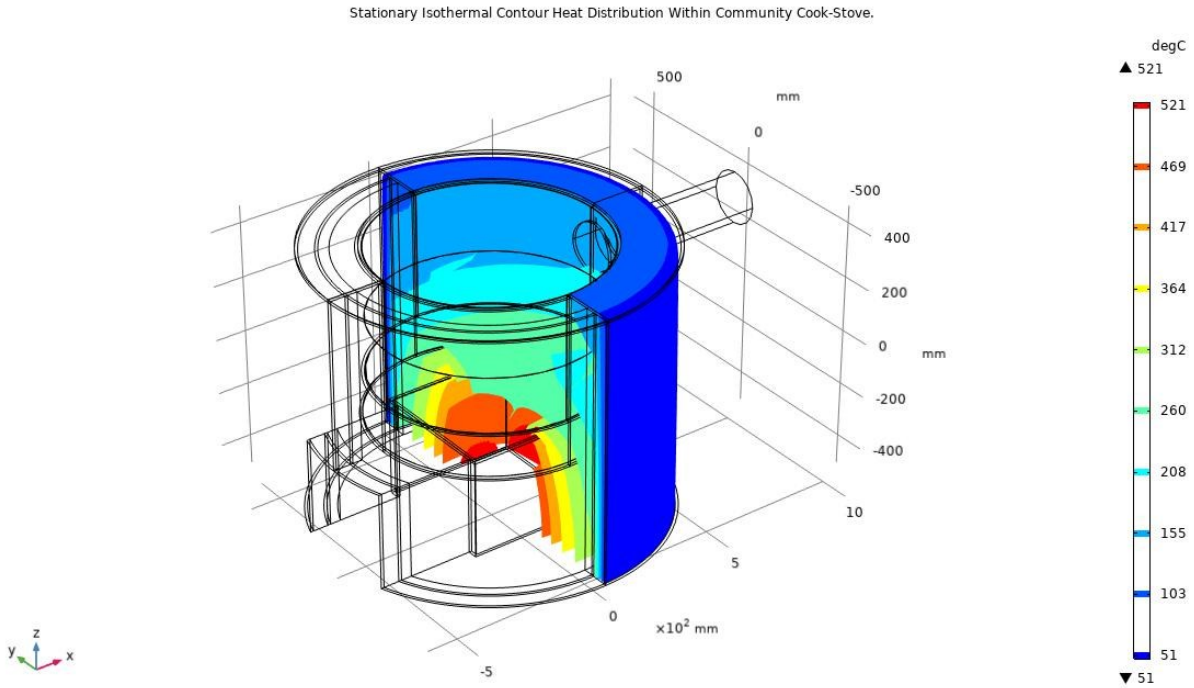


Figure 4.12: Stationary Isothermal Contour Distribution for Rectangular Combustion Chamber Model.

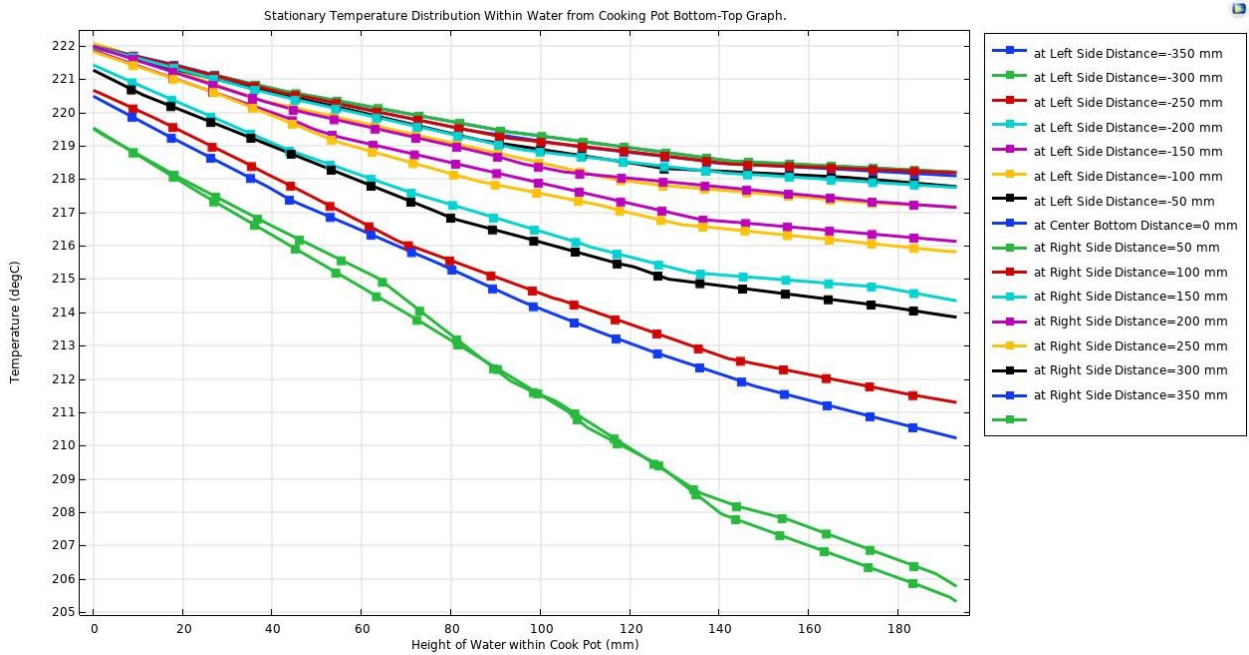


Figure 4.13 Stationary Temperature Distribution Within Water at each Point from Bottom to Top Layer of Rectangular Combustion Chamber Model.

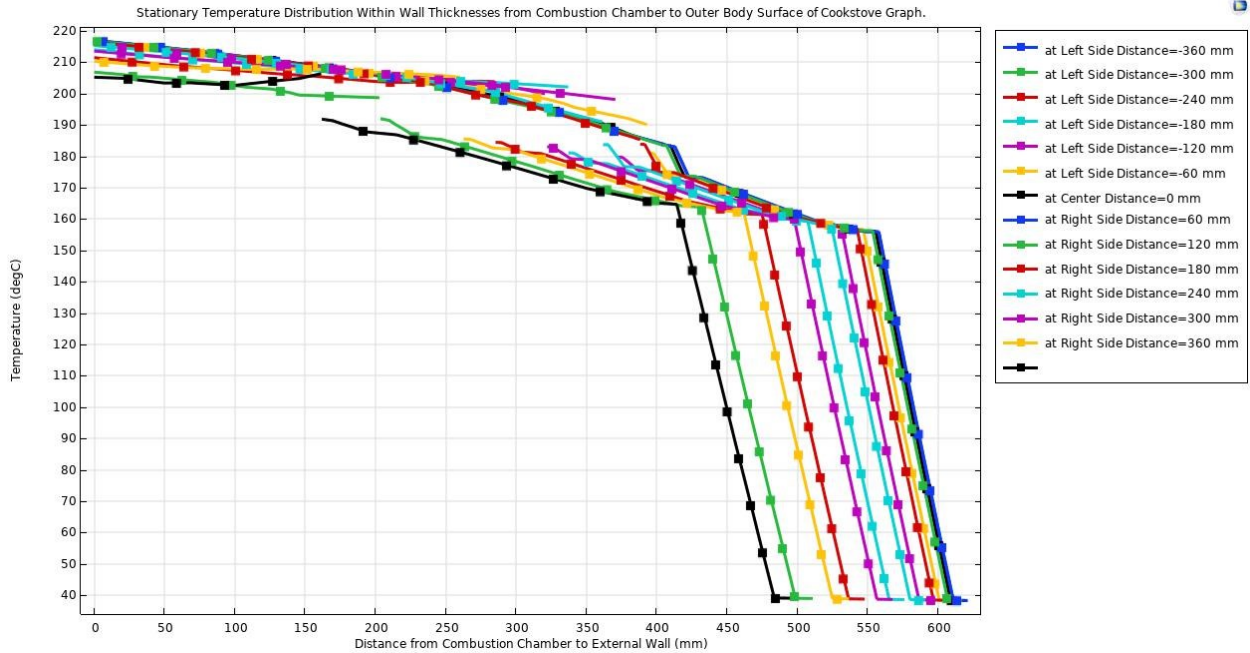


Figure 4.14 Stationary Temperature Distribution Within Cooking at each Point from Both Sides to External wall body Layer of Conical Combustion Chamber Model.

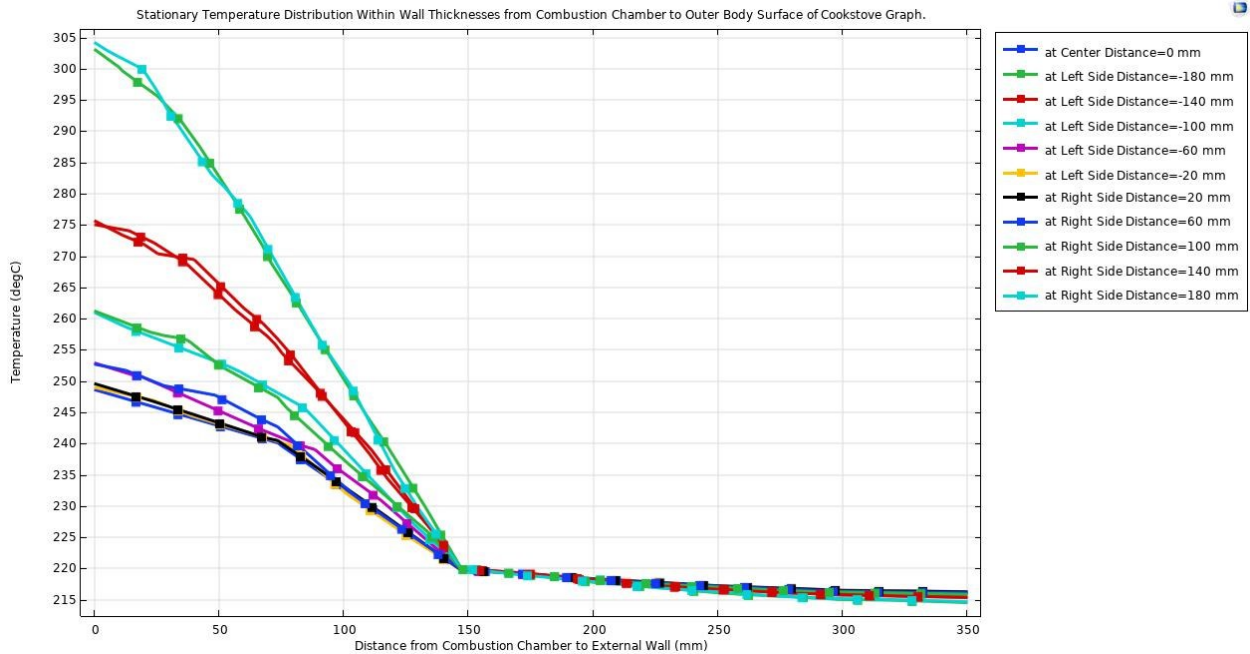


Figure 4.15 Stationary Temperature Distribution Within Wall Thickness from Rectangular Combustion Chamber to Outside Wall Surface.

## **4.1.2 Time Dependent Study of COMSOL Multi-physics Software based Simulation.**

Performing the time dependent study with COMSOL based simulation, allows showing the temperature distribution within the combustion chamber to each part of cooking pot for better performance of community cook-stove model.

This study analyzes the different combustion chamber geometry models that showing the temperature or heat distribution within the community cook-stove. Those the different combustion chamber geometry models are cylindrical combustion chamber model, conical combustion chamber model and square combustion chamber model.

### **4.1.2.1 Time Dependent Simulation Study of Cylindrical Combustion Chamber Geometry.**

Through conducting the time dependent study with COMSOL-based simulation, the boundary condition has initiated where the temperature used in combustion chamber have assumed that it will be 600 degrees Celsius. The heat source of  $2604.1 \text{ W}/(\text{m}^2)$  used and surface ambient temperature of  $25 \text{ }^\circ\text{C}$  (298K) used and outer surface temperature of the community cook-stove model assumed as  $25 \text{ }^\circ\text{C}$  (298K). the results have shown in the following figures such as shown in the fig 4.10, fig 4.11, fig 4.12 and fig 4.13.

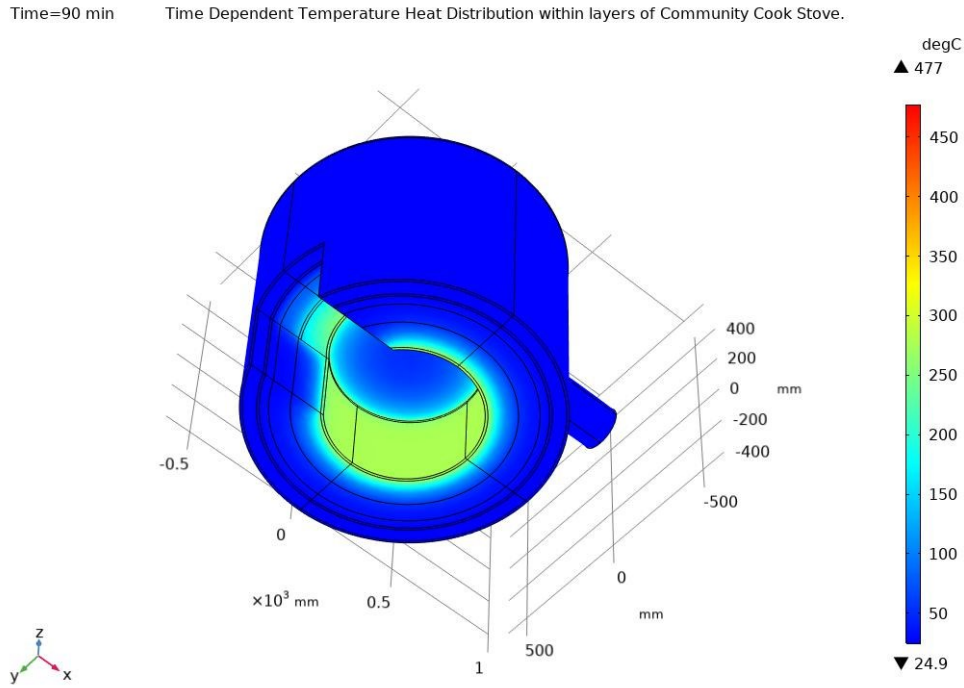


Fig 4.16 Temperature Heat Distribution for Cylindrical Combustion Chamber/ Time Dependent.

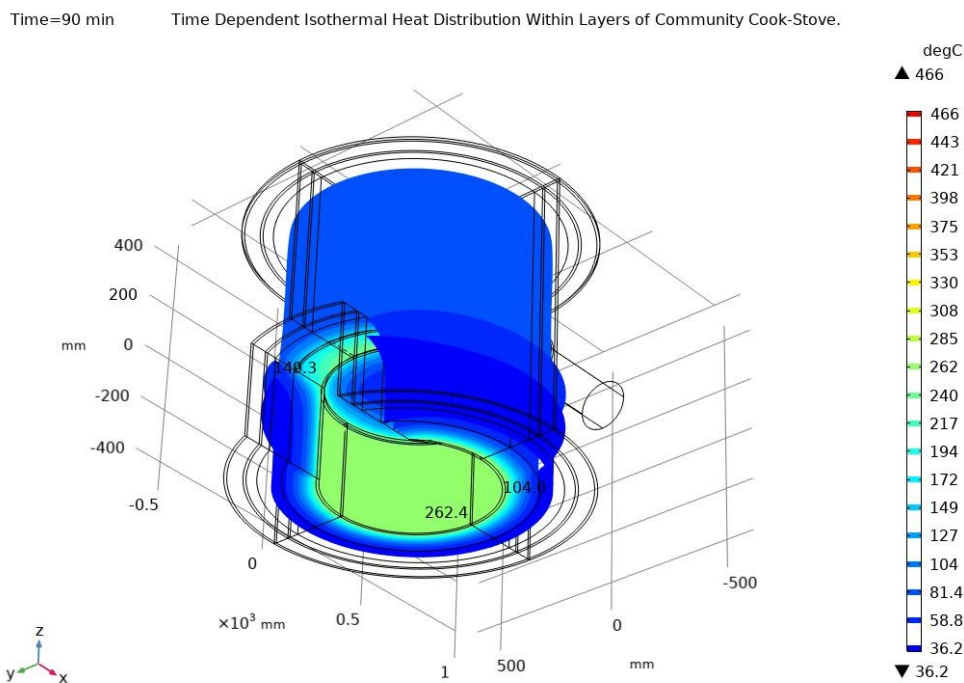


Fig 4.17 Isothermal Contour Distribution for Cylindrical Combustion Chamber/ Time Dependent.

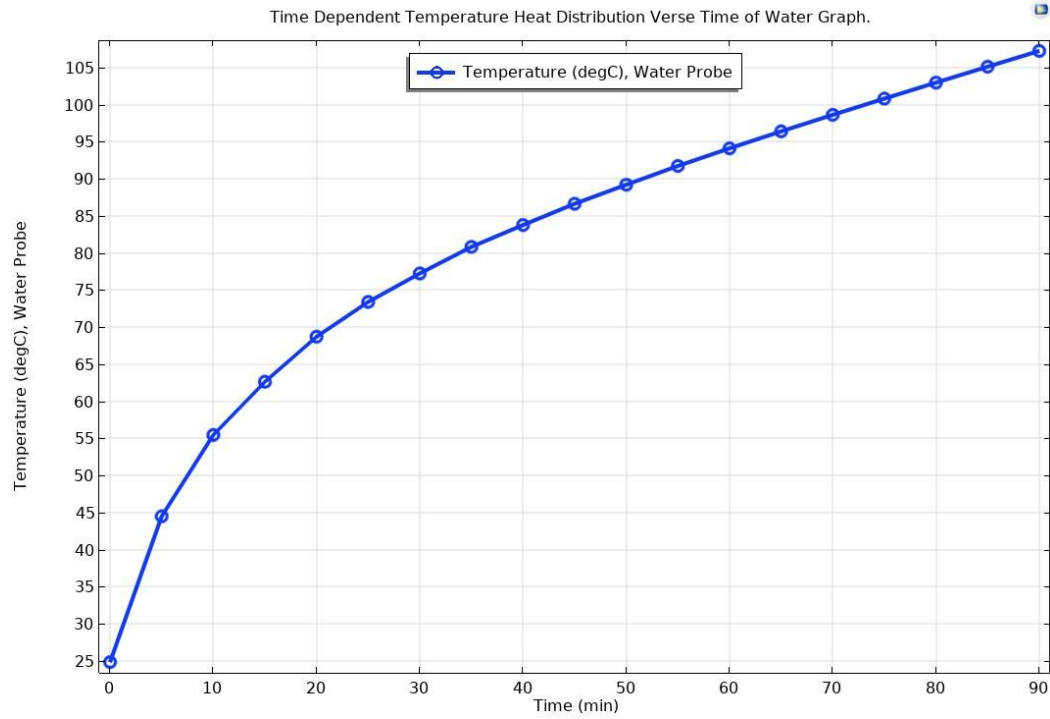


Fig 4.18 Time Dependent Graph of Temperature Heat Distribution within water Verse Time.

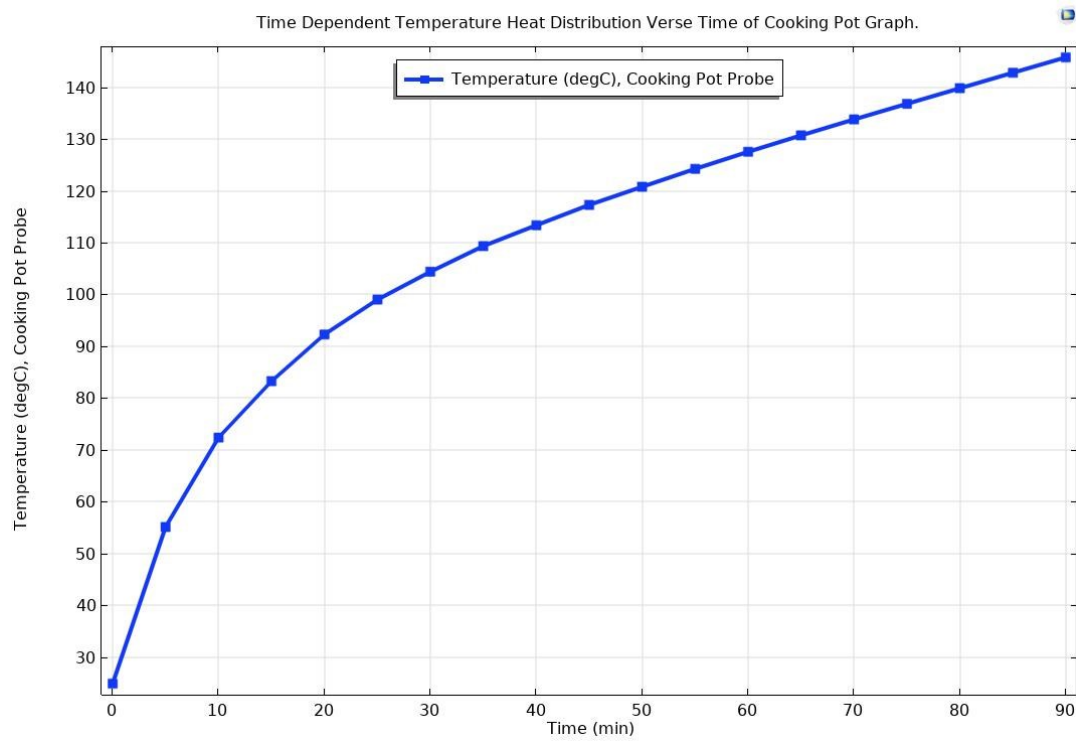


Fig 4.19 Time Dependent Graph of Temperature Heat Distribution within Cook-pot Verse Time.

### 4.1.2.2 Time Dependent Simulation Study of Conical Combustion Chamber Geometry.

Through conducting the time dependent study with comsol-based simulation, the boundary condition has initiated where the temperature used in combustion chamber have assumed that it will be 600 degrees Celsius. The heat source of  $2604.1 \text{ W}/(\text{m}^2)$  used and surface ambient temperature of  $25 \text{ }^\circ\text{C}$  (298K) used and outer surface temperature of the community cook-stove model assumed as  $25 \text{ }^\circ\text{C}$  (298K). The results have shown in the following figures such as shown in the fig 4.15, fig 4.16, fig 4.17, fig 4.0.18 and fig 4.19

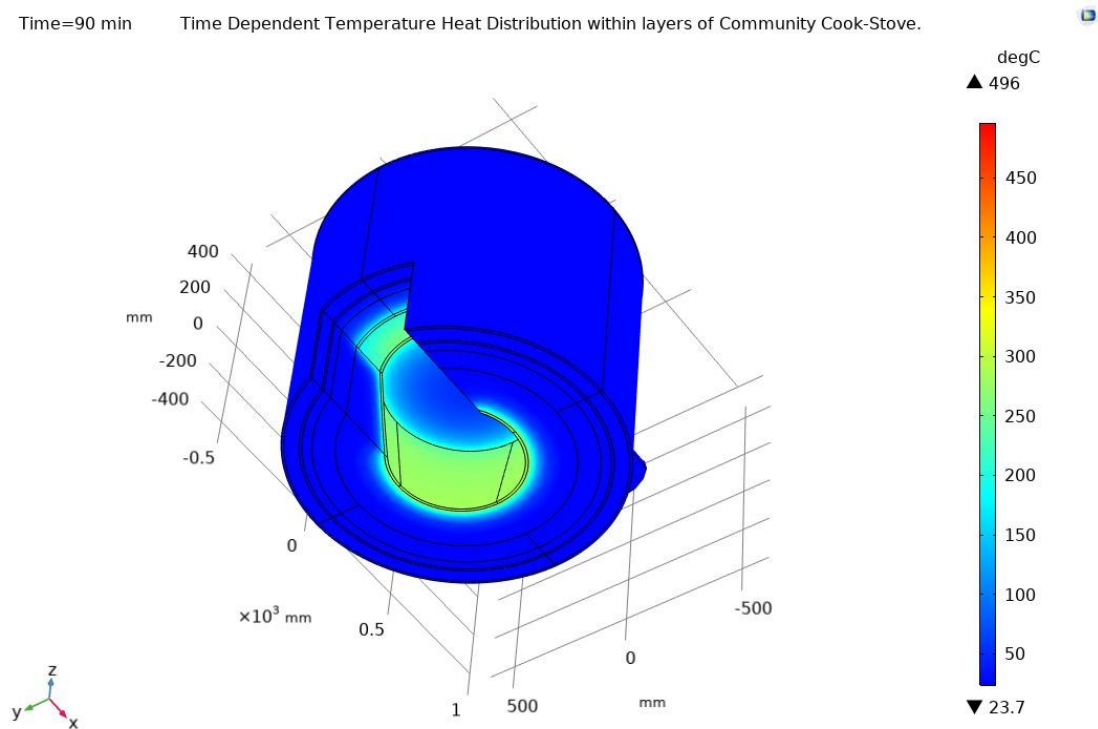


Fig 4.20 Temperature Heat Distribution for Conical Combustion Chamber/ Time Dependent.

Time=90 min

Isothermal surface Time Dependent Temperature Distribution Layers (degC)

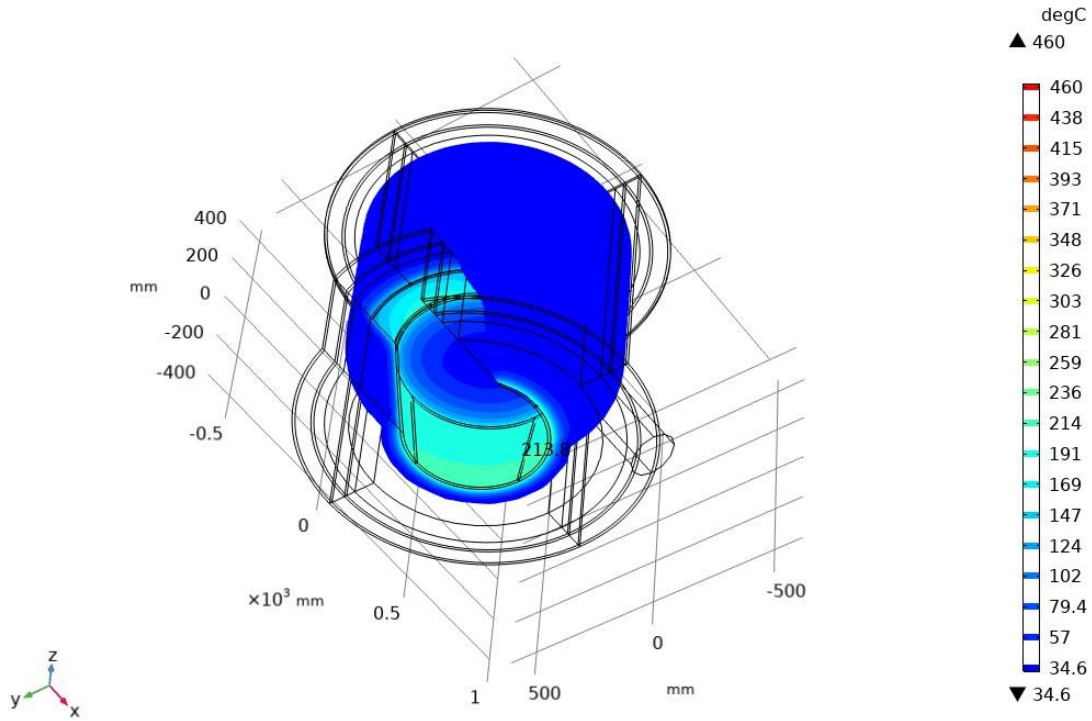


Fig 4.21 Isothermal Contour Distribution for Conical Combustion Chamber/ Time Dependent.

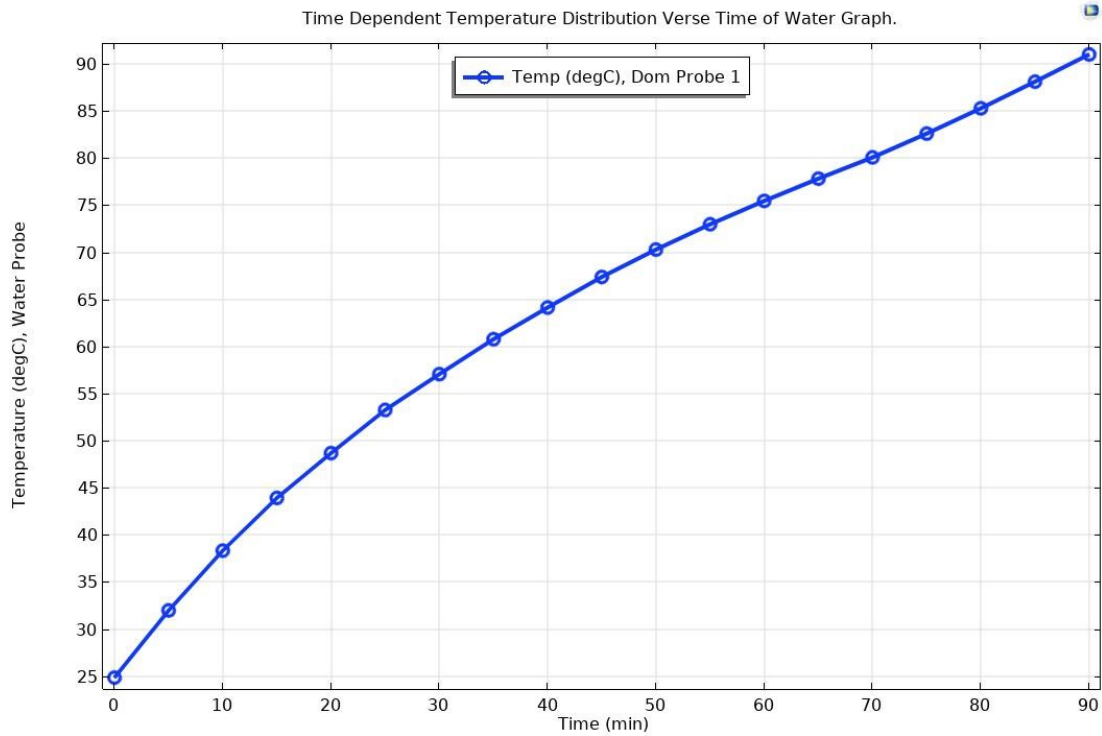


Fig 4.22 Time Dependent Graph of Temperature Heat Distribution within water Verse Time.

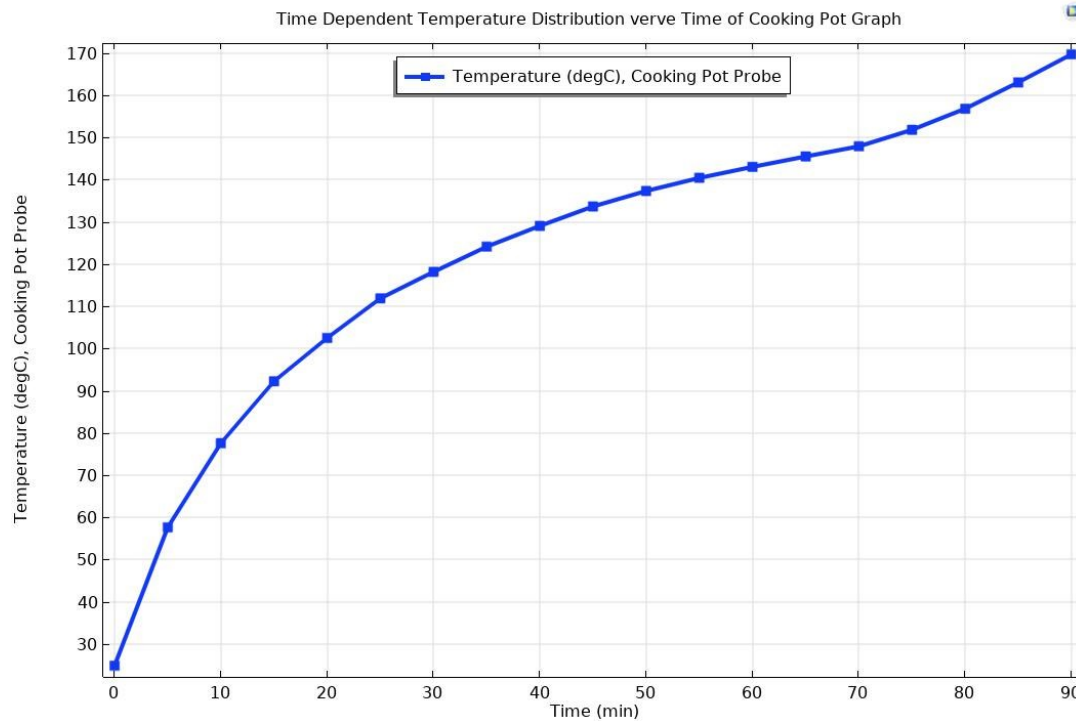


Fig 4.23 Time Dependent Graph of Temperature Heat Distribution within Cooking Pot Verse Time.

#### 4.1.2.3 Time Dependent Simulation Study of Rectangular Combustion Chamber Geometry.

Through conducting the time dependent study with Comsol-based simulation, the boundary condition has initiated where the temperature used in combustion chamber have assumed that it will be 600 degrees Celsius. The heat source of 2604.1 W/(m<sup>2</sup>) used and surface ambient temperature of 25 °C (298K) used and outer surface temperature of the community cook-stove model assumed as 25 °C (298K). The results have shown in the following figures such as shown in the fig 4.20, fig 4.21, fig 4.22, fig 4.23 and fig 4.24

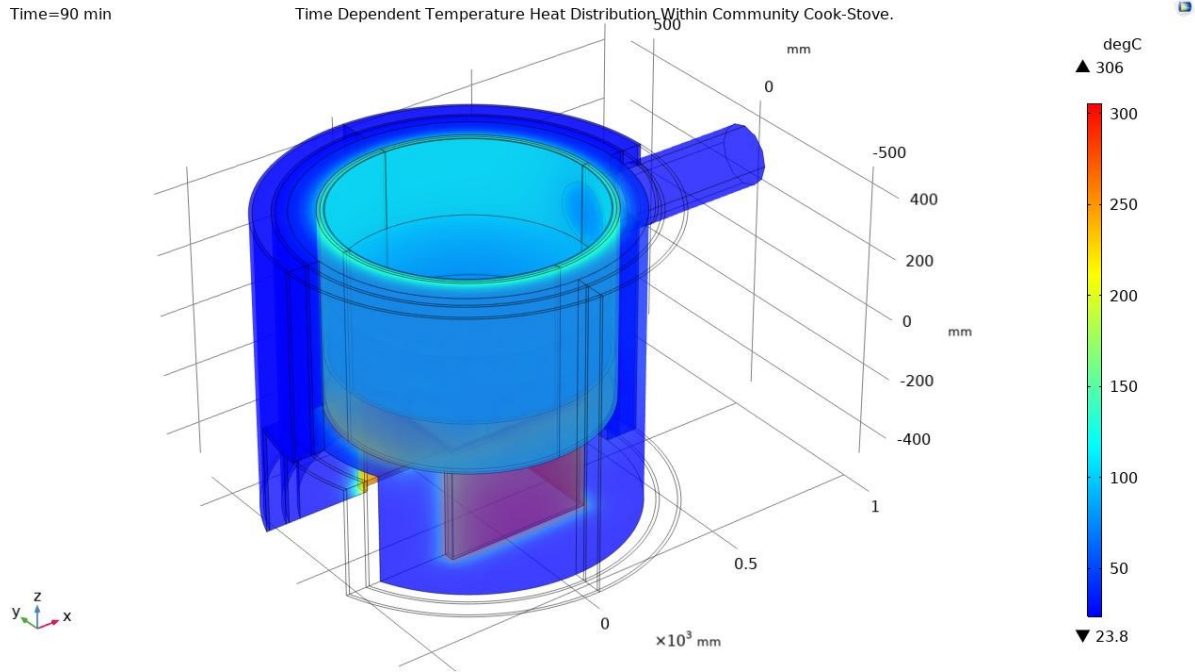


Fig 4.24 Temperature Heat Distribution for Rectangular Combustion Chamber/ Time Dependent.

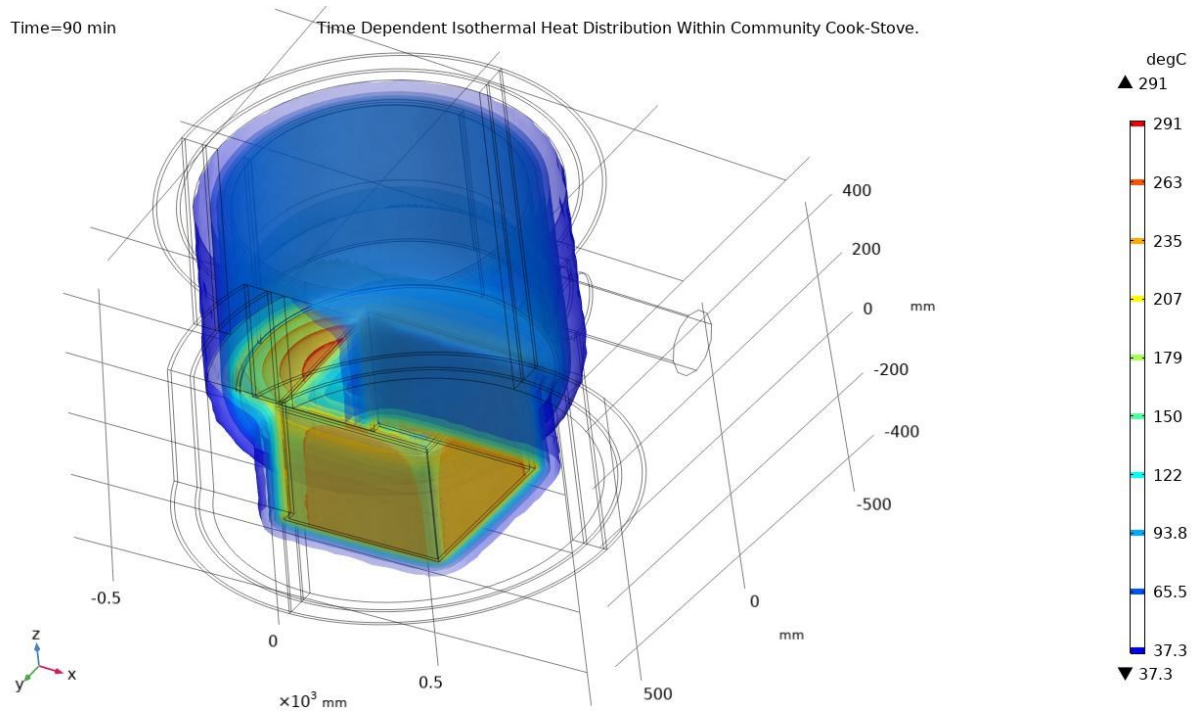


Fig 4.25 Isothermal Contour Distribution for Rectangular Combustion Chamber/ Time Dependent.

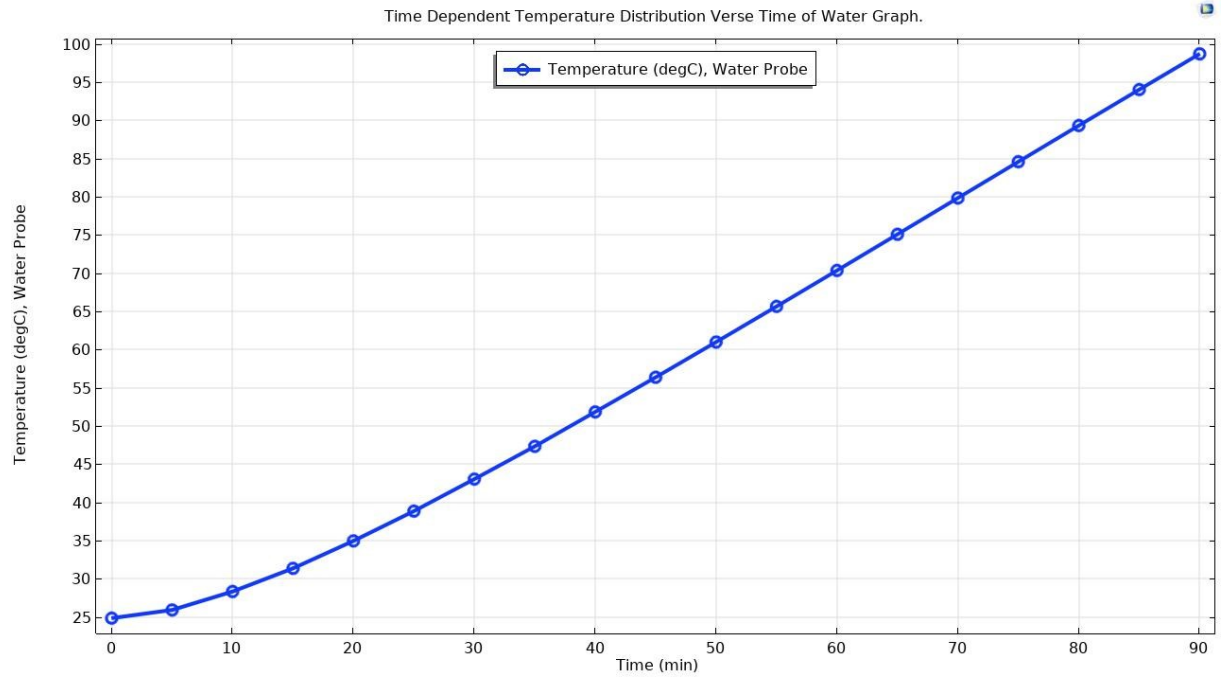


Fig 4.26 Time Dependent Graph of Temperature Heat Distribution within water Verse Time.

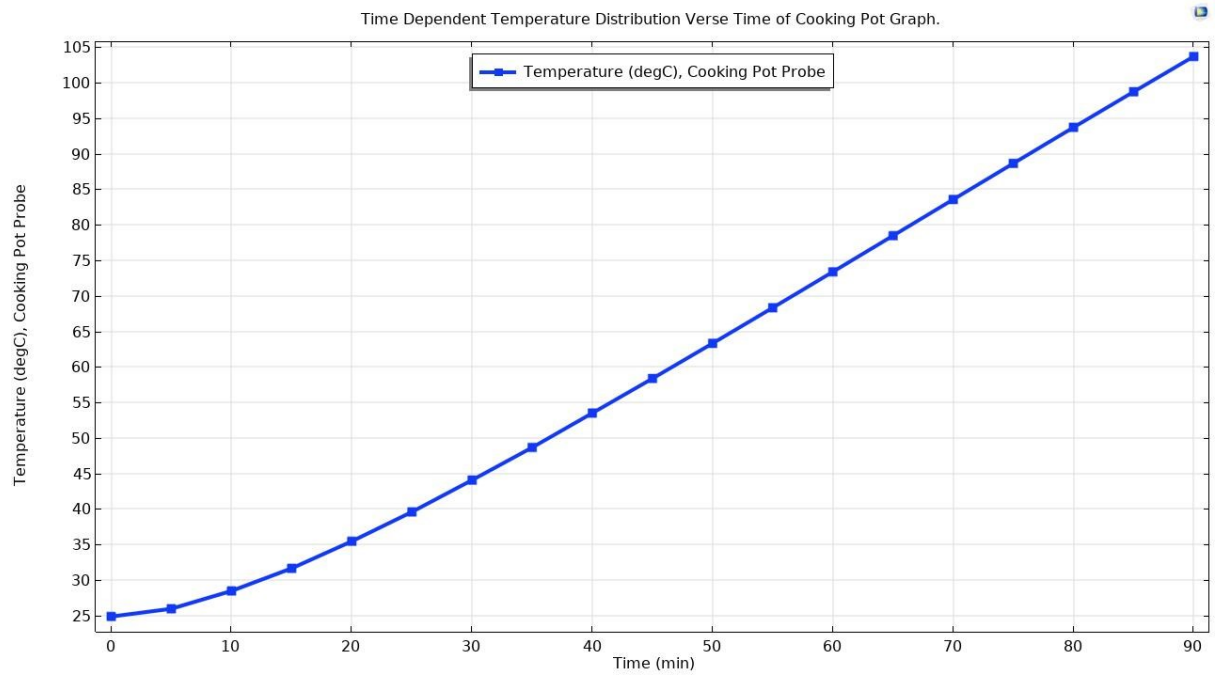


Fig 4.27 Time Dependent Graph of Temperature Heat Distribution within Cooking Pot Verse Time.

## 4.2 Discussion on Performance Comparison for All Geometry Models.

### 4.2.1 Data Analysis for All Combustion Chamber Geometries Comparison.

Basing on the simulation results, iteratively refine improvement the cook-stove design, and adjustments include optimizing the combustion chamber, improving insulation to further reduce heat loss and improve fuel efficiency. The study provide document that shows the entire design process, including technical drawings, and material specifications.

The main software used is Solid work, which is a computer-aided design (CAD) software and Comsol multi-physics. They use the principle of parametric design and generates three kinds of interconnected files. Solid work software allows the designer to enable very précised 3D objects. Same software has used to obtain the simulation results.

The comparison between the three different combustion chamber geometry models shown in fig 4.25 performed to analyze the best model that will lead to thermal performance basing on the boiling water at earlier time.

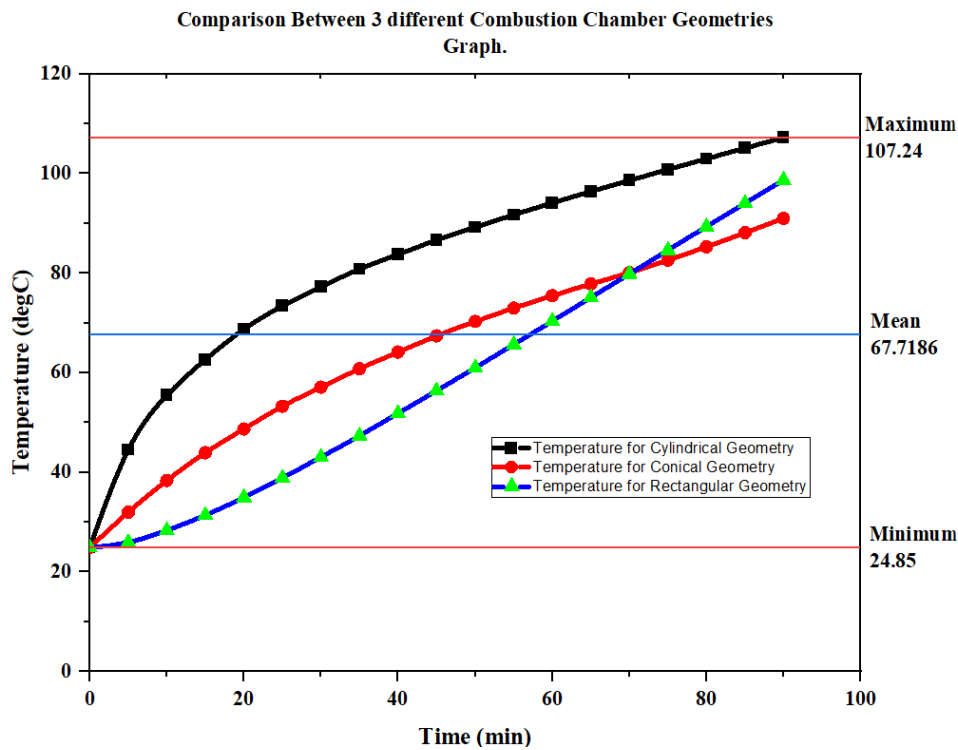


Fig 4.28 Temperature Heat Distribution within Water of the Three Different Combustion Chamber Geometries.

The Temperature distribution comparison analysis performed as shown in figure 4.26 to develop the critical difference of heat distribution within the cooking pot using the different combustion chamber geometries. This led to showing the model that will release much heat, and the conical combustion chamber geometry appears to be.

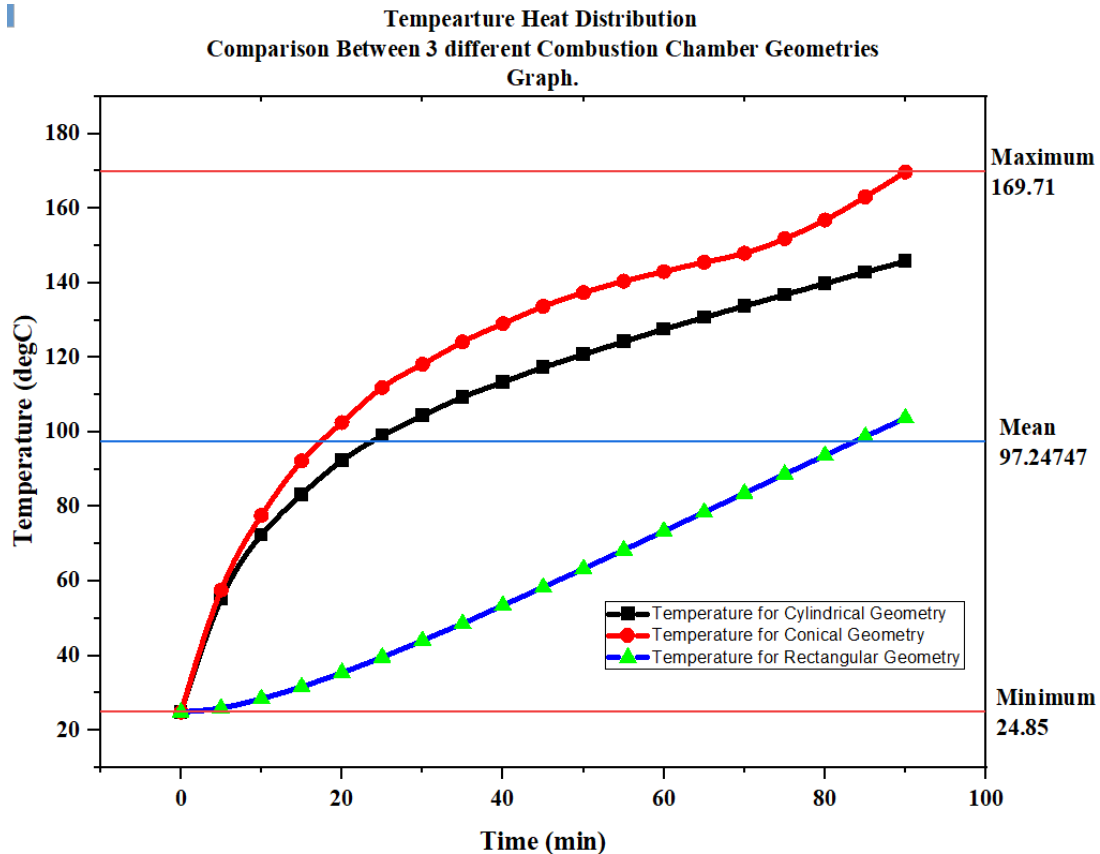


Figure 4.29 Temperature Heat Distribution within Cooking Pot of the Three Different Combustion geometry Models.

#### 4.2.2 Sensitivity Data Analysis for Different Insulation materials.

The insulation analysis comparison providing the reasonable outcomes by changing and using different insulators such as swamp air gap insulator, clay insulator, and Glass Fiber Blanket insulator. The graph below shows the comparison analysis for using the different thermal insulation as shown in the fig 4.27 and fig 4.28:

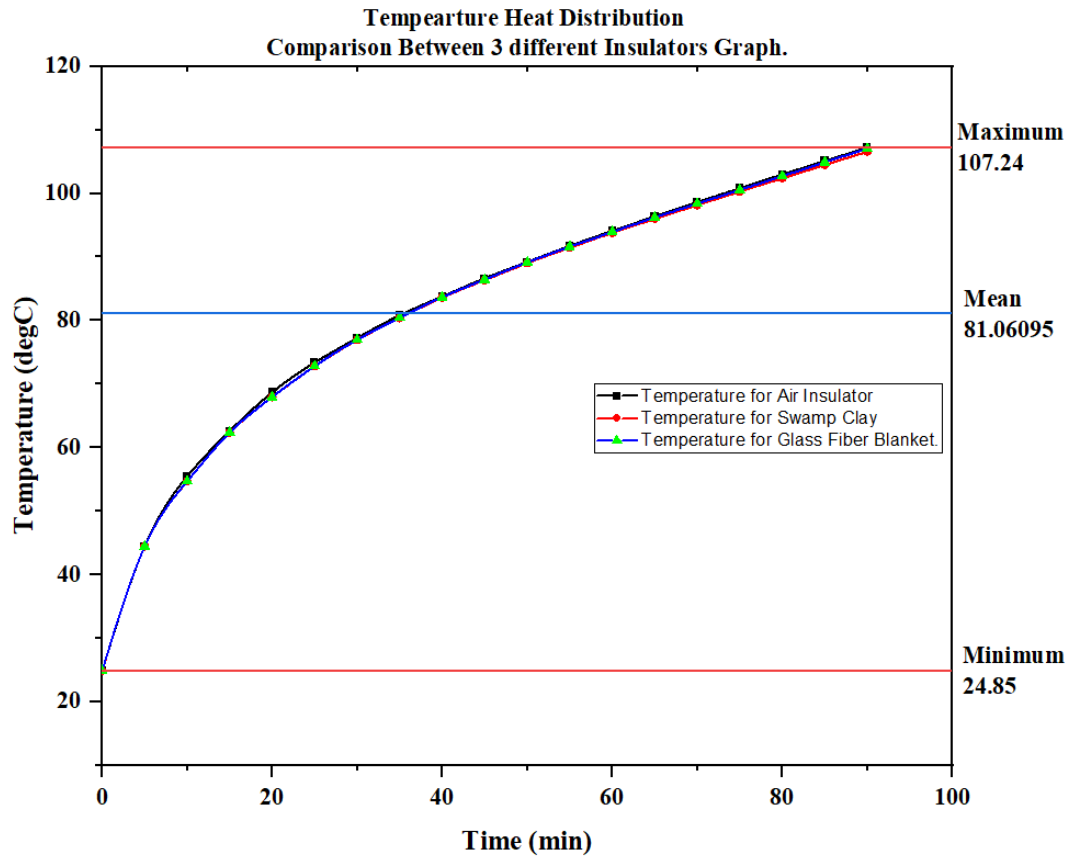


Fig 4.30 Temperature Heat Distribution within Water of the Three Different Insulators.

Table 4.1 Different temperature of insulators used for sensitivity analysis on cylindrical geometry.

Time min	Temperature degC	Temperature degC	Temperature degC
	Temperature for Air Insulator	Temperature for Swamp Clay	Temperature for Glass Fiber Blanket.
Time (min)	Temperature (degC)	Temperature (degC)	Temperature (degC)
0	24.85	24.85	24.85
5	44.503	44.462	44.46
10	55.466	54.692	54.692
15	62.637	62.365	62.365
20	68.712	67.966	67.974
25	73.403	72.81	72.83
30	77.244	76.943	76.976
35	80.827	80.414	80.463
40	83.773	83.622	83.687
45	86.639	86.365	86.452
50	89.211	89.047	89.155
55	91.738	91.496	91.628
60	94.112	93.798	93.957
65	96.401	96.014	96.208
70	98.628	98.162	98.397
75	100.82	100.29	100.57
80	102.98	102.4	102.74
85	105.12	104.5	104.91
90	107.24	106.59	107.07

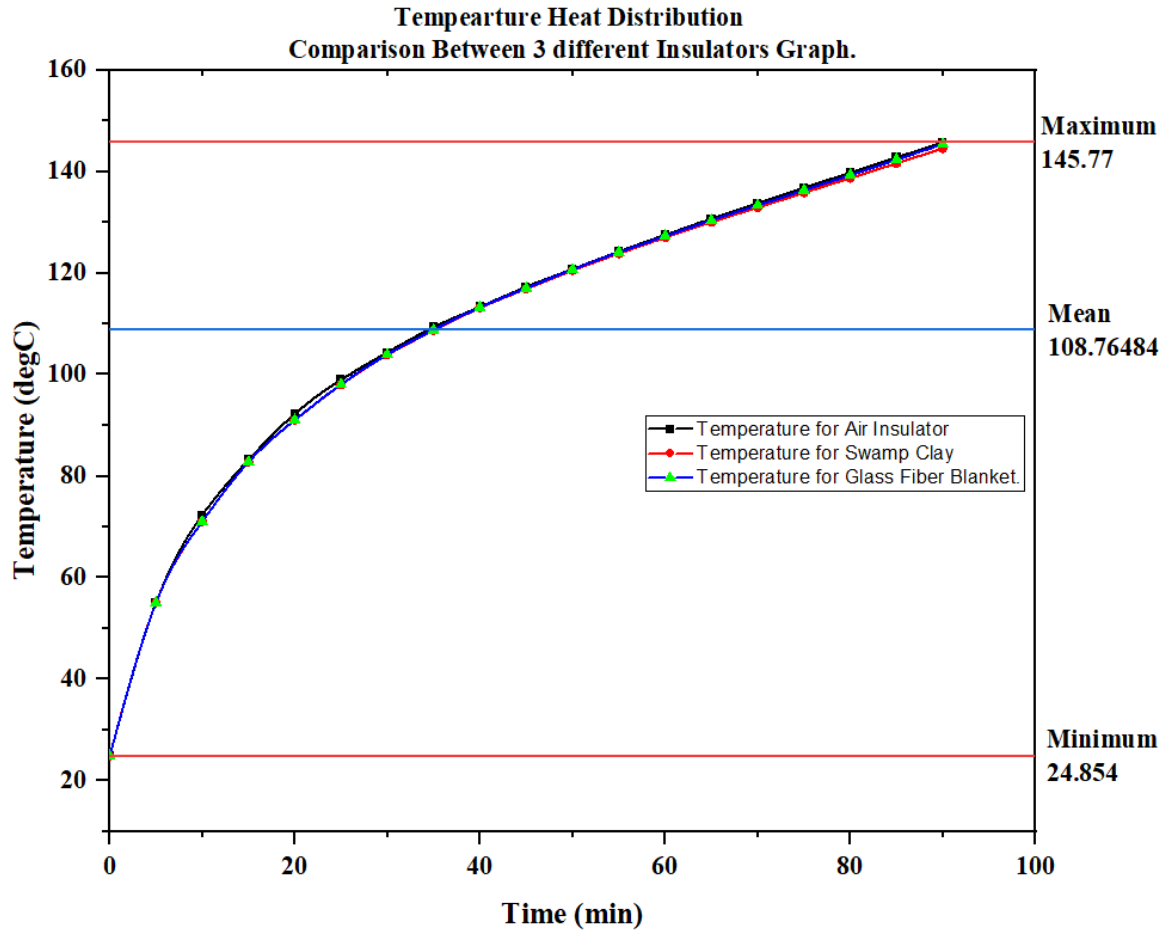


Fig 4.31 Temperature Heat Distribution within Cook Pot of the Three Different Insulators.

Through the variation of heat distribution within the community cook stove body, the recent concentration of heat within the combustion chamber enhanced by the good thermal insulations. Moreover, the analysis has performed using the three different insulators to see the heat variation within time of the community cook stove wall thicknesses.

The analysis has shown the best insulation material that can be useful within manufacturing the community cook stove.

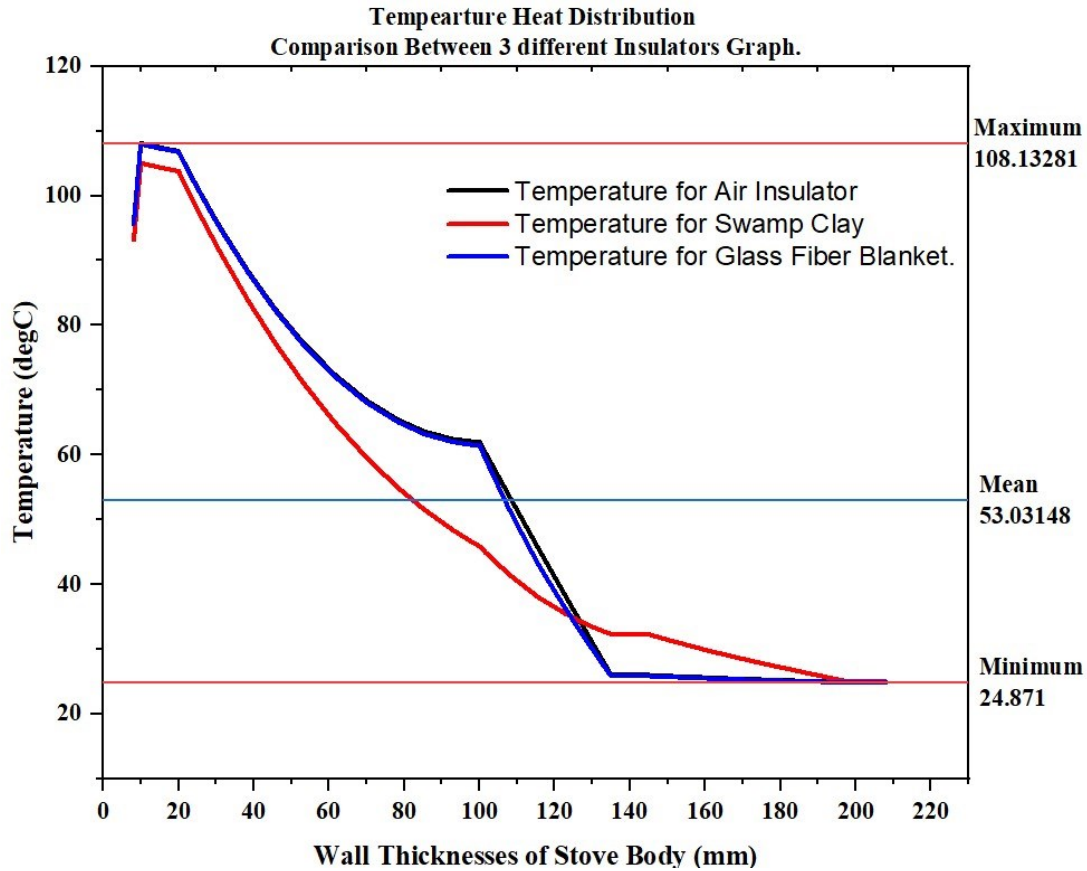


Fig 4.32 Temperature Heat Distribution within Cook Stove Wall Thickness for the Three Different Insulators.

Regarding the previous graph of fig 4.29 that shows the heat distribution and concentration using the different type of insulation for the same place or location during model building, the glass fiber blanket has the much effect on accumulation of the internal heat to enhance thermal efficiency of the stove.

## **Chapter 5. Conclusion and Recommendation.**

### **5.1 Conclusions.**

To gather data by using research approaches from many Articles, publication and Journals helps me to understand the Selection of better measurements in CDF Design Software. This aiming to show the design development for community cooking stoves that minimizes heat loss, optimizes fuel efficiency through improved heat transfer within the combustion chamber.

The proposed the simulation tool used in this work explained cook-stove design parameters that based, and acquire the full details on the heat distribution within the layers of community cook stove.

Based on the COMSOL Multi-physics results from simulations based, having the community cook-stove can help in increasing efficient, cost-effective, and environmentally friendly as well as improving the heat transfer within the combustion chamber. Moreover, it shows the selection of the final design model of combustion chamber that best meets the objectives as the cylindrical combustion chamber geometry model.

### **5.2 Recommendations.**

In all over the world, many improved cook-stoves design have developed where they show the improvement to addition on many biomasses cook stoves to increase the efficiency of the stoves.

the COMSOL Multi-physics software, is the one of the tools that every researcher on improved biomass cook stove are recommended to use due to many features for heat distribution analysis are there to perform thermal analysis in briefly good way.

The community cook-stove have shown the three (3) different models of combustion chamber geometries only. However, the other design models of combustion chamber geometries are recommended to see their temperature heat distribution such as hexagonal model design, square model design, trapezium model design, pentagon model design... etc.

Future research could focus on simplifying these processes and expanding the scope to enhance the applicability, impact of their findings, incorporating real-world testing and addressing health and safety considerations more comprehensively would further strengthen the practical relevance.

## References

- [1] D. Gómez-Heleria, J. Núñez, E. M. Fisher, V. M. Ruiz-García, and A. Beltrán, “Steady-state behavior of a biomass plancha-type cookstove: Experimental and 3D numerical study,” *Sustainable Energy Technologies and Assessments*, vol. 57, Jun. 2023, doi: 10.1016/j.seta.2023.103172.
- [2] N. S. Rathore, C. K. Singh, N. Rathore, and N. L. Panwar, “Thermal performance and heat storage behaviour of three pots improved cookstove,” *Energy Nexus*, vol. 6, Jun. 2022, doi: 10.1016/j.nexus.2022.100074.
- [3] U. Hayyat *et al.*, “CFD simulation of a forced draft biomass cookstove for different airflow conditions,” *Results in Engineering*, vol. 21, Mar. 2024, doi: 10.1016/j.rineng.2024.101928.
- [4] Dan Sweeney, “Handbook for Biomass Cookstove Research, Design, and Development A PRACTICAL GUIDE TO IMPLEMENTING RECENT ADVANCES,” 2016.
- [5] C. Samal, P. C. Mishra, S. Mukherjee, and D. Das, “Evolution of high performance and low emission biomass cookstoves-an overview,” in *AIP Conference Proceedings*, American Institute of Physics Inc., Dec. 2019. doi: 10.1063/1.5141191.
- [6] A. Pundle, B. Sullivan, P. Means, J. D. Posner, and J. C. Kramlich, “Predicting and analyzing the performance of biomass-burning natural draft rocket cookstoves using computational fluid dynamics,” *Biomass Bioenergy*, vol. 131, Dec. 2019, doi: 10.1016/j.biombioe.2019.105402.
- [7] S. F. Baldwin and Volunteers in Technical Assistance., *Biomass stoves : engineering design, development, and dissemination*. Volunteers in Technical Assistance, 1987.
- [8] J. Agenbroad, M. DeFoort, A. Kirkpatrick, and C. Kreutzer, “A simplified model for understanding natural convection driven biomass cooking stoves-Part 2: With cook piece operation and the dimensionless form,” *Energy for Sustainable Development*, vol. 15, no. 2, pp. 169–175, 2011, doi: 10.1016/j.esd.2011.04.002.
- [9] R. Shah and A. W. Date, “Steady-state thermochemical model of a wood-burning cookstove,” *Combustion Science and Technology*, vol. 183, no. 4, pp. 321–346, Apr. 2011, doi: 10.1080/00102202.2010.516617.

- [10] Hugh Burnham- Slipper Beng, “Breeding a better stove the use of Computational Fluid Dynamics and genetic Algorithm to Optimise a wood burning Stove for Eritrea”.
- [11] J. Phusrimuang and T. Wongwuttanasatian, “Improvements on thermal efficiency of a biomass stove for a steaming process in Thailand,” *Appl Therm Eng*, vol. 98, pp. 196–202, Apr. 2016, doi: 10.1016/j.applthermaleng.2015.10.022.
- [12] K. Xie, Y. Cui, J. Wang, and X. Qiu, “Theoretical and numerical investigation of heat transfer characteristics of an integrated cookstove under different atmospheric pressures based on theoretical models of solid flame and impingement heat transfer,” *International Communications in Heat and Mass Transfer*, vol. 127, Oct. 2021, doi: 10.1016/j.icheatmasstransfer.2021.105524.
- [13] T. Jain and P. N. Sheth, “Design of energy utilization test for a biomass cook stove: Formulation of an optimum air flow recipe,” *Energy*, vol. 166, pp. 1097–1105, Jan. 2019, doi: 10.1016/j.energy.2018.10.180.

## Appendix 1. Data Recording Process on Field.



(a).

(b).

(c).

Fig A.1 Data recording on field (a), final manufactured stove model (b), and construction chamber model (c) of Community Stove at RP IPRC Tumba Colledge.